

**Oxidation of Amino Acids by Peroxymonosulfate and
Sorption of Antibiotics to Natural Organic Matter**

by
Mercedes Ruiz Vélez

A dissertation submitted in partial fulfillment of
the requirements for the degree of

Doctor of Philosophy
(Environmental Chemistry & Technology)

at the
UNIVERSITY OF WISCONSIN-MADISON
2015

Date of final oral examination: 25 September 2015

Final oral committee:

Joel A. Pedersen, Professor, Soil Science

Lingjun Li, Professor, Chemistry

Robert J. Hamers, Professor, Chemistry

Christina Remucal, Assistant Professor, Civil and Environmental Engineering

Matt Ginder-Vogel, Assistant Professor, Civil and Environmental Engineering

© Copyright by Mercedes Ruiz Vélez 2015
All Rights Reserved

ACKNOWLEDGEMENTS

Thank you Joel A. Pedersen for your guidance and providing me with diverse research opportunities.

Thank you Sam Sibley and Tom Kuech for being great mentors.

I would like to thank my labmates – the old gang: Chad the Wookie, Christina, Christen, Clarissa, Lee, Kartik, Kurt, and Sarah; and the new crew: Ali, Arielle, Debra, Emily, Eric, Hannah, Ian, Liz, and Sara.

Thank you Megan McConville for showing me the ropes of the mass spec and always helping me out when I needed it.

Thanks to my family, particularly my Mom, my Grandma, and my brother (talisman power!), for all of your love and support.

Thank you Rafael for always making me laugh at the end of the day.

TABLE OF CONTENTS

ACKNOWLEDGEMENTS	ii
LIST OF FIGURES	iv
LIST OF TABLES	vi
Chapter 1. General Introduction	1
Chapter 2. Transformation of Amino Acids by Peroxymonosulfate	4
Chapter 2S. Supporting information for: Transformation of Amino Acids by Peroxymonosulfate	36
Chapter 3. Transformation of Amino Acids by Cobalt-activated Peroxymonosulfate	50
Chapter 3S. Supporting information for: Transformation of Amino Acids by Cobalt- activated Peroxymonosulfate	85
Chapter 4. Sorption of Clarithromycin and Tetracycline to Natural Organic Matter in the Presence of Calcium	98
Chapter 5. Summary, Conclusions, and Future Directions	131

LIST OF FIGURES

Chapter 2.2. Transformation of Amino Acids by Peroxymonosulfate

Figure 2.1. Oxidation of selected amino acids by peroxymonosulfate	31
Figure 2.2. Pseudo-first-order rate constants for the oxidation of selected amino acids by peroxymonosulfate.....	32
Figure 2.3. Dependence on pH of histidine (His) and tryptophan (Trp) transformation by peroxymonosulfate.....	33
Figure 2.4. Oxidation of tryptophan (Trp) by peroxymonosulfate in the presence of natural organic matter	34

Chapter 2S. Supporting Information for: Transformation of Amino Acids by Peroxymonosulfate

Figure 2S.1. Stability of peroxymonosulfate in the reaction conditions	44
Figure 2S.2. Transformation of alanine by peroxymonosulfate as a function of oxidant and salt concentrations	45
Figure 2S.3. Transformation of tryptophan by peroxymonosulfate as a function of oxidant and salt concentrations	46
Figure 2S.4. Ricin structure, solvent exposed residues	47
Figure 2S.5. Prion-trimer structure, solvent exposed residues..	48

Chapter 3. Transformation of Amino Acids by Cobalt-activated Peroxymonosulfate

Figure 3.1. Amino acid oxidation by cobalt-activated peroxymonosulfate	81
---	-----------

Figure 3.2. Pseudo first-order rate constants for amino acid by transformation by peroxymonosulfate and cobalt-activated peroxymonosulfate	82
Figure 3.3. Tryptophan oxidation by cobalt-activated peroxymonosulfate	83
Figure 3.4. The effect of (a) radical quenchers and (b) cobalt counterion on the oxidation of amino acid by cobalt-activated peroxymonosulfate	84
 Chapter 4. Sorption of Clarithromycin and Tetracycline to Natural Organic Matter in the Presence of Calcium	
Figure 4.1. Sorption of clarithromycin (CLA) to Elliott soil humic acid as a function of non-sorbed CLA at pH 8.7 and 9 (phosphate buffer)	123
Figure 4.2. Sorption of tetracycline (TC) to Elliott soil humic acid as a function of non-sorbed TC at pH 3, 4.3, 6.3 and 9.2 (phosphate buffer).....	124
Figure 4.3. Speciation as a function of pH, skeletal formulae and molecular electrostatic potentials (MEPs) of (a) clarithromycin and (b) tetracycline, and (c) MEP for sulfathiazole cation.	125
Figure 4.4. Sorption of tetracycline (TC) to Elliott soil humic acid as a function of pH ($I = 0.01$ M and 0.1 M). $[TC] = 1 \mu\text{M}$, $[DOC] = 37\text{-}43 \text{ mg}\cdot\text{L}^{-1}$	127
Figure 4.5. Sorption of antibiotics tetracycline (TC) and clarithromycin (CLA) to Elliott soil humic acid (ESHA) as a function of total calcium concentration.....	128
Figure 4.6. Organic carbon-normalized distribution coefficient (K_{OC} , $\text{L}\cdot\text{kg}^{-1}_{OC}$) as a function of pH 5.6 (succinate buffer) and 9 (borate buffer) and $[\text{Ca}^{+2}]_{\text{total}}$ (0, 0.1, $10 \mu\text{M}$)	129

Figure 4.7. Speciation of dissolved tetracycline (TC) as a function of pH in the presence of 2×10^{-4} M Ca^{2+} at $I = 0.01$ M and a total tetracycline concentration of 10^{-4} M..... **130**

LIST OF TABLES

Chapter 2. Transformation of Amino Acids by Peroxymonosulfate

Table 2.1. Second-order reaction rate constants (k') for the oxidation of selected amino acids by HSO_5^- , order of reaction with respect to HSO_5^- and activation energy (E_a). **29**

Table 2.2. Mass changes observed by LC-MS/MS and possible products of oxidation by HSO_5^- **30**

Chapter 2S. Supporting Information for: Transformation of Amino Acids by Peroxymonosulfate

Table 2S.1. Pseudo-first-order rate constants of amino acid oxidation by HSO_5^- **40**

Table 2S.2. HPLC mobile phases and gradients **41**

Table 2S.3. MRM parameters for amino acids and product standards **42**

Table 2S.4. Retention times of standards and observed products of oxidation **43**

Chapter 3. Transformation of Amino Acids by Cobalt-activated Peroxymonosulfate

Table 3.1. Reaction rate constants of ethanol and *tert*-butyl alcohol with sulfate, hydroxyl, and peroxymonosulfate reactions **79**

Table 3.2. Products of amino acid oxidation by $\text{HSO}_5^- + \text{Co}^{2+}$ **80**

Chapter 3S. Supporting Information for: Transformation of Amino Acids by Cobalt-Activated Peroxymonosulfate

Table 3S.1. Observed rate constants of amino acid transformation by $\text{HSO}_5^- + \text{Co}^{2+}$ **88**

Table 3S.2. Agilent 1050 HPLC mobile phases and gradients **89**

Table 3S.3. Agilent 1260 HPLC separation conditions	90
Table 3S.4. MRM parameters for amino acids and product standards	91
Table 3S.5. Stability constant of amino acid complexes with cobalt (II)	92
Table 3S.6. Reaction rates of some radical species.....	93
Table 3S.7. Retention times of standards and observed products of oxidation	95
Table 3S.8. Observed rate constants of amino acid transformation by $\text{HSO}_5^- + \text{Co}^{2+}$ in the presence of radical scavengers and HSO_5^- activated with CoSO_4	96

Chapter 4. Sorption of Clarithromycin and Tetracycline to Natural Organic Matter in the Presence of Calcium

Table 4.1. Freundlich parameters for tetracycline and clarithromycin sorption to dissolved Elliott soil humic acid.	122
---	------------

Chapter 1. General Introduction

Contaminants of emerging concern is a broad term for chemicals and microbes that either were previously not of concern, are not commonly monitored, or have just recently been discovered. Changes in perspective have come about partially due to newer instrumentation and better detection methods, increased understanding of low levels of toxicity, and changes in the disposal of contaminants into the environment. Chemicals might be newly synthesized and their impact, and toxicity is unknown or have been known for some time but available methods of detection were not viable for environmental samples. There are varied sources of these contaminants including microbial communities, the industrial, pharmaceutical and veterinary sectors, as well as common household items. There are different questions that must be answered about emerging contaminants, including their toxicological impact, fate and transport, transformation they undergo in the environment and what method effectively remove them. In my work I focused on two classes of emerging contaminants: proteinaceous/peptidic contaminants and antibiotics.

Proteinaceous materials (e.g., peptides and proteins) represent a class of emerging contaminants. Some examples are bacterial exotoxins, cyanotoxins, and proteins such as ricin and prions. The number of cyanotoxins is extensive, a water drinking limit has been established for at least one toxin, microcystin-LR.¹ Prion proteins can be released into the environment by infected animals and remain infectious once bound to soil particles.² A need exists to develop methods to detect and quantify these proteinaceous contaminants in the environment and to inactivate them. My study focused on the latter, current methods of inactivation of protein contaminants are not suited to *in situ* environmental (e.g., dry heating, autoclaving). In my work

I studied the oxidation of the free proteogenic amino acids (excluding cysteine) by peroxymonosulfate, since they are the building blocks of proteins and therefore a commonality shared between the proteogenic contaminants. Peroxymonosulfate is a strong oxidant by itself and can also be activated by transition metals to form radical species.³ I studied oxidation of amino acids by both peroxymonosulfate by itself and activated cobalt to generate sulfate radicals. I found both methods to be effective in the transformation of amino acids at different rates.

Polar organic contaminants represent another class of emerging contaminants. The sorption of ionic organic contaminants to natural organic matter is less well understood than that of non-polar contaminants. This is in part by the past focus on non-polar contaminants and the inherent complexity of ionic molecules. Sorption of polar-organics to natural organic matter will be driven in part by physical, chemical, and electrostatic interaction. Sorption of polar and ionizable compounds depends at various degrees on moisture content in sorbing system, the presence of exchangeable cations, ionic strength and pH. If such is the case, the ratio of different charged state of the molecule will change with changes in pH. Ionization state of polar-organic is going to change.⁴ I studied the sorption of two antibiotics, clarithromycin and tetracycline, to Elliott soil humic acid. The antibiotics selected have different speciation profiles, clarithromycin exists as a cation $\text{pH} < \text{p}K_{\text{a}}$, with a macroscopic $\text{p}K_{\text{a}} = 8.9$,⁵ whereas tetracycline is present as a cation at $\text{pH} < \text{p}K_{\text{a}1}$, a zwitterion at $\text{p}K_{\text{a}1} < \text{pH} < \text{p}K_{\text{a}2}$, a net monoanion exhibiting one positive and two negative charges at $\text{p}K_{\text{a}2} < \text{pH} < \text{p}K_{\text{a}3}$, and a dianion at $\text{pH} > \text{p}K_{\text{a}3}$ ($\text{p}K_{\text{a}} = 3.30, 7.68, 9.96$).⁶ The effect of ionic strength, pH, and competing cations was studied, and was found to differ between the two antibiotics.

REFERENCES

- (1) WHO. *Cyanobacterial Toxins: Microcystin-LR. In: Guidelines for Drinking-Water Quality, Addendum to Volume 2*; Geneva, 1998.
- (2) Johnson, C. J.; Pedersen, J. a; Chappell, R. J.; McKenzie, D.; Aiken, J. M. Oral Transmissibility of Prion Disease Is Enhanced by Binding to Soil Particles. *PLoS Pathog.* **2007**, *3*, e93.
- (3) Anipsitakis, G. P.; Dionysiou, D. D. Radical Generation by the Interaction of Transition Metals with Common Oxidants. *Environ. Sci. Technol.* **2004**, *38*, 3705–3712.
- (4) Delle Site, A. Factors Affecting Sorption of Organic Compounds in Natural Sorbent/water Systems and Sorption Coefficients for Selected Pollutants. A Review. *J. Phys. Chem. Ref. Data* **2001**, *30*, 187–439.
- (5) Nakagawa, Y.; Itai, S.; Yoshida, T.; Nagai, T. Physicochemical Properties and Stability in the Acidic Solution of a New Macrolide Antibiotic, Clarithromycin, in Comparison with Erythromycin. *Chem. Pharm. Bull. (Tokyo)*. **1992**, *40*, 725–728.
- (6) Mitscher, L. A. *The Chemistry of the Tetracycline Antibiotics.*; New York, 1978.

Chapter 2. Transformation of Amino Acids by Peroxymonosulfate

This chapter is part of a manuscript is going to be submitted with the following co-author:

Joel A. Pedersen

Environmental Chemistry and Technology Program, University of Wisconsin, Madison, WI
53706, USA

ABSTRACT. A variety of peptidic and proteinaceous contaminants (e.g., proteins, toxins, biological agents) present in the environment may pose risk human health and wildlife. Deactivation methods for these contaminants used in laboratory and industrial settings (e.g., autoclaving, dry heating) are not necessarily applicable to *in situ* environmental remediation. Peroxymonosulfate is a strong oxidant (HSO_5^- , $E_H^0 = 1.82 \text{ V}$) reactive towards a variety of organic moieties (e.g., sulfides, amines, alkenes) and could potentially be used for the deactivation of proteinaceous contaminants. Relatively little quantitative rate information exists on the reaction of peroxymonosulfate with free amino acids. Here we studied the kinetics and products of 19 of the 20 standard proteinogenic amino acids (all except cysteine) oxidation by peroxymonosulfate. The rates of amino acid oxidation by peroxymonosulfate transformation decrease in the order methionine > tryptophan > tyrosine > histidine > alanine for the amino acids studied. Amino acids that possess sulfur-containing, heteroaromatic or substituted aromatic side chains acids were the most susceptible to peroxymonosulfate oxidation as have been observed with reactive oxygen species. Methionine sulfoxide and sulfone were confirmed as products of oxidation by LC-MS/MS. The rate of oxidation of tryptophan did not decrease in the presence of natural organic matter (Suwannee River NOM isolate). Our results demonstrate that unactivated peroxymonosulfate is capable of oxidizing 19 amino acids at various rates with methionine and tryptophan being liable targets of oxidation in peptides and proteins.

INTRODUCTION

A variety of naturally occurring toxins and potential biological warfare agents are peptidic or proteinaceous in nature. These include some classes of cyanotoxins (e.g., microcystins, nodularins), bacterial exotoxins (e.g., tetanus toxin, diphtheria toxin, botulinum toxin, *Staphylococcus* enterotoxin type B), and the protein ricin. Proteinaceous toxins can be

present in the environment (e.g., water, soil, sediments), sources include microbes, shedding and excretion by infected animals, and deliberate dissemination of toxins in the case of potential biological warfare agents. Cyanobacteria, found in freshwaters, pose a human health risk due to the release of cyanotoxins (e.g., microcystins, nodularins). Microcystins are nonribosomal, cyclic heptapeptides composed of two variable L-amino acids, three common D-amino acids or their derivatives, and two novel D-amino acids. Of the >50 different congeners discovered to date, microcystin-LR has received the most study and is found in lakes and drinking water.^{1,2} The World Health Organization has set a provisional drinking water guideline of 1 $\mu\text{g}\cdot\text{L}^{-1}$ for microcystin-LR.³ Although the U.S. Environmental Protection Agency (EPA) does not have regulations for cyanotoxins, it does have Health Advisories recommendations for microcystins (represented by microcystin-LR) levels of exposures of no more than 0.3 $\mu\text{g}\cdot\text{L}^{-1}$ and of 1.6 $\mu\text{g}\cdot\text{L}^{-1}$ for children younger than six and adults respectively.⁴ Ricin is a toxic carbohydrate-binding (lectin) protein produced by the castor oil plant (*Ricinus communis*). The enterotoxins botulinum toxin and *Staphylococcus* enterotoxin type B are produced by *Clostridium botulinum* and *Staphylococcus aureus* respectively, and cause food poisoning. Botulinum toxin, *Staphylococcus* enterotoxin type B, and ricin could be used as biological agents,⁵ they are stable at ambient conditions and can be inactivated by exposure to dry heat > 100 °C for 10 min.⁶ We note that *Staphylococcus* enterotoxin type B can be reactivated after heating due to refolding of the protein.⁶ Chemical inactivation in laboratory settings can be achieved by exposure to sodium hypochlorite for 30 min at various concentrations: ricin (> 1.0%), botulinum toxin (>0.1%), *Staphylococcus* enterotoxin type B (> 0.5%), and microcystin ($\geq 0.5\%$).⁶

In addition to toxins, pathogens may be composed of proteins (prions)⁷ or encapsulated by them (viruses). Prions are notoriously difficult to inactivate,⁸ being resistant to sterilization

methods that are effective against conventional pathogens. Treatments effective in reducing prion infectivity (defined as $< 3\log_{10}$ reduction in 18 min to 3 h) include autoclaving at 121-132 °C for 1 h (gravity displacement sterilizer) or 121 °C for 30 min (prevacuum sterilizer) and exposure to sodium hydroxide (NaOH), 0.09 N or 0.9 N, for 2 h followed by autoclaving at 121 °C for 1 h (gravity displacement sterilizer).⁹ The aforementioned treatments, especially dry heating and autoclaving, cannot be readily applied in environmental settings, prompting the search for alternative inactivation methods.

Advanced oxidation processes (AOPs) are defined as processes that generate strong chemical oxidants (e.g., hydroxyl radical, sulfate radical) to oxidize organic pollutants. Peroxymonosulfate (HSO_5^-) holds promise as an oxidant for treating wastewater and contaminated soils.¹⁰ Peroxymonosulfate has two ionization constants ($pK_{a1} < 1$, $pK_{a2} = 9.4$); and decomposes at alkaline pH values $\geq pK_{a2}$ (≈ 8).¹¹ The oxidation of S(IV) by HSO_5^- proceeds at a similar rate and yields the same product as oxidation by H_2O_2 .¹² Like hydrogen peroxide and persulfate, peroxymonosulfate contains a peroxide bond but in the case of peroxymonosulfate this bond is asymmetrical and so can be considered a monosubstituted peroxide. Most prior studies have focused on the production of sulfate radical from peroxymonosulfate,^{13–22} but HSO_5^- itself can oxidize organic molecules. Peroxymonosulfate has a standard reduction potential of 1.82 V ($\text{HSO}_5^- + 2\text{H}^+ + 2\text{e}^- \rightarrow \text{HSO}_5^- + \text{H}_2\text{O}$),²³ comparable to that of hydrogen peroxide (1.8 V; $\text{H}_2\text{O}_2 + 2\text{H}^+ + 2\text{e}^- \rightarrow 2\text{H}_2\text{O}$).²⁴ Peroxymonosulfate is capable of oxidizing acetals to esters,²⁵ aldehydes to carboxylates,²⁶ sulfides to sulfoxides and sulfones,²⁷ and phosphines to phosphine oxides.²⁸ Oxidation of phenol to benzene-1,4-diol and cyclohexanone to ϵ -caprolactone has been reported.²⁹ Peroxymonosulfate has been used to delignify wood in the

paper making process and as a pool shock treatment to reduce the concentrations of organic molecules in water and thereby decrease chlorine demand.³⁰⁻³²

In the present study, we focus on the oxidation of proteinogenic amino acids because they represent the building blocks of proteins. Understanding the oxidation of amino acids is a prerequisite for elucidating the pathways of protein transformation by HSO_5^- . The transformation of several aliphatic amino acids by peroxymonosulfate has been reported: glycine, alanine, leucine, valine, serine, and threonine at 30-45 °C and $\text{pH} \leq 5.2$. These studies reported rate constants determined by following the concentration of HSO_5^- and not the amino acid; the products of reaction were determined by a spot test and found to be aldehydes in all cases.^{33,34,35} Oxidation of methionine- and tryptophan-containing peptides by HSO_5^- has also been studied, but rate constants were not determined.³⁶ In the case of methionine the product of oxidation was found to be methionine sulfone; no transformation product was reported for Trp.³⁶ Studies of amino acid transformation by other oxidants (e.g., hydroxyl radical, ozone, singlet oxygen) consistently show the highest rates of oxidation for sulfur-containing and aromatic amino acids. The kinetics of HSO_5^- reaction with these amino acids has not been studied. Systematic investigation of the reactivity of HSO_5^- towards individual amino acids is therefore needed.

The objectives of this study were to systematically investigate the kinetics of proteinogenic amino acid oxidation by HSO_5^- , and to identify the products of oxidation of the most rapidly reacting amino acids. Kinetic studies were conducted to determine initial rates of reaction of 19 of 20 standard proteinogenic amino acids (all except cysteine) under controlled conditions (pH, temperature) in batch and quench-flow reactors. Product identification was achieved by liquid chromatography with tandem mass spectrometry.

MATERIALS AND METHODS

Chemicals. Peroxymonosulfate (Oxone®), valine (Val, 99%), and methionine sulfoxide (99.7%) were purchased from Alfa Aesar. Arginine (Arg, 99%) and asparagine (Asn, >99%) were purchased from TCI. Phenylalanine (Phe, $\geq 99\%$), formic acid ($\sim 98\%$), and niacin (USP grade) were obtained from Fluka. Alanine (Ala, 99%), aspartic acid (Asp, >99%), glutamic acid (Glu, $\geq 99.5\%$), glycine (Gly 99%), histidine (His, >99%), leucine (Leu, 98%), lysine (Lys, $\geq 98\%$), methionine (Met, $\geq 98\%$), serine (Ser, $\geq 99\%$), threonine (Thr, $\geq 98\%$), tryptophan (Trp, $\geq 98\%$), quinolinic acid (99%), melatonin (>98%), 5-hydroxytryptophan (98%), and methionine sulfone ($\geq 98\%$) were procured from Sigma-Aldrich. Tyrosine (Tyr, >99%), sodium thiosulfate pentahydrate (ACS grade), Na_2HPO_4 (ACS grade), NaH_2PO_4 (>99%), and dry acetonitrile were from Acrōs Organics. Isoleucine (Ile) and proline (Pro) were acquired from MPBiomedicals. Sodium acetate trihydrate (ACS grade), HCl (ACS grade), di(*N*-succinimidyl) carbonate (DCS, 98%), and 6-aminoquinoline (AQM, 98%) were procured from Fisher.

Suwannee River Natural Organic Matter (SRNOM) isolate (1R101N) was obtained from the International Humic Substances Society (IHSS). We prepared the SRNOM stock solution ($40 \text{ mg}_{\text{OC}} \cdot \text{L}^{-1}$) was prepared as follows. The isolate was dissolved in ultrapure water with pH adjusted to 10 with NaOH, and the solution was stirred for 24 h in the dark, filtered ($0.22 \mu\text{m}$ Millex PES filter), and stored in amber glass dark at 4°C .

Synthesis of the derivatization reagent. To allow fluorometric determination of amino acid concentrations, we synthesized the derivatizing reagent 6-aminoquinolyl-*N*-hydroxysuccinimidyl carbamate (AQC) as described previously.^{37,38} Briefly, DCS (12 mM) was dissolved in dry acetonitrile and heated under reflux. A solution of AQM (10 mM) in dry acetonitrile was added dropwise over 30 min. The reaction was allowed to reflux for an

additional 30 min. The solution was concentrated to half its volume and cooled for 24 h. The resulting crystals were washed with dry acetonitrile.

Kinetic experiments: Batch reactors. For all amino acids except methionine (*vide infra*), kinetic experiments were conducted in amber borosilicate glass bottles under continuous stirring on a magnetic stir plate. The initial amino acid and HSO_5^- concentrations in these reactions were 0.45 mM and 4.5 mM, respectively, in 0.1 M phosphate buffer (pH 7) at room temperature (25 °C) unless otherwise noted. Reactions were conducted at $\text{pH} < 9$ because at higher pH values HSO_5^- dissociates to SO_5^{2-} and decomposes.¹¹ The concentration of HSO_5^- exceeded that of the amino acids by a factor of 10 to maintain pseudo-first order reaction conditions. Reactions were initiated by adding HSO_5^- to the amino acid solution. Aliquots were withdrawn as a function of time and quenched with equal volume of 1 M thiosulfate.¹⁴ The order of reaction with respect to HSO_5^- , of selected reactions, was obtained via the method of initial rates. Activation energies for the transformation of Trp, Tyr, and His by HSO_5^- were calculated from reaction rate constants obtained over a range of temperatures (20-30 °C) using the linearized Arrhenius equation. No reactions were conducted at high temperatures because HSO_5^- can be decompose to produce sulfate radical at elevated temperatures (> 70 °C).³⁹

Kinetic experiments: Quench-flow reactor. The kinetics for methionine transformation by HSO_5^- was too rapid to monitor using batch reactors. We therefore employed a quench-flow system (System 1000, Update Instruments) to study the rates of methionine transformation at room temperature. The experimental set-up consisted of two syringes (one filled with the amino acid solution, the other with the HSO_5^- solution), a grid mixer, and a reactor line. Solvent lines from the syringes meet at the grid mixer, the reaction takes place in the reactor line, and the sample is collected in equal volume of thiosulfate (1 M) to quench the reaction. The length of the

reactor line (nylon 6/6) was selected to achieve the desired reaction time. A ram controller allowed selection of syringe displacement and displacement velocities. The grid mixer causes high turbulence to ensure complete mixing of the syringe components.

High performance liquid chromatography with fluorescence detection (HPLC-FD).

Amino acid concentrations were determined by HPLC-FD. Tryptophan and tyrosine are intrinsically fluorescent and were analyzed directly. The remaining amino acids required derivatization prior to fluorescence detection. Amino acids were derivatized using AQC as previously described.^{37,38} Briefly, an aliquot (50 μ L) of an amino acid sample was added to borate buffer (0.1 M, pH 9) followed by addition of 25 μ L of AQC (2 g·L⁻¹), immediately after which the reaction mixture was vortexed (5 s). Fresh AQC solutions were prepared weekly and stored at 4 °C.

Quantification of amino acids was performed on an Agilent 1050 HPLC equipped with a fluorescent detector (Agilent 1110). The mobile phases were 15.6 mM acetate buffer (pH 5) and 60% acetonitrile in H₂O for all amino acids with the exception of Asp and Glu for which 0.1% formic acid in H₂O and 60% acetonitrile in H₂O were used as the mobile phases. Samples were separated (see SI) in an AccQ·Tag Waters column (C18, 3.9 \times 150 mm, 4 μ m, 60 Å, Wat052885) equipped with a Nova-Pak® (C-18, 3.9 \times 200 mm, 4 μ m, 60 Å, Wat044380). Excitation and emission wavelengths were $\lambda_{\text{ex/em}} = 280/350$ nm for Trp, $\lambda_{\text{ex/em}} = 229/310$ nm for Tyr, and $\lambda_{\text{ex/em}} = 245/395$ nm for the AQC-derivatized amino acids.

Liquid chromatography-tandem mass spectrometry. Product identification was performed on an Agilent 6460 triple quadrupole LC-MS with an electrospray ionization source. The mobile phases were 10 mM pH 7.5 ammonium acetate buffer with 10% acetonitrile and acetonitrile. Products were separated (gradient elution, see SI for details) with the column used

for HPLC-fluorescence detection described above. To prevent inorganic salts from reaching the detector, the eluate was diverted to waste from (0-4.5 and 29-30 min), and data were recorded from 4.5-29 min. The source parameters were: gas temperature 300 °C, gas flow 7 L·min⁻¹, nebulizer 45 psi, sheath gas temperature 350 °C, sheath gas flow 10 L·min⁻¹, capillary voltage 3500 V, nozzle voltage 500 V.

Initially a full scan (MS2 mode) in the range of 100-800 *m/z* was performed, and new peaks appearing in the reaction mixtures were recorded. Standards of potential transformation products of amino acids with similar mass were acquired when available. Samples and standards were then analyzed in the multiple reaction monitoring (MRM) mode and the fragmentation pattern were compared (see the Supporting Information).

RESULTS AND DISCUSSION

All amino acids investigated were transformed by HSO₅⁻. Figure 2.1 shows the transformation of the most rapidly reacting amino acids as a function of time. Reactivity declined in the order Met > Trp > Tyr > His > Ala. We determined pseudo first-order reaction rate constants for the transformation of 19 of the 20 common proteinogenic amino acids by HSO₅⁻. These are displayed in Figure 2.2 and tabulated in Table 2S.1. The amino acids were stable under the reaction conditions in the absence of HSO₅⁻ (see the Supporting Information). In the absence of amino acids, peroxymonosulfate was stable over the time periods used in our experiments (up to 1 hour) (Figure 2S.1).

The sulfur-containing amino acid Met was transformed the most rapidly with a pseudo first-order rate constant, $k_{\text{obs}} = 17.8 \pm 0.8 \text{ s}^{-1}$ (half-life $t_{1/2} = 3.9 (\pm 0.2) \times 10^{-3} \text{ s}$). Amino acids with substituted aromatic or heterocyclic side chains had k_{obs} ranging from $2.1 (\pm 0.2) \times 10^{-3} \text{ s}^{-1}$

to $1.5 (\pm 0.1) \times 10^{-4} \text{ s}^{-1}$ (half-lives ranging from $3.3 (\pm 0.3) \times 10^2 \text{ s}$ to $4.6 (\pm 0.3) \times 10^3 \text{ s}$). Sulfur-containing and aromatic amino acids are among the most susceptible to oxidation by ozone⁴⁰ and singlet oxygen.⁴¹ Contrary to expectations based on the reactivity of other oxidants towards amino acids, the aromatic amino acid Phe did not rank among those with highest oxidation rates, while the aliphatic amino acid Ala was the fifth most reactive amino acid. Among the aromatic amino acids Trp, Tyr have resonance electron-donating groups (hydroxyl group, heterocyclic nitrogen atoms), which activate the aromatic ring toward reactions such as hydroxylation; in contrast Phe lacks an electron-donating group. The second-order rate constants for the most rapidly reacting five amino acids ranged from $k' = 3400 \pm 170 \text{ M}^{-1}\cdot\text{s}^{-1}$ (Met) to $0.035 \pm 0.002 \text{ M}^{-1}\cdot\text{s}^{-1}$ (His) at pH 7 (Table 2.1).

Reaction order with respect to HSO_5^- . We determined the reaction order with respect to HSO_5^- for the amino acids with largest rate constants (Met, Trp, Tyr, His, Ala) by the method of initial rates. We determined initial rates of amino acid transformation as a function of HSO_5^- loading (4.5, 6, 9, and 18 mM). Table 2.1 summarizes the order of reaction for Met, Trp, Tyr, and His. Rates of reaction increased with increasing HSO_5^- loading for Met, Trp, Tyr, and His. The order of reaction was 1 for Met, Trp, and His, and 0.62 ± 0.07 for Tyr (Table 2.1).

The effect of pH. Of the amino acids investigated, only His possessed a sidechain with an ionization constant such that the ionization state of the sidechain varies over the pH range typical of environmental systems ($\text{p}K_{\text{a,r}} = 6.0$). At the pH of the experiments described above, both the His cation and the net neutral species were present in appreciable concentrations. We hypothesized that rate of reaction would be affected by pH due to the reactivity of the ionized species. We therefore examined the transformation of His by HSO_5^- at pH 6 and 7. Experiments were not conducted at high pH values where His would be present as only as the neutral species

because peroxymonosulfate is sensitive to pH and starts to decompose at pH values $\gtrsim pK_{a2}$.¹¹ As a control, we examined the transformation kinetics of Trp, an amino acid that does not change speciation over the pH range examined. The rate of His oxidation decreased by an order of magnitude when pH decreased from 7 to 6 (Figure 2.3). At pH 6 the pseudo first-order reaction rate constant for His was $4.1 (\pm 0.3) \times 10^{-5} \text{ s}^{-1}$; at pH 7 it is $1.5 (\pm 0.6) \times 10^{-4} \text{ s}^{-1}$. The difference in reactivity for His is attributed to the charge state of the imidazole ring. At pH 7 the concentration of the base (the fractions present as the base are 0.50 and 0.91 at pH 6 and 7, respectively). Higher rates of reactions were also observed in the oxidation of His residues and free His in the presence of singlet oxygen,^{42,43} and ozone,⁴⁴ as the neutral species became more dominant. Consistent with expectations, the rate of Trp transformation by HSO_5^- did not vary appreciably with pH; pseudo first-order reaction rate constants at pH 6 and 7 were $3.3 (\pm 0.2) \times 10^{-3} \text{ s}^{-1}$ and $2.2 (\pm 0.2) \times 10^{-3} \text{ s}^{-1}$.

Activation energies. We determined the activation energies for the three aromatic amino acids with highest oxidation rates (Trp, Tyr, His). Temperature-controlled reactions (20-35 °C) were conducted in a water bath with overhead stirring. The activation energy was obtained from the linearized Arrhenius equation and decreased in the order of His \approx Tyr > Trp (Table 2.1). No value for the activation energy of Met is reported as we were unable to control temperature in the quench-flow reactor. The values (35 ± 4 to $97 \pm 13 \text{ kJ}\cdot\text{mol}^{-1}$) are at or below the range of the apparent activation energy of other oxidants used in *in situ* chemical oxidation. For example, in the transformation of chlorinated ethenes to dechlorinated products by sulfate radicals produced by heat-activated persulfate, the apparent activation energies were found to range from 101 ± 4 to $144 \pm 5 \text{ kJ}\cdot\text{mol}^{-1}$.⁴⁵

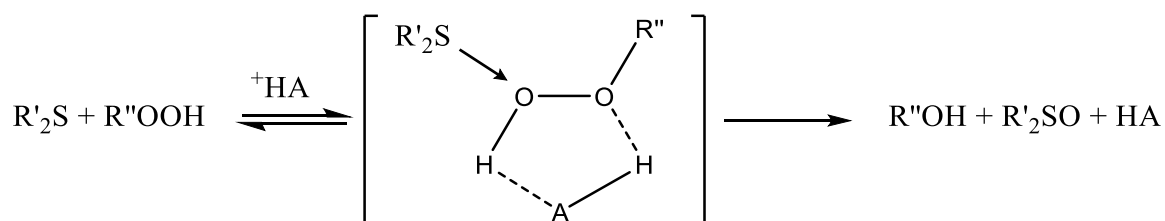
The effect of natural organic matter on Trp transformation by HSO_5^- . Natural organic matter is likely to be present in environments that would be subjected to *in situ* chemical remediation. We therefore studied the transformation of Trp by HSO_5^- in the presence of SRNOM. We hypothesized that the presence of natural organic matter would decrease the observed reaction rate by serving as a sink for HSO_5^- (Figure 2.5). We selected Trp for this experiment because it was the second fastest reacting amino acid and can be detected directly by fluorescence. We employed Suwannee River NOM isolate because it is a well-characterized unfractionated reference aquatic natural organic matter.⁴⁶ We found that HSO_5^- transformed Trp in the presence of $5 \text{ mg}_{\text{OC}}\cdot\text{L}^{-1}$ SRNOM. Inclusion of SRNOM did not affect the kinetics of Trp transformation by HSO_5^- ($p > 0.05$). The reported impact of NOM on *in situ* chemical oxidation methods varies; different effects have been observed for permanganate, persulfate and Fenton's reagent.²⁴ In the case of peroxymonosulfate, the presence of transition metals in the NOM sample could activate HSO_5^- to produce radical species (e.g., $\text{SO}_4^{\cdot-}$, $\cdot\text{OH}$),⁴⁷ thereby increasing degradation efficiency while at the same time the NOM acts as a sink for radicals.^{48,49}

We determined the concentrations of metals in SRNOM by ICP-OES (see SI). Iron, which can activate HSO_5^- to form sulfate radical (Fe(II,III)),⁴⁷ was found in a concentration equivalent to $0.13 \pm 0.01 \text{ }\mu\text{M}$ in the reaction matrix. To test the hypothesis that radical species contributed to the transformation of Trp in reactions conducted in the presence of SRNOM, we added ethanol to scavenge sulfate and hydroxyl radicals. The observed reaction rate constants decreased from $1.71 (\pm 0.04) \times 10^{-3} \text{ s}^{-1}$ in the absence to $8.4 (\pm 0.4) \times 10^{-4} \text{ s}^{-1}$ in the presence of ethanol confirming the contribution of sulfate or hydroxyl radicals to the reaction. We therefore conclude that the equal overall rates of Trp transformation in the absence and presence of

SRNOM were due to the production of radicals and consumption of reactants by SRNOM in the latter.

Transformation products. We first examined our HPLC-FD chromatograms for evidence of amino acid transformation products. Products of oxidation with primary or secondary amines can be derivatized by AQC.³⁷ Only AQC derivatives or products of oxidation with intrinsic fluorescence at $\lambda_{\text{ex/em}} = 245/395$ nm present at sufficiently high concentrations would have been detected with the instrumental setting used. The only transformation product detected by HPLC-FD was in the Met reaction product mixture, eluting earlier than the parent compound and observed starting at the earliest time point (12 ms). This product had the same retention time as the AQC derivative of methionine sulfoxide (Met-Ox).

We next examined product mixtures from the reaction of Met with HSO_5^- by LC-MS/MS to confirm the presence of Met-Ox and to identify further products of Met transformation. Mass changes observed by LC-MS/MS are summarized in Table 2.2. The formation of Met-Ox was further confirmed by LC-MS/MS using MRM scan. The sample peaks had the same retention time as the standards and the same fragmentation pattern. Mass changes of +16 and +32 m/z corresponding to addition of oxygen were observed for Met corresponding to the products Met-Ox and methionine sulfone. The use of authentic standards allowed us to confirm Met-Ox and Met-sulfone as products of oxidation of Met, in agreement with products observed for the oxidation of sulfides with HSO_5^- .²⁷ The oxidation of organic sulfides by peroxides, in the presence of protic solvents, is proposed to occur by a nucleophilic attack by the sulfide to an oxygen molecule in the peroxide, which forms a solvent complex intermediate (Scheme 2.1).⁵⁰



Scheme 1. Oxidation of organic sulfides by peroxide in protic solvents. (R' and R'' denote to the remainder of the molecule attached to the sulfide and the peroxide respectively).

We examined the reaction mixtures of the next three fastest reacting amino acids by LC-MS/MS. The total ion count (TIC) from the Trp reaction mixture contained five of transformation products. One product was 221 *m/z* (Trp + 16 *m/z*) indicative of a hydroxylated product. Hydroxylated Trp products have been observed in the H₂O₂ and hydroxyl radical oxidation of Trp.^{51,52} Peroxymonosulfate is capable of hydroxylating aromatic rings. For example, HSO₅[−] reacts with phenol to form benzene-1,4-diol.²⁹ The retention time and fragmentation pattern of the commercially available standard of 5-hydroxy tryptophan (5-OH-Trp) differed from those of the transformation product (retention time 5.6 and 7 min for 5-OH-Trp and Trp + 16 *m/z* respectively) (Table 2S.4). The dissimilarity in retention time relative to 5-OH-Trp may indicate that the product is not hydroxylated on the aromatic ring. Another possible product with the same mass shift is oxindolylalanine, which is also formed in the reaction of Trp with H₂O₂.⁵¹ Other Trp transformation products had mass shifts of +20, −37, and −81 *m/z*, possible products include hydroxykynurenine, quinolic acid, and niacin respectively. Standards of quinolic acid and niacin had different retention time and fragmentation pattern differed from the observed products. The lower *m/z* products may reflect ring-cleavage products. Although a mass shift (+20 *m/z*) that could correspond to hydroxykynurenine was observed we were unable to obtain an authentic standard to verify this product. Hydroxykynurenine is an oxidation product

of kynurenine (+4 m/z), formed due to the hydrolysis and loss of the carbonyl group of *N*-formylkynurenine (+32 m/z) that in part results from the addition of two oxygen atoms to Trp followed by cleavage of the indole ring.⁵² Mass shifts corresponding to kynurenine (+4 m/z) and *N*-formylkynurenine (+32 m/z) were not present in detectable amounts the reaction mixture for the time point analyzed. The samples analyzed were from the end of the reaction; analysis at earlier timepoints may yield evidence of kynurenine and *N*-formylkynurenine .

For Tyr a mass change of (+48 m/z) was observed, which may reflect addition of three oxygen atoms. The double hydroxylation of Tyr (+32 m/z) has been observed in its reaction with sulfate radical, but so far we have not found evidence in the literature for a triple-hydroxylated Tyr product.⁵³ Dakin products have been observed in the reaction of peroxymonosulfate with electron-rich aromatic rings.²⁶ Tyrosine has an electron-donating hydroxyl group. The Dakin products for Tyr would be 89 and 110 m/z , but these products were not present in our study. Further study on the transformation products of Tyr is required.

Two mass changes were observed for His possibly corresponding to oxo-histidine (+16 m/z) and (+17 m/z). No authentic standards were commercially available for these products. Oxo-histidine is formed in the reaction of His with hydroxyl radical and hydrogen peroxide.^{54,55} In the case of hydroxyl radical, the radical attacks the imidazole ring forming an allyl-type radical that reacts with oxygen leading to the formation of a peroxy radical that can undergo further reactions to form 2-oxohistidine.^{54,56,57} Formation of nitric oxides by peroxymonosulfate occurs indirectly by dimethyloxirane, which is formed by the reaction of HSO_5^- with acetone.⁵⁸ Our reaction mixtures lacked acetone, and we therefore we do not expect the formation of nitric oxide derivatives.

Environmental Implications. Our results indicate that unactivated peroxymonosulfate may be useful for the *in situ* remediation of proteinogenic contaminants. Amino acids with sulfur-containing, substituted aromatic, or heterocyclic side chains react the most rapidly with HSO_5^- . The transformation of cyanotoxin microcystin-LR by peroxymonosulfate at low Co^{2+} concentration ($0.1 \mu\text{g}\cdot\text{L}^{-1}$) at pH 5.8, was found to have an initial pseudo first-order rate constant of $2.59 \times 10^{-4} \text{ s}^{-1}$ (the reaction was followed by 1 h).⁵⁹ The primary oxidant in that study was sulfate radical, the ratio for $\text{HSO}_5^-:\text{Co}^{2+}$ was 5000:1, lower than the optimal ratio 100:1 found for the degradation of 2,4-dichlorophenol.¹⁴ Microcystins are cyclic heptapeptides containing only two proteogenic amino acid residues. In the case of microcystin-LR those are Arg and Leu, which do not rank among those rapidly transformed by unactivated HSO_5^- (the pseudo first-order rate constants for Arg and Leu are $7.6 (\pm 0.9) \times 10^{-5} \text{ s}^{-1}$ and $3.1 (\pm 0.4) \times 10^{-5} \text{ s}^{-1}$, respectively; Table S1). Assuming that the rate of transformation of amino acids in a peptide is the same as the free amino acids then in the absence of Co^{2+} the pseudo first-order rate constant of microcystin-LR should be $1.1 (\pm 0.1) \times 10^{-4} \text{ s}^{-1}$. Common microcystins include (LR (Leu, Arg), RR (Arg Arg), YR (Tyr, Arg) and LA (Leu, Ala)). The results of the present study suggest that HSO_5^- would be able to oxidize the Tyr residue in microcystin-YR.

The transformation of peptidic contaminants could be carried out under ambient conditions (i.e., no extreme temperatures or pH values), and without the use of a metal catalysis (e.g., cobalt).⁴⁷ The concentrations of NOM used in this study ($\text{mg}_{\text{OC}}\cdot\text{L}^{-1}$ SRNOM) did not affect the kinetics of Trp oxidation, but the effect of NOM warrants further study. Transition metals that activate peroxymonosulfate can be present in natural organic matter, as is the case in SRNOM, which leads to the formation of radical species (i.e. hydroxyl radical, sulfate radical).⁴⁷ The use of ethanol, a radical scavenger, allowed us to confirm the activation of HSO_5^- in the

presence of SRNOM. At the same time NOM can act as a radical sink and increasing NOM concentrations decreases the degradation of organic contaminants by hydroxyl radicals.^{48,49} Natural organic matter has the potential to impact contaminant degradation by peroxymonosulfate. Peptidic toxicants and proteins with external Met, Trp, Tyr, His, and Ala residues are expected to be especially amenable to oxidation by HSO_5^- including ricin and prion proteins (Figures S4 and S5). Hydroxyl and sulfate radicals react with amino acids and proteins to form carbon- and nitrogen-centered radicals that can lead to cleavage of the peptide backbone (see reviews by Roeser et al. and Hawkins et al.)^{60,61} Further study with peroxymonosulfate is required to determine if it can cleave the peptide backbone, which can result in protein inactivation.^{62,63} The reaction kinetics of amino acid residues in a protein differ from those of free amino acids in part due to their location in the tertiary structure. This difference in reactivity can be used to determine solvent accessibility.^{53,60} Lundeen et al. quantified the kinetics of photooxidation of some amino acids (Cys, His, Met, Trp, Tyr) by singlet oxygen in an intact protein (glyceraldehyde-3-phosphate dehydrogenase) and found that the rates of oxidation of free amino acid and residues in peptides was faster than in proteins. Solvent-accessible amino acid residues reacted at higher rates than those present in the inside of the protein.⁶⁴ The oxidation of Trp by H_2O_2 decreases in the order of free Trp > short peptides containing Trp > protein (lysozyme).⁵¹ Protein conformation is expected to affect which residues are susceptible to transformation, and residues with higher solvent accessibility are the most prone to transformations.⁶⁴⁻⁶⁷ Therefore, we expect the transformation of amino acid residues in a protein to occur at a slower rate than observed in the reaction between free amino acids and peroxymonosulfate, with the solvent-accessible residues being the least affected.

ACKNOWLEDGEMENTS

This work was funded in part by the United States Geological Survey (G10AC00676). MR was funded by a Graduate Engineering Research Scholars fellowship. We thank Christy Remucal and Megan McConville for use of the LC-MS/MS instrument and helpful discussions, Brian Fox for use of the quench flow reactor, Isabel U. Foreman-Ortiz for laboratory assistance, and Holger Wille for providing us with the prion trimer PDB file.

REFERENCES

- (1) Park, H. D.; Watanabe, M. F.; Harda, K.; Nagai, H.; Suzuki, M.; Watanabe, M.; Hayashi, H. Hepatotoxin (microcystin) and Neurotoxin (anatoxin-A) Contained in Natural Blooms and Strains of Cyanobacteria from Japanese Freshwaters. *Nat. Toxins* **1993**, *1*, 353–360.
- (2) Kotak, B. G.; Zurawell, R. W. Cyanobacterial Toxins in Canadian Freshwaters: A Review. *Lake Reserv. Manag.* **2007**, *23*, 109–122.
- (3) WHO. *Cyanobacterial Toxins: Microcystin-LR. In: Guidelines for Drinking-Water Quality, Addendum to Volume 2*; Geneva, 1998.
- (4) U.S. Environmental Protection Agency. *Recommendations for Public Water Systems to Manage Cyanotoxins in Drinking Water*; 2015.
- (5) Darling, R. G.; Woods, J. B. *USAMRIID's Medical Management of Biological Casualties*; 5th ed.; 2004.
- (6) US Department of Health and Human Services. Appendix I — Guidelines for Work with Toxins of Biological Origin. In *Biosafety in Microbiological and Biomedical Laboratories*; 2009; pp. 385–393.
- (7) Prusiner, S. B. Prions. *Proc. Natl. Acad. Sci. U. S. A.* **1998**, *95*, 13363–13383.
- (8) Taylor, D. M. Inactivation of Transmissible Degenerative Encephalopathy Agents: A Review. *Vet. J.* **2000**, *159*, 10–17.
- (9) Rutala, W. A.; Weber, D. J. Guideline for Disinfection and Sterilization of Prion-Contaminated Medical Instruments. *Infect. Control Hosp. Epidemiol.* **2010**, *31*, 107–117.
- (10) Kotronarou, A.; Hoffmann, M. R. Peroxymonosulfate : An Alternative to Hydrogen Peroxide for the Control of Hydrogen Sulfide. *J. Water Pollut. Control Fed.* **1991**, *63*, 965–970.
- (11) Ball, D. L.; Edwards, J. O. The Kinetics and Mechanism of the Decomposition of Caro's

- Acid. I. *J. Am. Chem. Soc.* **1956**, 78, 1125–1129.
- (12) Betterton, E. A.; Hoffmann, M. R. Oxidation of Aqueous SO₂ by Peroxymonosulfate. *J. Phys. Chem.* **1988**, 92, 5962–5965.
 - (13) Anipsitakis, G. P.; Dionysiou, D. D. Degradation of Organic Contaminants in Water with Sulfate Radicals Generated by the Conjunction of Peroxymonosulfate with Cobalt. *Environ. Sci. Technol.* **2003**, 37, 4790–4797.
 - (14) Anipsitakis, G. P.; Dionysiou, D. D.; Gonzalez, M. A. Cobalt-Mediated Activation of Peroxymonosulfate and Sulfate Radical Attack on Phenolic Compounds. Implications of Chloride Ions. *Environ. Sci. Technol.* **2006**, 40, 1000–1007.
 - (15) Chan, K. H.; Chu, W. Degradation of Atrazine by Cobalt-Mediated Activation of Peroxymonosulfate: Different Cobalt Counteranions in Homogenous Process and Cobalt Oxide Catalysts in Photolytic Heterogeneous Process. *Water Res.* **2009**, 43, 2513–2521.
 - (16) He, X.; de la Cruz, A. a.; Dionysiou, D. D. Destruction of Cyanobacterial Toxin Cylindrospermopsin by Hydroxyl Radicals and Sulfate Radicals Using UV-254nm Activation of Hydrogen Peroxide, Persulfate and Peroxymonosulfate. *J. Photochem. Photobiol. A Chem.* **2013**, 251, 160–166.
 - (17) Zhang, T.; Zhu, H.; Croué, J.-P. Production of Sulfate Radical from Peroxymonosulfate Induced by a Magnetically Separable CuFe₂O₄ Spinel in Water: Efficiency, Stability, and Mechanism. *Environ. Sci. Technol.* **2013**, 47, 2784–2791.
 - (18) Pagano, M.; Volpe, A.; Mascolo, G.; Lopez, A.; Locaputo, V.; Ciannarella, R. Peroxymonosulfate-Co(II) Oxidation System for the Removal of the Non-Ionic Surfactant Brij 35 from Aqueous Solution. *Chemosphere* **2012**, 86, 329–334.
 - (19) Zhu, Y.; Chen, S.; Quan, X.; Zhang, Y. Cobalt Implanted TiO₂ Nanocatalyst for Heterogeneous Activation of Peroxymonosulfate. *RSC Adv.* **2013**, 3, 520.
 - (20) Saputra, E.; Muhammad, S.; Sun, H.; Patel, A.; Shukla, P.; Zhu, Z. H.; Wang, S. α-MnO₂ Activation of Peroxymonosulfate for Catalytic Phenol Degradation in Aqueous Solutions. *Catal. Commun.* **2012**, 26, 144–148.

- (21) Rastogi, A.; Al-Abed, S. R.; Dionysiou, D. D. Sulfate Radical-Based Ferrous–peroxymonosulfate Oxidative System for PCBs Degradation in Aqueous and Sediment Systems. *Appl. Catal. B Environ.* **2009**, *85*, 171–179.
- (22) Do, S.-H.; Jo, J.-H.; Jo, Y.-H.; Lee, H.-K.; Kong, S.-H. Application of a Peroxymonosulfate/cobalt (PMS/Co(II)) System to Treat Diesel-Contaminated Soil. *Chemosphere* **2009**, *77*, 1127–1131.
- (23) Steele, W. V.; Appelman, E. H. The Standard Enthalpy of Formation of Peroxymonosulfate (HSO_5^-) and the Standard Electrode Potential of the Peroxymonosulfate-Bisulfate Couple. *J. Chem. Thermodyn.* **1982**, *14*, 337–344.
- (24) Huling, S. G.; Pivetz, B. E. *In-Situ Chemical Oxidation*; 2006.
- (25) Curini, M.; Epifano, F.; Marcotullio, M. C.; Rosati, O. Oxone[®] : A Convenient Reagent for the Oxidation of Acetals. *Synlett* **1999**, *6*, 777–779.
- (26) Webb, K. S.; Ruzskay, S. J. Oxidation of Aldehydes with Oxone[®] in Aqueous Acetone. *Tetrahedron* **1998**, *54*, 401–410.
- (27) Trost, B. M.; Curran, D. P. Chemoselective Oxidation of Sulfides to Sulfones. *Tetrahedron Lett.* **1981**, *22*, 1287–1290.
- (28) Wozniak, L. A.; Stec, W. J. Oxidation in Organophosphorus Chemistry : Potassium Peroxymonosulphate. *Tetrahedron Lett.* **1999**, *40*, 2637–2640.
- (29) Kennedy, R. J.; Stock, A. M. The Oxidation of Organic Substances by Potassium Peroxymonosulfate. *J. Org. Chem.* **1960**, *25*, 1901–1906.
- (30) Springer, E. L.; McSweeney, J. D. Bleaching Kraft Pulps with Peroxymonosulfate and Oxygen. In *Pulping Conference*; 1993.
- (31) Springer, E. L. Potential Uses for Peroxymonosulfate in Pulping and Bleaching. In *AIChE Forest Products Symposium*; 1992; pp. 113–120.

- (32) Anipsitakis, G. P.; Tufano, T. P.; Dionysiou, D. D. Chemical and Microbial Decontamination of Pool Water Using Activated Potassium Peroxymonosulfate. *Water Res.* **2008**, *42*, 2899–2910.
- (33) Kannan, R. S.; Ramachandran, M. S. Studies on the Autocatalyzed Oxidation of Amino Acids by Peroxomonosulfate. *Int. J. Chem. Kinet.* **2003**, *35*, 475–483.
- (34) Sundar, M.; Easwaramoorthy, D.; Kutti Rani, S.; Palanichamy, M. Mechanistic Investigation of the Oxidation of Lysine by Oxone. *J. Solution Chem.* **2007**, *36*, 1129–1137.
- (35) Ramachandram, M. S.; Vivekanandam, T. S. Kinetics and Mechanism of the Oxidation of Amino Acids by Peroxomonosulphate. Part 1. *J. Chem. Soc. Perkin Trans. 2* **1984**, 1341.
- (36) Ekkati, A. R.; Kodanko, J. J. Targeting Peptides with an Iron-Based Oxidant: Cleavage of the Amino Acid Backbone and Oxidation of Side Chains. *J. Am. Chem. Soc.* **2007**, *129*, 12390–12391.
- (37) Cohen, S. a; Michaud, D. P. Synthesis of a Fluorescent Derivatizing Reagent, 6-Aminoquinolyl-N-Hydroxysuccinimidyl Carbamate, and Its Application for the Analysis of Hydrolysate Amino Acids via High-Performance Liquid Chromatography. *Anal. Biochem.* **1993**, *211*, 279–287.
- (38) Remucal, C. K.; McNeill, K. Photosensitized Amino Acid Degradation in the Presence of Riboflavin and Its Derivatives. *Environ. Sci. Technol.* **2011**, *45*, 5230–5237.
- (39) Yang, S.; Wang, P.; Yang, X.; Shan, L.; Zhang, W.; Shao, X.; Niu, R. Degradation Efficiencies of Azo Dye Acid Orange 7 by the Interaction of Heat, UV and Anions with Common Oxidants: Persulfate, Peroxymonosulfate and Hydrogen Peroxide. *J. Hazard. Mater.* **2010**, *179*, 552–558.
- (40) Kotiaho, T.; Eberlin, M. N.; Vainiotalo, P.; Kostiainen, R. Electrospray Mass and Tandem Mass Spectrometry Identification of Ozone Oxidation Products of Amino Acids and Small Peptides. *J. Am. Soc. Mass Spectrom.* **2000**, *11*, 526–535.

- (41) Boreen, A. L.; Edhlund, B. L.; Cotner, J. B.; McNeill, K. Indirect Photodegradation of Dissolved Free Amino Acids: The Contribution of Singlet Oxygen and the Differential Reactivity of DOM from Various Sources. *Environ. Sci. Technol.* **2008**, *42*, 5492–5498.
- (42) Chu, C.; Lundeen, R. a.; Remucal, C. K.; Sander, M.; McNeill, K. Enhanced Indirect Photochemical Transformation of Histidine and Histamine through Association with Chromophoric Dissolved Organic Matter. *Environ. Sci. Technol.* **2015**, *49*, 5511–5519.
- (43) Murachi, T.; Tsudzuki, T.; Okumura, K. Photosensitized Inactivation of Stem Bromelain. Oxidation of Histidine, Methionine, and Tryptophan Residues. *Biochemistry* **1975**, *14*, 249–255.
- (44) Pryor, W. A.; Giamalva, D. H.; Church, D. F. Kinetics of Ozonation. 2. Amino Acids and Model Compounds in Water and Comparisons to Rates in Nonpolar Solvents. *J. Am. Chem. Soc.* **1984**, *106*, 7094–7100.
- (45) Waldemer, R. H.; Tratnyek, P. G.; Johnson, R. L.; Nurmi, J. T. Oxidation of Chlorinated Ethenes by Heat-Activated Persulfate: Kinetics and Products. *Environ. Sci. Technol.* **2007**, *41*, 1010–1015.
- (46) Averett, R. C.; Leenheer, J. A.; McKnight, D. M.; Thorn, K. A. *Humic Substances in the Suwannee River, Georgia: Interactions, Properties, and Proposed Structures. Paper 2373*; 1994.
- (47) Anipsitakis, G. P.; Dionysiou, D. D. Radical Generation by the Interaction of Transition Metals with Common Oxidants. *Environ. Sci. Technol.* **2004**, *38*, 3705–3712.
- (48) Page, S. E.; Logan, J. R.; Cory, R. M.; McNeill, K. Evidence for Dissolved Organic Matter as the Primary Source and Sink of Photochemically Produced Hydroxyl Radical in Arctic Surface Waters. *Environ. Sci. Process. Impacts* **2014**, *16*, 807–822.
- (49) Lindsey, M. E.; Tarr, M. a. Inhibition of Hydroxyl Radical Reactio with Aromatics by Dissolved Natural Organic Matter. *Environmantal Sci. Technol.* **2000**, *34*, 444–449.
- (50) Dankleff, M. A. P.; Curci, R.; Edwards, J. O.; Pyun, H.-Y. The Influence of Solvent on the Oxidation of Thioxane by Hydrogen Peroxide and by Tert-Butyl Hydroperoxide. *J. Am. Chem. Soc.* **1968**, *90*, 3209–3218.

- (51) Simat, T.; Steinhart, H. Oxidation of Free Tryptophan and Tryptophan Residues in Peptides and Proteins. *J. Agric. Food Chem.* **1998**, *46*, 490–498.
- (52) Finley, E. L.; Dillon, J.; Crouch, R. K.; Schey, K. L. Identification of Tryptophan Oxidation Products in Bovine Alpha-Crystallin. *Protein Sci.* **1998**, *7*, 2391–2397.
- (53) Gau, B. C.; Chen, H.; Zhang, Y.; Gross, M. L. Sulfate Radical Anion as a New Reagent for Fast Photochemical Oxidation of Proteins. *Anal. Chem.* **2010**, *82*, 7821–7827.
- (54) Uchida, K.; Kawakishi, S. 2-Oxo-Histidine as a Novel Biological Marker for Oxidatively Modified Proteins. *FEBS Lett.* **1993**, *332*, 208–210.
- (55) Finnegan, M.; Linley, E.; Denyer, S. P.; McDonnell, G.; Simons, C.; Maillard, J.-Y. Mode of Action of Hydrogen Peroxide and Other Oxidizing Agents: Differences between Liquid and Gas Forms. *J. Antimicrob. Chemother.* **2010**, *65*, 2108–2115.
- (56) Schöneich, C. Mechanisms of Metal-Catalyzed Oxidation of Histidine to 2-Oxo-Histidine in Peptides and Proteins. *J. Pharm. Biomed. Anal.* **2000**, *21*, 1093–1097.
- (57) Lassmann, G.; Eriksson, L. a.; Himo, F.; Lendzian, F.; Lubitz, W. Electronic Structure of a Transient Histidine Radical in Liquid Aqueous Solution: EPR Continuous-Flow Studies and Density Functional Calculations. *J. Phys. Chem. A* **1999**, *103*, 1283–1290.
- (58) Brik, M. E. Oxidation of Secondary Amines to Nitroxides with Oxone in Aqueous Buffered Solution. *Tetrahedron Lett.* **1995**, *36*, 5519–5522.
- (59) Antoniou, M. G.; de la Cruz, A.; Dionysiou, D. D. Degradation of Microcystin-LR Using Sulfate Radicals Generated through Photolysis, Thermolysis and E⁻ Transfer Mechanisms. *Appl. Catal. B Environ.* **2010**, *96*, 290–298.
- (60) Roeser, J.; Bischoff, R.; Bruins, A. P.; Permentier, H. P. Oxidative Protein Labeling in Mass-Spectrometry-Based Proteomics. *Anal. Bioanal. Chem.* **2010**, *397*, 3441–3455.
- (61) Hawkins, C. L.; Davies, M. J. Generation and Propagation of Radical Reactions on

Proteins. *Biochim. Biophys. Acta* **2001**, *1504*, 196–219.

- (62) Attwood, D.; Poust, R. I. Chemical Kinetics and Drug Stability. In *Modern Pharmaceutics, Two Volume Set*; CRC Press, 2009; pp. 203–254.
- (63) Walsh, G. Protein Purification and Characterization. In *Proteins: Biochemistry and Biotechnology*; Wiley-Blackwell, 2014; pp. 91–139.
- (64) Lundeen, R. a.; McNeill, K. Reactivity Differences of Combined and Free Amino Acids: Quantifying the Relationship between Three-Dimensional Protein Structure and Singlet Oxygen Reaction Rates. *Environ. Sci. Technol.* **2013**, *47*, 14215–14223.
- (65) Gau, B. C.; Chen, H.; Zhang, Y.; Gross, M. L. Sulfate Radical Anion as a New Reagent for Fast Photochemical Oxidation of Proteins. *Anal. Chem.* **2010**, *82*, 7821–7827.
- (66) Xu, G.; Chance, M. R. Radiolytic Modification and Reactivity of Amino Acid Residues Serving as Structural Probes for Protein Footprinting. *Anal. Chem.* **2005**, *77*, 4549–4555.
- (67) Roeser, J.; Bischoff, R.; Bruins, A. P.; Permentier, H. P. Oxidative Protein Labeling in Mass-Spectrometry-Based Proteomics. *Anal. Bioanal. Chem.* **2010**, *397*, 3441–3455.

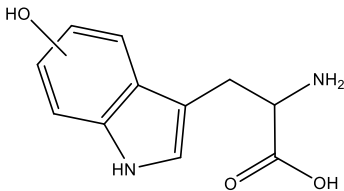
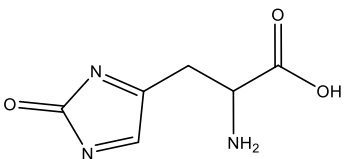
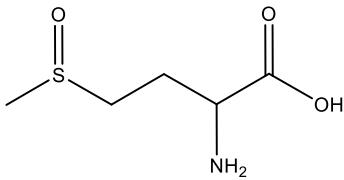
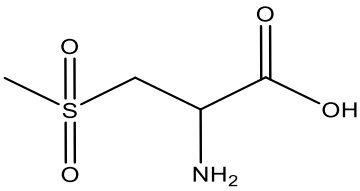
Table 2.1. Second-order reaction rate constants (k') for the oxidation of selected amino acids by HSO_5^- , order of reaction with respect to HSO_5^- , and activation energy (E_a).

Amino Acid	k' ($\text{M}^{-1}\text{s}^{-1}$)	Reaction order with respect to HSO_5^-	E_a ($\text{kJ}\cdot\text{mol}^{-1}$)
Met	3400 ± 170	0.93 ± 0.08	ND
Trp	0.49 ± 0.04	0.96 ± 0.08	35 ± 4
Tyr	0.0092 ± 0.0007	0.62 ± 0.07	81 ± 8
His	0.035 ± 0.002	0.99 ± 0.07	97 ± 13

$R^2 \geq 0.99$ and ≥ 0.96 for the linear regression fit used to calculate k' and reaction order, and the activation energy respectively.

ND, not determined

Table 2.2. Mass changes observed by LC-MS/MS and possible products of oxidation by HSO_5^-

Amino Acid	$\text{M}+\text{H}^+$ (m/z)	Possible products	
		Name	Structure
Trp	221	hydroxy-tryptophan	
His	172	2-oxo-histidine	
Met	166	methionine sulfoxide	
	182	methionine sulfone	

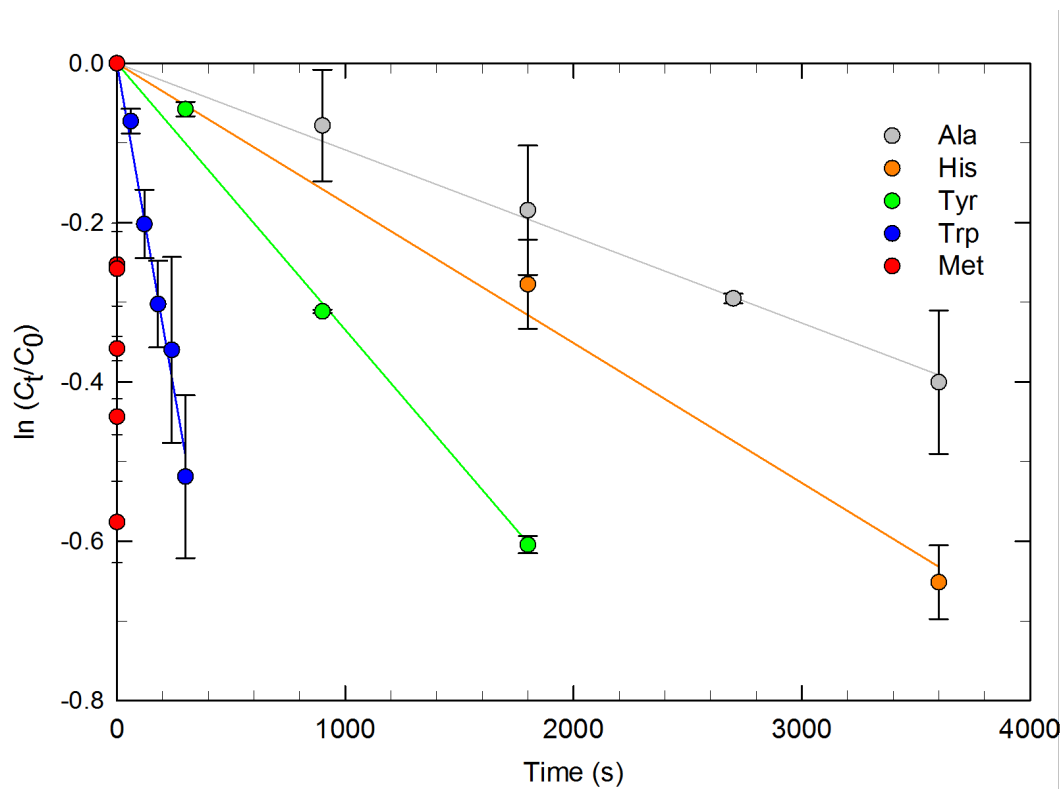
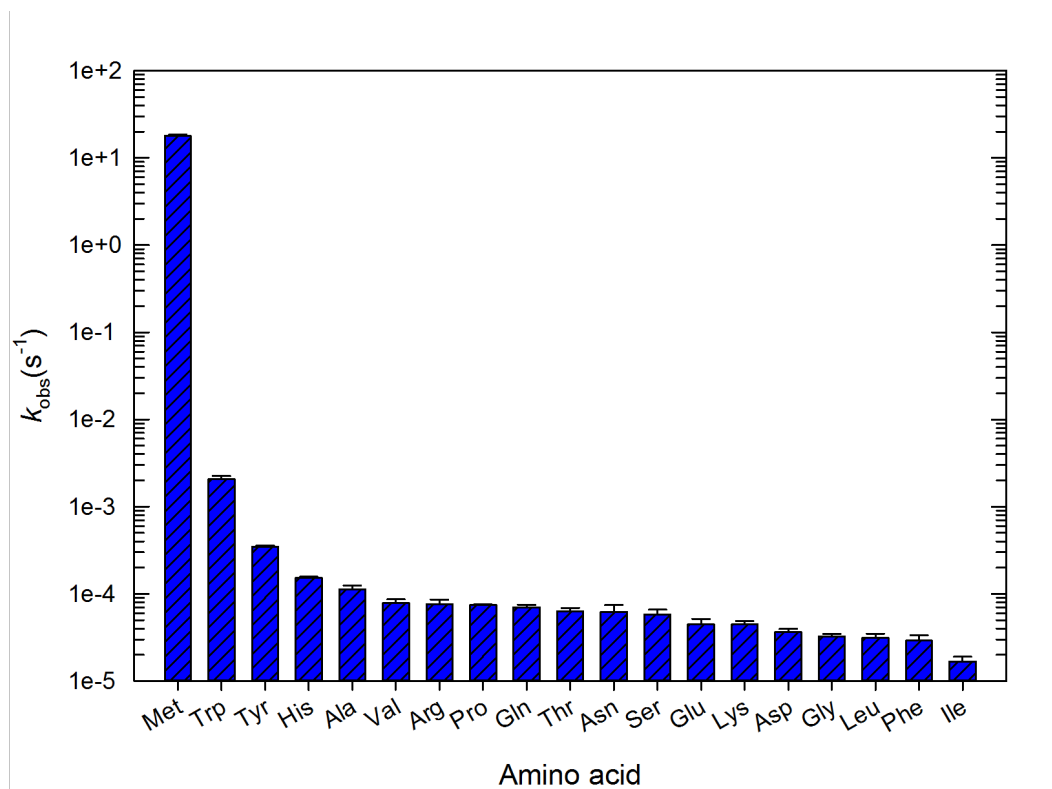


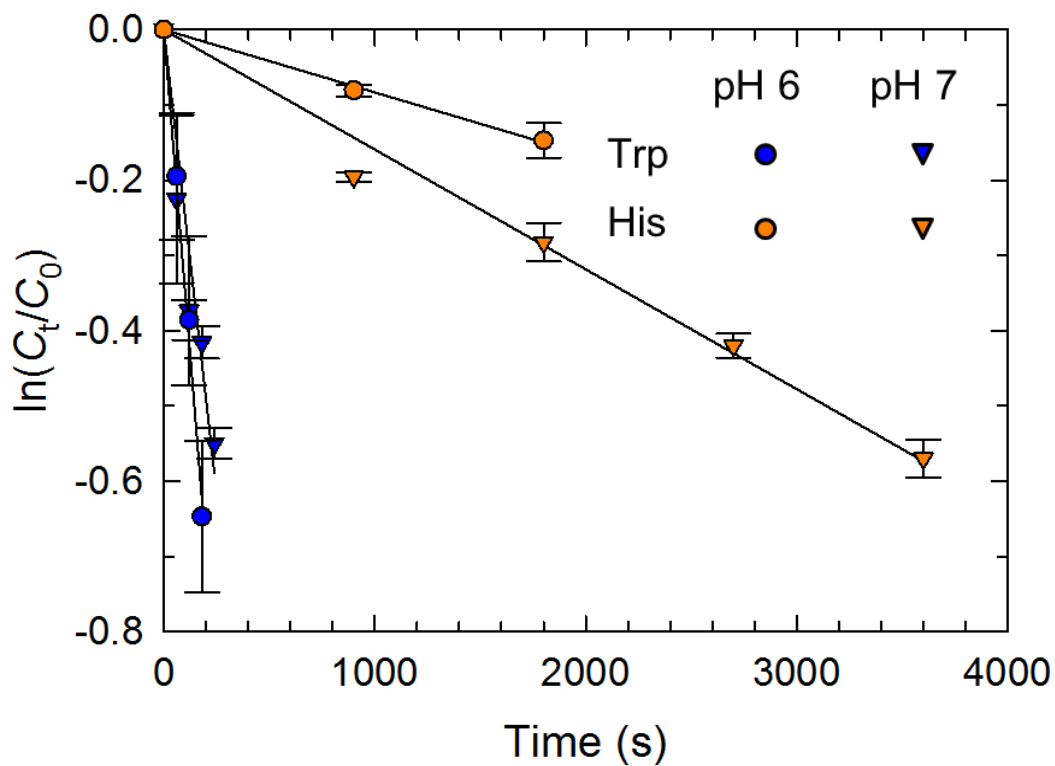
Figure 2.1. Oxidation of selected amino acids by peroxymonosulfate. Experimental conditions: [amino acid]₀ = 0.45 mM, [HSO₅[−]]₀ = 4.5 mM, pH 7 (0.1 M phosphate). Error bars represent one standard deviation ($n = 3$). Pseudo-first-order rate constants are presented in Table 2.1.

6



7

8 **Figure 2.2.** Pseudo-first-order rate constants for the oxidation of selected amino acids by
 9 peroxymonosulfate. Experimental conditions: $[\text{amino acid}]_0 = 0.45 \text{ mM}$, $[\text{HSO}_5^-]_0 = 4.5 \text{ mM}$, pH
 10 7 (0.1 M phosphate). Error bars represent one standard deviation ($n = 3$).



11

12 **Figure 2.3.** Dependence on pH of histidine (His) and tryptophan (Trp) transformation by

13 peroxymonosulfate. Experimental conditions: [amino acid]₀ = 0.45 mM, [HSO₅⁻]₀ = 4.5 mM,

14 phosphate buffer 0.1 M, pH 6 or 7. Error bars represent one standard deviation ($n = 3$).

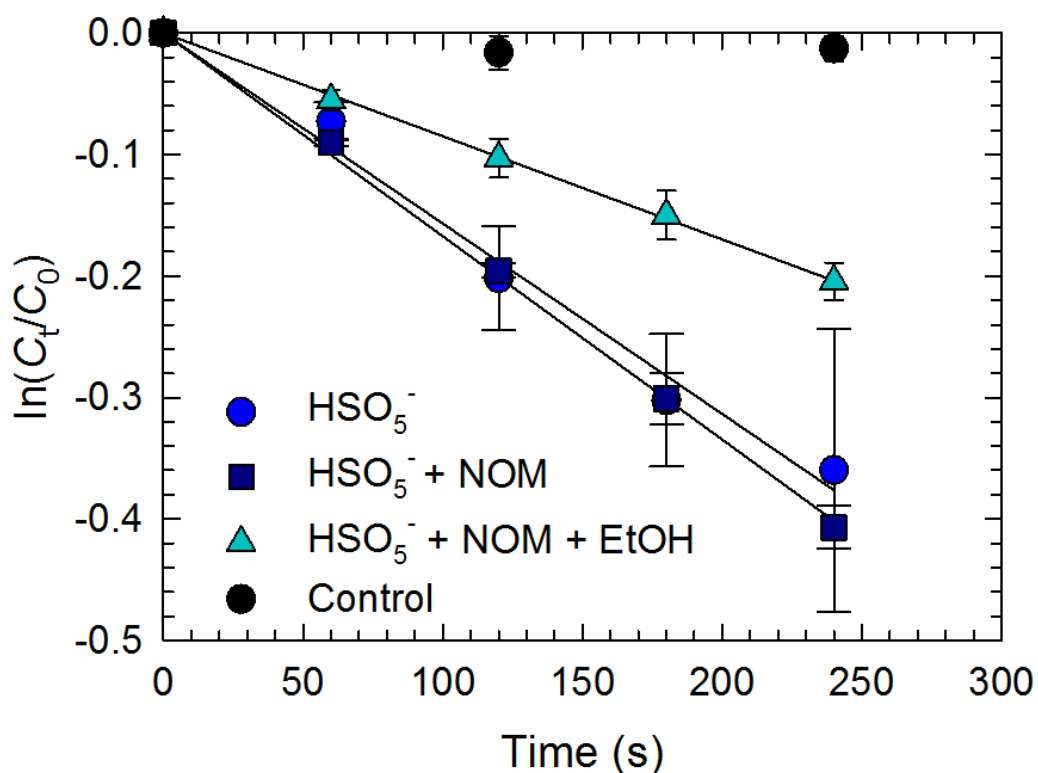


Figure 2.4. Oxidation of tryptophan (Trp) by peroxydisulfate in the presence of natural organic matter and ethanol (EtOH). Experimental conditions: $[\text{Trp}]_0 = 0.45 \text{ mM}$, $[\text{HSO}_5^-]_0 = 4.5 \text{ mM}$, $[\text{NOM}]_0 = 5 \text{ mg}_{\text{OC}} \cdot \text{L}^{-1}$, $[\text{EtOH}] = 4.5 \text{ M}$, 0.1 M phosphate buffer, pH 7. The control was Trp with NOM in the absence of HSO_5^- . Error bars represent one standard deviation ($n = 3$).

**Chapter 2S. Supporting information for: Transformation of Amino Acids by
Peroxymonosulfate**

This chapter is part of a manuscript is going to be submitted with the following co-author:

Joel A. Pedersen

Environmental Chemistry and Technology Program, University of Wisconsin, Madison, WI
53706, USA

Text 2S.1. Materials

Text 2S.2. ICP-OES

Text 2S.3. Amino acid stability

Text 2S.4. Iodometric titration of peroxymonosulfate

Text 2S.5. Effect of ionic salt concentration on the rate of oxidation of alanine

Table 2S.1. Pseudo first-order observed rate constant of amino acid oxidation by HSO_5^-

Table 2S.2. HPLC mobile phases and gradients

Table 2S.3. MRM parameters for amino acids and product standards

Table 2S.4. Retention times of standards and observed products of oxidation

Figure 2S.1. Peroxymonosulfate stability in reaction conditions

Figure 2S.2. Transformation of alanine by peroxymonosulfate as a function of oxidant and salt concentrations

Figure 2S.3. Transformation of tryptophan by peroxymonosulfate as a function of oxidant and salt concentrations

Figure 2S.4. Ricin structure, solvent exposed residues.

Figure 2S.5. Prion-trimer structure, solvent exposed residues.

2S.1. Materials

Potassium sulfate (ACS grade) was obtained from Reagent World. HCl (ACS Plus grade) was obtained from Fisher. ICP-OES metal standards ($1000 \text{ mg} \cdot \text{L}^{-1} \pm 2 \text{ mg} \cdot \text{L}^{-1}$) were from Fluka Analytical.

2S.2 ICP-OES

Sample preparation. A Suwannee River natural organic matter isolate (SRNOM) sample ($40 \text{ mg}_{\text{OC}} \cdot \text{L}^{-1}$) was acidified to pH 2 with HCl (12.1 N) to dissolve metals present in solution. To separate SRNOM from solution the sample was filtered using centrifugal concentrators (30 min, 14000 g, Sartorius Vivacon 500®, 2000 MWCO).

Standards preparation. Two calibration solutions with final concentrations of $0.1 \text{ g} \cdot \text{L}^{-1}$ and $1.0 \text{ g} \cdot \text{L}^{-1}$ were prepared from standard and used for the low and high points of the calibration. In the case of Fe and Mg the bounding concentration used were 0.01 and $0.1 \text{ g} \cdot \text{L}^{-1}$ respectively. Winlab 32 software was used to process raw instrumental data to obtain final concentration values for these metals.

ICP-OES Parameters. Argon was used to generate the plasma ($15 \text{ L} \cdot \text{min}^{-1}$), as the nebulizer gas ($0.6 \text{ L} \cdot \text{min}^{-1}$) and the auxiliary gas ($0.2 \text{ L} \cdot \text{min}^{-1}$), and the instrument was run using an RF Plasma source (1500 W). The sample introduction rate was $1 \text{ mL} \cdot \text{min}^{-1}$, with an axial plasma view to increase sensitivity. Initially the sample was screened for Co, Fe, Mn, Ag, Ni, Ru, and V which are known to activate peroxymonosulfate,¹ and Si, Ala, and Mg that are commonly present in the environment. Of these metals Fe, Mg, and Si were present in the sample at levels above the detection limit, and were quantified with the use of metal standards. The concentrations of Fe, Si, and Mg were 0.8 ± 0.07 , 11.09 ± 0.01 , and $0.16 \pm 0.01 \text{ } \mu\text{m} \cdot \text{mg}_{\text{NOM}}^{-1}$

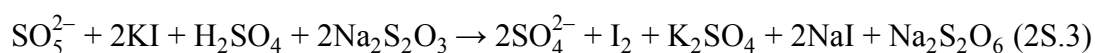
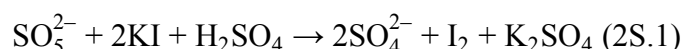
respectively in the SRNOM sample, errors represent the standard deviation of the concentration calculated from three measurements.

2S.3. Amino Acid Stability

The concentrations of amino acid were monitored under the reaction conditions (0.1 M phosphate buffer, pH 7) in the absence of HSO_5^- . At the end of the experiment the concentration of amino acid did not change considerably ($\leq 9\%$) for all the amino acids studied.

2S.4. Determination of Peroxymonosulfate Concentration

Iodimetric titration was used to determine the concentration of HSO_5^- . Briefly, an aliquot (10 mL) of HSO_5^- was added to a flask containing a known amount of potassium iodine and 10 mL of 20 % (v/v) of sulfuric acid, resulting in a yellow solution from the oxidation of iodide to iodine. The iodine is titrated with sodium thiosulfate until the solution turns a pale yellow. Starch is then added, to obtain a more distinct end point, due to the formation of iodine-starch clathrate. The titration is continued until a colorless endpoint is achieved. The titration was carried out in an ice-bath to maintain the temperature $<20^\circ\text{C}$.



2S.5. Effect of Salt Concentration on the Rate of Oxidation of Alanine

The rates of Met, Trp and His transformation were proportional to the concentration of HSO_5^- . The non-integer order of reaction for Tyr suggests a complex reaction mechanism. In the

case of Ala a negative order was obtained. A negative order of reaction could indicate a rapid step preceding the rate-determining step² or the formation of an inhibitory intermediate.³ Further experiments are required to explain this observation.

The rate of reaction of alanine (Ala) decreased with increasing peroxymonosulfate concentration (Figure 2S.2a). Peroxymonosulfate was used as the triple salt $2\text{KHSO}_5 \cdot \text{KHSO}_4 \cdot \text{K}_2\text{SO}_4$. Increasing peroxymonosulfate concentration therefore also increases the ionic strength of the solution. To test the hypothesis that an increase in ionic strength decreased the rate of reaction experiments were performed at different K_2SO_4 concentrations with Ala and tryptophan (Trp). Increasing the salt concentration resulted in a decreased of the rate of reaction of Ala (Figure 2S.2b) but not Trp (Figure 2S.3). Further experiments are required to explain this observation.

Table 2S.1. Pseudo-first-order rate constants of amino acid oxidation by HSO_5^-

Amino acid	$k_{\text{obs}} (\text{s}^{-1})$	R^2
Met	17.8 ± 0.8	0.97
Trp	$2.1 (\pm 0.2) \times 10^3$	0.90
Tyr	$3.45 (\pm 0.1) \times 10^4$	0.99
His	$1.52 (\pm 0.06) \times 10^4$	0.98
Ala	$1.1 (\pm 0.1) \times 10^4$	0.89
Val	$7.8 (\pm 0.8) \times 10^4$	0.89
Arg	$7.6 (\pm 0.9) \times 10^5$	0.82
Pro	$7.4 (\pm 0.2) \times 10^5$	0.99
Gln	$7.0 (\pm 0.5) \times 10^5$	0.95
Thr	$6.3 (\pm 0.6) \times 10^5$	0.91
Ans	$6.0 (\pm 1) \times 10^5$	0.72
Ser	$5.8 (\pm 0.8) \times 10^5$	0.81
Glu	$4.5 (\pm 0.7) \times 10^5$	0.82
Lys	$4.5 (\pm 0.4) \times 10^5$	0.93
Asp	$3.6 (\pm 0.3) \times 10^5$	0.94
Gly	$3.3 (\pm 0.2) \times 10^5$	0.96
Leu	$3.1 (\pm 0.4) \times 10^5$	0.90
Phe	$2.9 (\pm 0.4) \times 10^5$	0.82
Ile	$1.7 (\pm 0.2) \times 10^5$	0.88

Table 2S.2. HPLC mobile phases and gradients

Amino acid	Mobile phase	Gradient
Glu, Asp	A = Formic acid 0.1 % B = 60:40 ACN:H ₂ O	0 min 80% A, 20 min 50 % A, 21 min 50 % A. 21.01 min 80 % A, 28 min 80% A.
Tyr	A = NaAc 15 mM, pH 5 B = ACN	0-0.5 min 90% A, 0.6-2 min 80 % A, 2.01-8 min 65 % A, 8.05-12 min 90 % A.
Trp	A = NaAc 15 mM, pH 5 B = ACN	0-2 min 90% A, 2.01-5 min 75 % A, 5.01-6 min 65 % A, 7.01-8.0 min 90 % A.
Remaining	A = NaAC 15 mM, pH 5 B = 60:40 ACN:H ₂ O	0 min 80% A, 20 min 50 % A, 21 min 50 % A, 21.01 min 80 % , 28 min 80% A.

Abbreviations: ACN, acetonitrile; NaAc, sodium acetate.

Table 2S.3. MRM parameters for amino acids and product standards

Compound Name	Precursor Ion (<i>m/z</i>)	Product Ion (<i>m/z</i>)	Dwell Time (ms)	Fragmentor Voltage (V)	Collision Energy (eV)
Trp-OH	221.1	204.1	75	85	8
Trp-OH	221.1	162.1	75	85	20
Kyn	209.1	146.1	75	90	20
Kyn	209.1	94.1	75	90	12
Kyn	209.1	65.1	75	90	64
Trp	205.2	188.1	75	80	8
Trp	205.2	146.1	75	80	16
Met-sulfone	182	56	75	90	24
Quinolinic acid	168	168	75	130	0
Met-sulfoxide	166	74	75	85	12
Met-sulfoxide	166	56.1	75	85	24
Met	150	104	75	95	8
Met	150	56	75	95	16
Niacin	124	80	75	120	24
Niacin	124	78	75	120	28
Melatonin	233	233	75	100	0
Tyr	182.1	136.1	200	90	12
Tyr	182.1	91.1	200	90	36
His	156.1	110.1	200	90	16
His	156.1	56.2	200	90	40

All samples were analyzed in positive mode with a cell accelerator voltage of 4 V.

Table 2S.4. Retention times of standards and observed products of oxidation

<i>m/z</i>	Standard		Sample
	Standard	Retention time (min)	Retention time (min)
221	5-hydroxy tryptophan	5.6	7
209	Kynurenine	6.8	6.8
205	Trp	8.7	8.7
168	Quinolinic acid	4.7	13
124	Niacin	4.6	9-9.9

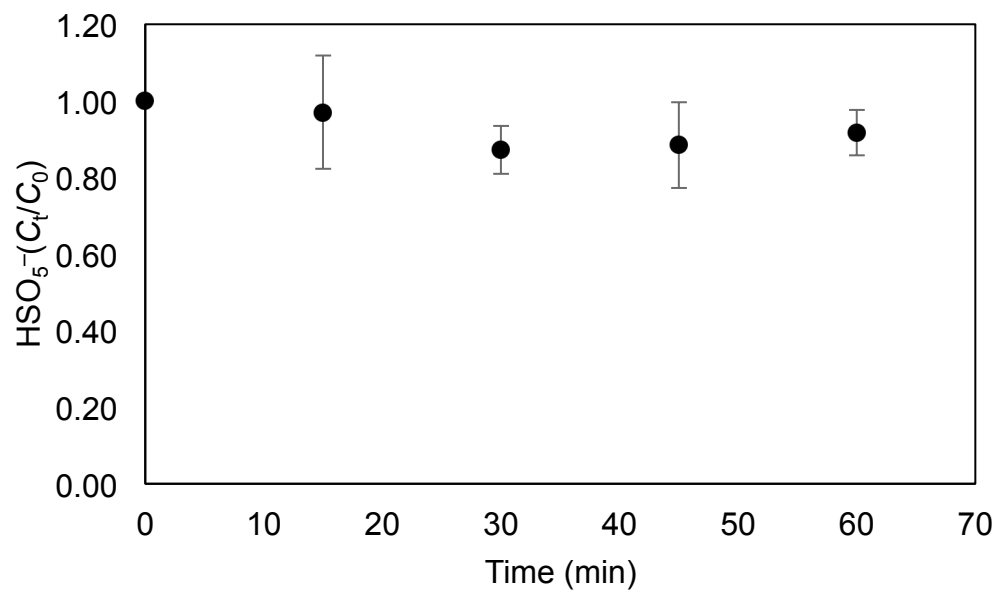


Figure 2S.1. Stability of peroxymonosulfate in the reaction conditions. Reaction conditions $[\text{HSO}_5^-]_0 = 4.5 \text{ mM}$, 0.1 M phosphate buffer, pH 7. The concentration of HSO_5^- did not appreciably change in the reaction conditions.

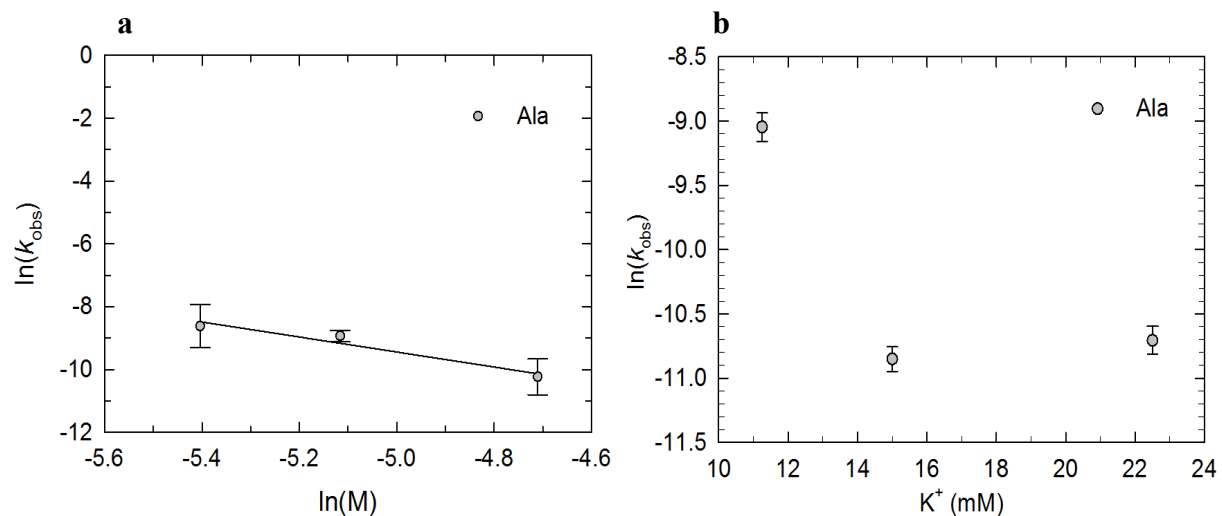


Figure 2S.2. Transformation of alanine by peroxymonosulfate as a function of oxidant and salt concentrations. (a) Determination of the order of Ala reaction with respect to $[\text{HSO}_5^-]_0$ (in $\text{mol}\cdot\text{L}^{-1}$). Initial conditions were, $[\text{Ala}]_0 = 0.45 \text{ mM}$, $[\text{HSO}_5^-]_0 = 4.5, 6, \text{ or } 9 \text{ mM}$, 0.1 M phosphate buffer, pH 7. The rate of reaction decreased with increasing HSO_5^- concentration. (b) Transformation of Ala as a function of sulfate concentration. Experimental conditions were $[\text{Ala}]_0 = 0.45 \text{ mM}$, $[\text{HSO}_5^-]_0 = 4.5 \text{ mM}$, 0.1 M phosphate buffer, pH 7. Peroxymonosulfate is a component of the triple salt $2\text{KHSO}_5\cdot\text{KHSO}_4\cdot\text{K}_2\text{SO}_4$. The 4.5 mM solution of HSO_5^- contained 11.25 mM K^+ . The $(\text{HSO}_5^- + \text{K}_2\text{SO}_4 \text{ } 1.88 \text{ mM})$ reaction contains 15 mM K^+ , and the $(\text{HSO}_5^- + \text{K}_2\text{SO}_4 \text{ } 5.63 \text{ mM})$ reaction contains 22.5 mM K^+ , which are equivalent to the amount of potassium present in $[\text{HSO}_5^-]_0 = 6 \text{ mM}$ and $[\text{HSO}_5^-]_0 = 9 \text{ mM}$ respectively. The rate of reaction decreased as K_2SO_4 concentration increased.

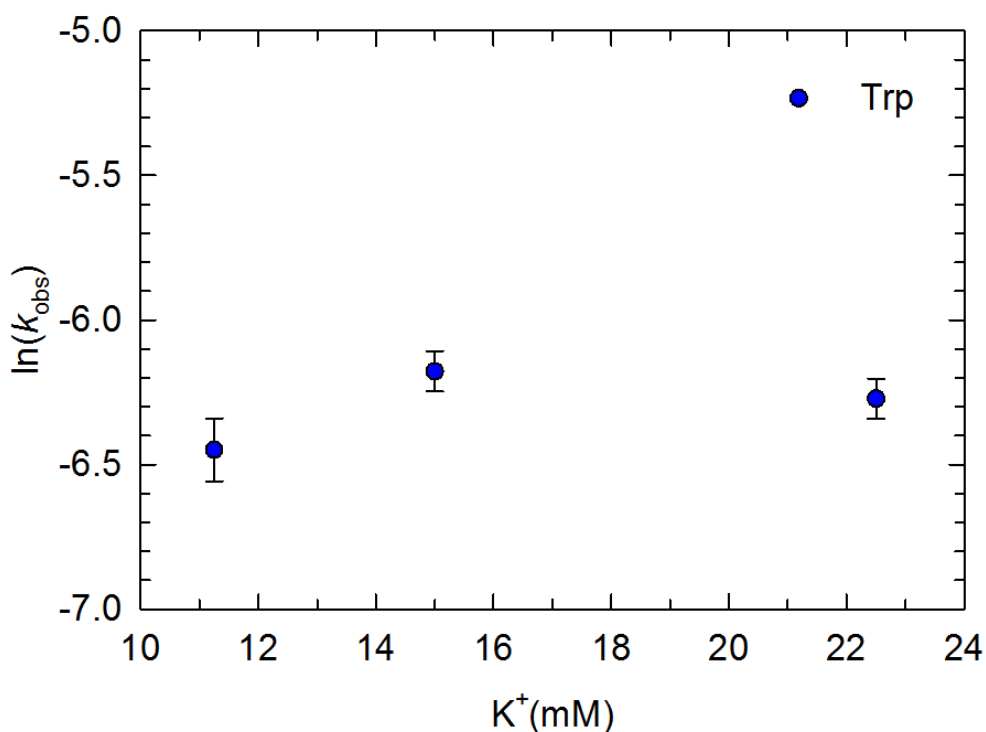


Figure 2S.3. Transformation of tryptophan by peroxymonosulfate as a function of oxidant and salt concentrations. Experimental conditions: $[Trp]_0 = 0.45$ mM, $[HSO_5^-]_0 = 4.5$ mM, phosphate buffer 0.1 M, pH 7. Peroxymonosulfate is a component of the triple salt $2KHSO_5 \cdot KHSO_4 \cdot K_2SO_4$, a 4.5 mM solution of HSO_5^- is 11.25 mM K^+ . The ($HSO_5^- + K_2SO_4$ 1.88 mM) reaction is 15 mM K^+ and the ($HSO_5^- + K_2SO_4$ 5.63 mM) reaction is 22.5 mM K^+ , which are equivalent to the amount of potassium present in $[HSO_5^-]_0 = 6$ mM and $[HSO_5^-]_0 = 9$ mM respectively. Increasing K_2SO_4 concentration did not affect the rate of reaction of Trp.

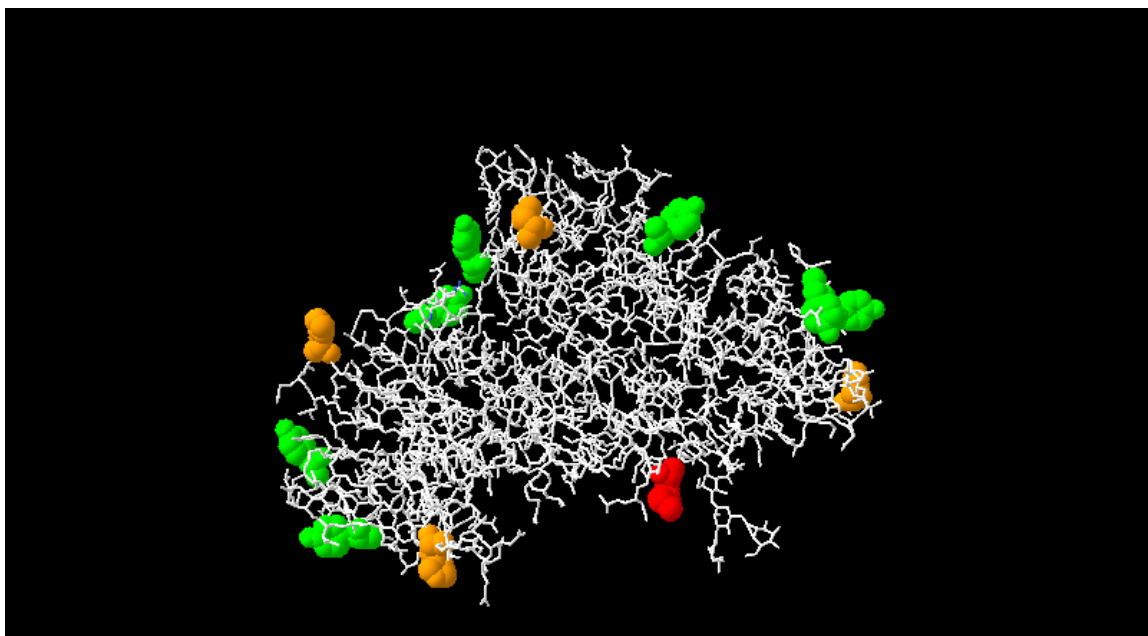


Figure 2S.4. Ricin structure, solvent exposed residues. Image constructed in Swiss-PdbViewer DeepView (<http://spdbv.vital-it.ch/>).⁴ PBD ID 2AAI.⁵ Residues with > 50% solvent accessibility A His 65; > 37% solvent accessibility A Tyr 115, A Tyr 194, B Met 5, B His 29, B Tyr 67, B Tyr 148, B Tyr 228; > 30% solvent accessibility A His 94, A Tyr 153, B Tyr 69, B His 251. Color code His orange, Met red, Tyr green. Ricin is composed of two protein chains, A refers to the ribosome inactivating protein, and B to the ricin-type beta-trefoil lectin domain.

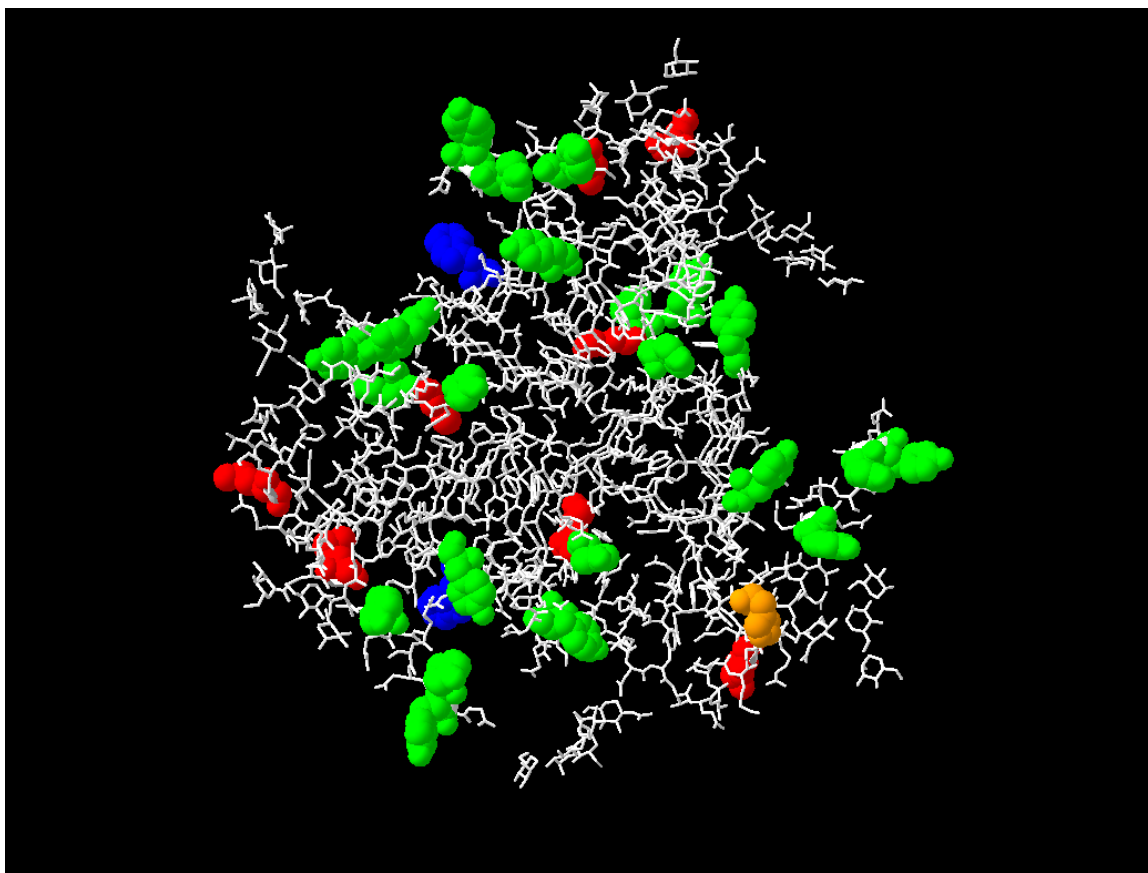


Figure 2S.5. Prion-trimer structure, solvent exposed residues. Image constructed in Swiss-PdbViewer DeepView (<http://spdbv.vital-it.ch/>).⁴ PBD file provided by Holger Wille. Residues with > 60% solvent accessibility A Tyr 224, A Tyr 225, B Tyr 224, B Tyr 225, C Tyr 224, and C Tyr 225; > 50% solvent accessibility A (Tyr 148, Met 153, Tyr 154, Tyr 162, Tyr 168, His 176, Met 204, Tyr 217), B (Tyr 98, Tyr 148, Met 153, Tyr 156, Tyr 162, Tyr 168, Met 204, Met 212, Try 217), and C (Tyr 98, Tyr 148, Met 153, Tyr 154, Tyr 156, Tyr 162, Tyr 168, Met 204, Met 212, Tyr 217). Color code His orange, Met red, Trp blue, Tyr green.

REFERENCES

- (1) Anipsitakis, G. P.; Dionysiou, D. D. Radical Generation by the Interaction of Transition Metals with Common Oxidants. *Environ. Sci. Technol.* **2004**, *38*, 3705–3712.
- (2) Wilkins, R. G. *Kinetics and Mechanism of Reactions of Transition Metal Complexes*; 2002; Vol. 6.
- (3) Helfferich, F. G. *Kinetics of Multistep Reactions*; Elsevier Science, 2004.
- (4) Guex, N.; Peitsch, M. C. SWISS-MODEL and the Swiss-PdbViewer: An Environment for Comparative Protein Modeling. *Electrophoresis* **1997**, *18*, 2714–2723.
- (5) Rutenber, E.; Katzin, B. J.; Ernst, S.; Collins, E. J.; Mlsna, D.; Ready, M. P.; Robertus, J. D. Crystallographic Refinement of Ricin to 2.5 Å. *Proteins* **1991**, *10*, 240–250.
- (6) Govaerts, C.; Wille, H.; Prusiner, S. B.; Cohen, F. E. Evidence for Assembly of Prions with Left-Handed Beta-Helices into Trimers. *Proc. Natl. Acad. Sci. U. S. A.* **2004**, *101*, 8342–8347.

Chapter 3. Transformation of Amino Acids by Cobalt-activated Peroxymonosulfate

This chapter is part of a manuscript is going to be submitted with the following co-author:

Joel A. Pedersen

Environmental Chemistry and Technology Program, University of Wisconsin, Madison, WI
53706, USA

ABSTRACT. Proteinaceous contaminants (e.g., proteins, peptides, biological agents) can be present in the environment and remain active. Current inactivation methods (e.g., autoclaving, dry heating) used for these contaminants are difficult to apply in environmental settings, prompting the development of new approaches. Cobalt-activated peroxymonosulfate (HSO_5^-) has been demonstrated to degrade diverse contaminants (e.g., phenols, microcystin-LR, diesel fuel). Inactivation methods applicable in environmental settings require further study. Here we investigated kinetics and products of oxidation of 18 of the 20 standard proteinogenic amino acids (all except cysteine and methionine) by cobalt (II)-activated HSO_5^- . Cobalt catalyzes the decomposition of HSO_5^- into sulfate radicals ($\text{SO}_4^{\cdot-}$); other radical species (e.g., $\cdot\text{OH}$, $\text{HSO}_5^{\cdot-}$, $\text{Cl}\cdot$) can be formed due to propagation reactions. Overall rates of amino acid transformation by $\text{HSO}_5^- + \text{Co(II)}$ exceeded those of reaction with unactivated HSO_5^- by at least an order of magnitude (Ruiz et al., 2015). Rates of transformation decreased in the order tryptophan > leucine \approx lysine \gtrsim isoleucine \gtrsim arginine \gtrsim threonine \gtrsim serine \gtrsim phenylalanine \gtrsim tyrosine \gtrsim glycine \gtrsim valine \gtrsim glutamic acid \gtrsim aspartic acid \gtrsim alanine \gtrsim glutamine \gtrsim asparagine \gtrsim histidine \gtrsim proline. Use of radical scavengers and varying the counterion of the cobalt salt allowed us to determine the major oxidants in the reactions. For tryptophan the major oxidant was sulfate radical. We examined the effect of the counter ion of the cobalt salt (viz. Cl^- and SO_4^{2-}) and higher transformation rates in the presence of chlorine than sulfate for alanine, isoleucine, leucine, lysine, and tryptophan. The major oxidants were determined by using alcohols with different reaction rate constants (viz ethanol and *tert*-butanol) toward radicals as radical scavengers. The major oxidants were found to be $\text{SO}_4^{\cdot-}$ and $\cdot\text{OH}$ for tryptophan, and $\text{SO}_4^{\cdot-}$ and/or $\cdot\text{OH}$ for alanine and histidine. For the aliphatic amino acids leucine and valine, and the basic amino acid lysine, other oxidants appeared to dominate the reaction. Products of

reaction confirmed by mass spectrometry with the use of authentic standards include kynurenine for tryptophan and methionine oxide and methionine sulfone for methionine.

INTRODUCTION

Some proteins and peptides can be present in the environment as contaminants and pose a risk to humans and wildlife. Proteinaceous and peptidic contaminants include cyanotoxins (e.g., microcystins, nodularin), bacterial exotoxins (e.g., botulinum toxin, *Staphylococcus* enterotoxin type B), and proteins such as ricin and prions. Microcystin-LR is a non-ribosomal peptide produced by cyanobacteria and has been detected in surface and drinking water.^{1,2} Ricin, a protein produced by the castor bean plant, and botulinum toxin, produced by *Clostridium botulinum*, have the potential to be used as biowarfare agents.³ Prions, composed primarily if not exclusively of misfolded conformers of the prion protein, cause neurodegenerative diseases in mammals and can persist in the environment and remain infectious when bound to soil components.⁴⁻⁷ The presence of toxic proteinaceous material in the environment demands the development of *in situ* remediation technologies. Although methods exist to decontaminate a variety of peptide and proteins, not all can be readily adapted for application to environmental matrices. Harsh methods are required to inactivate these proteins such as chemical denaturation (exposure to sodium hypochlorite for 30 min) and high temperature (dry heat > 100 °C for 10 min) to inactivate ricin and botulinum toxin,³ or autoclaving (121-132 °C for 1 hour gravity displacement sterilizer)⁸ to inactivate prions. The aforementioned methods are ill suited for *in situ* remediation.

In situ chemical oxidation is approved by the U.S. Environmental Protection Agency (EPA) to treat hazardous waste sites.⁹ Common oxidants used in *in situ* chemical oxidation include permanganate, Fenton reagent (hydrogen peroxide + ferrous iron), modified Fenton reagent (e.g. in the presence of iron chelates)¹⁰, ozone, and persulfate.^{11,12} The reactive species of

these oxidants are the permanganate ion, hydroxyl radicals ($\cdot\text{OH}$) in the case of the (modified) Fenton reagents, hydroxyl radicals and ozone in the case of ozone, and sulfate radical ($\text{SO}_4^{\cdot-}$) in the case of persulfate. Sulfate and hydroxyl radicals are strong oxidants (formal potentials of 2.7 V and 2.5 V at pH 7, respectively) capable of oxidizing organic contaminants. Sulfate radical has gained more attention for *in situ* chemical oxidation application studies due in part by the assumption that it is a more selective radical than $\cdot\text{OH}$,¹³ and observed higher initial degradation rates compared to hydroxyl radical.¹⁴ Sulfate radical is thought to be more selective than $\cdot\text{OH}$ by reacting mainly via electron transfer whereas hydroxyl radical can be rapidly depleted by engaging in hydrogen abstraction reactions, both sulfate and hydroxyl radicals can abstract hydrogen from organic molecules, but this reaction is believed to occur at a lower rate for sulfate relative to hydroxyl radical.^{13,15}

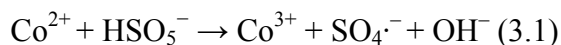
Several limitations inhere in the use of the Fenton reagent to produce hydroxyl radical for remediation of contaminated soils and sediments. The main constraint on the environmental application of the Fenton reagent is the need to maintain acidic conditions ($\text{pH} < 5$) to minimize precipitation of iron (III).¹⁰ *In situ* application of the Fenton reagent may rely on naturally occurring iron minerals and be conducted in neutral and alkaline conditions; the efficiency of target contaminant degradation depends iron content and oxidation state, mineral and oxide composition.¹⁶ Furthermore, hydroxyl radical reacts rapidly with H_2O_2 depleting both hydroxyl radical and its precursor.^{17,18} Generation of sulfate radical from persulfate or peroxymonosulfate is not subject to these constraints.

Peroxymonosulfate decomposes into radical species (so-called activation) in the presence of transition metal catalysis,^{14,19,20} UV light ($\lambda < 254 \text{ nm}$),²¹ and heat (80°C).²² Activated HSO_5^- can be employed over a wider range of pH (up to pH 12) than Fenton reagent to form sulfate

radicals.²³ The formation of hydroxyl radical via UV activation of HSO_5^- increases at $\text{pH} > 9$, due in part to reaction of sulfate radical with hydroxide ion.²³ Among these activation pathways, activation by transition metals is the most viable option for *in situ* soil decontamination UV is not viable since the photoic zone is approximately the top 0.5 mm of the soil surface.²⁴

Cobalt-activated HSO_5^- has been demonstrated to be effective in oxidizing a variety of organic contaminants including atrazine, microcystin-LR, 2,4-dichlorophenol, and diesel fuel.^{25,26,14,27} Using pulse radiolysis and flash photolysis techniques, the rates of free amino acid reaction with sulfate radical have been studied for nine amino acids: alanine (Ala), arginine (Arg), glycine (Gly), histidine (His), methionine (Met), serine (Ser), tryptophan (Trp), tyrosine (Tyr), valine (Val).²⁸⁻³⁰ Rate constants have been reported for eight of these amino acids but products of transformation were not reported.²⁸⁻³⁰ In a previous correspondence, we demonstrated the oxidation of amino acid by peroxymonosulfate (HSO_5^-); in this contribution we studied the transformation of amino acids by radicals species generated by the decomposition of HSO_5^- catalyzed by cobalt (II). To the best of our knowledge a kinetic study of the oxidation of free amino acids by cobalt-activated HSO_5^- has not been conducted. Cobalt activation of HSO_5^- results in the formation of primarily sulfate radical.¹⁴ Nonetheless, sulfate radical may not be the predominant major oxidant in the reactions with some amino acids, as other radicals can be formed through propagation reaction.

Among the transition metals investigated for catalyzing the decomposition of HSO_5^- into radial species (Co^{2+} , Ru^{3+} , $\text{Fe}^{+2/+3}$, Ce^{+3} , V^{+3} , Mn^{+2} , Ni^{+2}),¹⁴ cobalt(II) salts have been shown to be the most effective in producing sulfate radicals, based on the initial transformation of 2,4-dichlorophenol.¹⁴ The decomposition of peroxymonosulfate proceeds as:¹⁴

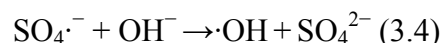


Equations 3.2 and 3.3 describe equation 1 in more detail. The formation of the sulfate radical by cobalt activation proceeds as:^{31,32}



First, Co(II) reacts with water to form cobalt hydroxide (eq 3.2), then cobalt hydroxide reduces HSO_5^- to yield Co(III)O^+ , sulfate radical, and water (eq 3.3). In the regeneration of the cobalt catalyst, Co(III) is reduced by peroxymonosulfate (standard reduction potential, $E_H^0 = 1.82 \text{ V}$, $\text{HSO}_5^- + 2\text{H}^+ + 2\text{e}^- \rightarrow \text{HSO}_5^- + \text{H}_2\text{O}$, $pK_{a1} < 1$, $pK_{a2} = 9.4$).^{33,34} Increasing the pH of the reaction results in the formation of $\cdot\text{OH}$ (eq 3.4). The reaction between HSO_5^- with either $\text{SO}_4^{\cdot-}$ or $\cdot\text{OH}$ (eq 3.5, 3.6) produces HSO_5^- radical ($\text{SO}_5^{\cdot-}$).³⁵

Propagation reactions (eqs 3.4-3.6) can generate hydroxyl radicals and peroxymonosulfate radicals:



The objectives of the study were to determine the rates of amino acid transformation by cobalt-activated HSO_5^- , and for selected amino acids to identify the dominant oxidant in selected reactions (viz. sulfate, hydroxyl, or HSO_5^- radicals) and determine the products of oxidation. To achieve these objectives we conducted kinetic studies to determine the initial rates of reaction of 18 of the common proteinogenic amino acids (excluding Met and Cys) with cobalt-activated HSO_5^- . The kinetics of transformation of Met and Cys were not studied due to their rapid rates of

reactions with different oxidants.³⁶ In our previous correspondence (Ruiz et. al, 2005) the second order rate constant of Met by HSO_5^- was $k' = 3400 \pm 170 \text{ M}^{-1}\text{s}^{-1}$. The identification of the dominant oxidant was accomplished by the use of quenching agents differing in reactivity towards the radical species under consideration and by examining the effect of the counterion in the cobalt salt. Product identification was achieved by liquid chromatography with tandem mass spectrometry.

MATERIALS AND METHODS

Chemicals. Peroxymonosulfate (Oxone[®]), valine (Val, 99%), and methionine sulfoxide (99.7%) were purchased from Alfa Aesar. Arginine (Arg, 99%), asparagine (Asn, >99%), and *tert*-butyl alcohol (99.0%) were procured from TCI. Phenylalanine (Phe, $\geq 99\%$) and formic acid ($\sim 98\%$) were obtained from Fluka. Alanine (Ala, 99%), aspartic acid (Asp, >99%), glutamic acid (Glu, $\geq 99.5\%$), glycine (Gly 99%), histidine (His, >99%), leucine (Leu, 98%), lysine (Lys, $\geq 98\%$), methionine (Met, $\geq 98\%$), serine (Ser, $\geq 99\%$), threonine (Thr, $\geq 98\%$), tryptophan (Trp, $\geq 98\%$), 5-hydroxytryptophan (98%), and methionine sulfone ($\geq 98\%$) were bought from Sigma-Aldrich. Tyrosine (Tyr, >99%), sodium thiosulfate pentahydrate (ACS grade), Na_2HPO_4 (ACS grade), NaH_2PO_4 (>99%), $\text{CoSO}_4 \cdot (\text{H}_2\text{O})_7$ (99%) and dry acetonitrile were acquired from Acrös Organics. Isoleucine (Ile), proline (Pro), and $\text{CoCl}_2 \cdot (\text{H}_2\text{O})_6$ were from MPBiomedicals. Sodium acetate trihydrate (ACS grade), HCl (ACS grade), formic acid (88%), *N,N'*-disuccinimidyl carbonate (98%), and 6-aminoquinoline (AQM: 98%) were ordered from Fisher. K_2SO_4 (ACS grade) was obtained from Reagent World. Ethanol (>99.9%) was bought from Pharmco-AAPER. The derivatizing reagent 6-aminoquinolyl-*N*-hydroxysuccinimidyl carbamate (AQC) was synthesized as previously described.³⁷

Kinetic experiments. We conducted kinetic experiments at room temperature (25 °C) in amber borosilicate glass bottles under continuous stirring on a magnetic stir plate. Unless otherwise noted, the initial reactant concentrations were 0.45 mM of amino acid, 4.5 mM HSO_5^- , and 9 μM CoCl_2 in 0.1 M phosphate buffer at pH 7. Reactions were initiated by adding HSO_5^- to the amino acid/cobalt solution. Aliquots were withdrawn as a function of time and quenched with equal volume of 1 M thiosulfate. All samples were filtered (0.2 μm , regenerated cellulose Corning 4 mm syringe filter) prior to derivatization (except for Trp and Tyr; *vide infra*) and analysis by high performance liquid chromatography with fluorescence detection (HPLC-FD). Loss of amino acid to the filter was not observed (see Supporting Information).

Quenching studies. To determine the free radical species responsible for amino acid transformation in reactions containing HSO_5^- and Co^{2+} , we added ethanol or *tert*-butanol to reaction vessels before initiating reactions. Alcohols containing an α -hydrogen react rapidly with both sulfate and hydroxyl radicals (ethanol, $k'_{\text{EtOH},i} > 10^7 \text{ M}^{-1}\cdot\text{s}^{-1}$), but HSO_5^- radical has a substantially lower rate of reaction with α -hydrogen (ethanol, $k'_{\text{EtOH},\text{SO}_5^-} < 10^3 \text{ M}^{-1}\cdot\text{s}^{-1}$) (Table 3.1). This difference in reactivities allows differentiation of sulfate and hydroxyl radicals from HSO_5^- radical. To discriminate between sulfate and hydroxyl radicals *tert*-butanol was used. This alcohol rapidly quenches hydroxyl radicals ($k'_{t\text{BA},\text{OH}} = 6 \times 10^8 \text{ M}^{-1}\cdot\text{s}^{-1}$) but reacts at a slower rate with sulfate radicals ($k'_{t\text{BA},\text{SO}_4^{\cdot-}} = 4 \times 10^4 \text{ M}^{-1}\cdot\text{s}^{-1}$) (Table 3.1).

Amino acid analysis by HPLC-FD. Amino acid analysis was conducted as described in our previous publication (Ruiz et al., 2015). Amino acids lacking an intrinsic fluorophore (i.e., all except Trp and Tyr) were derivatized using AQC as previously described.³⁷ Briefly, an aliquot (50 μL) of an amino acid sample was added to borate buffer (0.1 M, pH 9) followed by

an aliquot of AQC (25 μL), immediately after which the reaction mixture was vortexed (5 s). Fresh AQC solutions (2 $\text{g}\cdot\text{L}^{-1}$) were prepared weekly and stored at 4 $^{\circ}\text{C}$.

Quantification of amino acids was performed on an Agilent 1050 HPLC equipped with a fluorescent detector (Agilent 1110). The mobile phases were 15.6 mM acetate buffer (pH 5) and 60% acetonitrile in H_2O for all amino acids with the exception of Asp and Glu for which 0.1% formic acid in H_2O and 60% acetonitrile in H_2O were used as the mobile phases. Samples were separated (see SI) on an AccQ-Tag Waters column (C18, 3.9×150 mm, 4 μm , 60 \AA , Wat052885) equipped with a Nova-Pak® guard column (C-18, 3.9×200 mm, 4 μm , 60 \AA , Wat044380). Excitation and emission wavelengths were $\lambda_{\text{ex/em}} = 280/350$ nm for Trp, $\lambda_{\text{ex/em}} = 229/310$ nm for Tyr, and $\lambda_{\text{ex/em}} = 245/395$ nm for the AQC-derivatized amino acids.

An additional system, Agilent 1260 HPLC equipped with a fluorescent detector, was used to quantify amino acid concentrations of some reactions (alcohol quenching, CoSO_4 for Ala, His, Ile, Val). Separation was achieved with a Poroshell 120 (EC-C18, 3.0×50 mm, 2.7 μm , 120 \AA , 699975-302) equipped with a Poroshell 120 (EC-C18, 2.1×5.0 mm, 2.7 μm) guard column. The mobile phases used were (A) 15 mM sodium acetate pH 5 with 10% ACN and (B) ACN. Injection volume was 50 μL ; the flow rate of the mobile phase was $0.75 \text{ mL}\cdot\text{min}^{-1}$. Mobile phase details and gradient used are summarized in Table 3S.1. Excitation and emission wavelengths remained the same.

Analysis by LC-MS/MS. Product identification was performed on an Agilent 6460 triple quadrupole LC-MS with an electrospray ionization source. The mobile phases were 10 mM pH 7.5 ammonium acetate buffer with 10% ACN and ACN. The source parameters were: gas temperature 300 $^{\circ}\text{C}$, gas flow $7 \text{ L}\cdot\text{min}^{-1}$, nebulizer 45 psi, sheath gas temperature 350 $^{\circ}\text{C}$, sheath gas flow $10 \text{ L}\cdot\text{min}^{-1}$, capillarity voltage 3500 V, nozzle voltage 500 V.

Products were separated (gradient elution, see SI for details) with the column used for HPLC-fluorescence detection described above. To prevent inorganic salts from reaching the detector, the eluate was diverted to waste from (0-4.5 and 29-30 min), and data were recorded from 4.5-29 min. Authentic standards were acquired for possible products when available (Table 3S.4). Possible products were confirmed when the retention time and the fragmentation pattern of the products of reaction matched those of the standard.

RESULTS AND DISCUSSION

All amino acids investigated were transformed by cobalt-activated HSO_5^- . Plots of the most rapidly transformed amino acids (Trp, Lys, Leu) are presented in Figure 3.1. The transformation of Trp was the most rapid, followed by Lys and Leu. Observed rate constants (k_{obs}) for the transformation of the 18 amino acids investigated by cobalt-activated HSO_5^- are presented in Figure 3.2; their values are tabulated in Table 3S.1. Observed reaction rate constants ranged from $1.7 \times 10^{-3} \text{ s}^{-1}$ (Pro) to $6.2 \times 10^{-2} \text{ s}^{-1}$ (Trp). The rate amino acid transformation by Co^{2+} -activated HSO_5^- exceeded that of unactivated HSO_5^- by more than an order of magnitude (Figure 3.2). The rates of amino acid oxidation by Co^{2+} -activated HSO_5^- decreased in the order of $\text{Trp} > \text{Lys} \approx \text{Leu} \gtrsim \text{Ile} \gtrsim \text{Arg} \gtrsim \text{Thr} \gtrsim \text{Ser} \gtrsim \text{Phe} \gtrsim \text{Tyr} \gtrsim \text{Gly} \gtrsim \text{Val} \gtrsim \text{Glu} > \text{Asp} \gtrsim \text{Ala} \gtrsim \text{Gln} \gtrsim \text{Asn} \gtrsim \text{His} \gtrsim \text{Pro}$. The rates of oxidation by hydroxyl radical for these amino acids decrease in the order of $\text{Trp} \approx \text{Tyr} > \text{Phe} > \text{His} > \text{Arg} > \text{Ile} > \text{Leu} > \text{Val} > \text{Pro} > \text{Gln} > \text{Thr} > \text{Lys} > \text{Ser} > \text{Glu} > \text{Ala} > \text{Asp} > \text{Asn} > \text{Gly}$, and the ranking for sulfate radical is $\text{Trp} > \text{Trp} > \text{Met} > \text{Ser} > \text{Ala} \approx \text{Gly} > \text{His}$.³⁸ The disparity in ranking order in the transformation of amino acids by cobalt activated peroxymonosulfate and sulfate radical suggests the participation of additional oxidants in some of the reactions with Co^{2+} -activated peroxymonosulfate. The rates of amino acid transformation by unactivated HSO_5^- decreased in the order of (Met >) $\text{Trp} > \text{Tyr} > \text{His} >$

Ala (Ruiz et al., 2015). In the unactivated HSO_5^- system the only oxidant present is peroxymonosulfate; in the cobalt-activated HSO_5^- system in addition to sulfate radical, other radical species may also be produced (i.e., $\text{SO}_5^{\cdot-}$, $\cdot\text{OH}$, $\text{Cl}\cdot$, HOCl eq 3.5-3.13) that may also react differentially with the different amino acids.

Identification of dominant oxidants. Sulfate radical ($\text{SO}_4^{\cdot-}$) is the main radical species formed in the activation of HSO_5^- by Co(II) (eq 3.3); however, other radical species can be produced in propagation reactions (eq 3.7-3.11). For example, peroxymonosulfate radical ($\text{SO}_5^{\cdot-}$) can be formed in the regeneration of the Co(II) catalyst (eq 3.5). Prior work on reactions of organic molecules by Co^{2+} -activated HSO_5^- has demonstrated radical species other than $\text{SO}_4^{\cdot-}$ sometimes contribute to the transformation of the molecule (oxidation of caffeine and 2,4-dichlorophenol by $\cdot\text{OH}$).^{39,40}

To deduce the dominant oxidants operative in selected reactions with cobalt-activated HSO_5^- , we employed radical quenchers (viz. ethanol, *tert*-butanol) or altered the counterion in the Co(II) salt in the reactions. Radical scavengers with different rates of reaction with radicals (Table 3.1) were used to determine the primary oxidant. Ethanol reacts rapidly with both $\text{SO}_4^{\cdot-}$ and $\cdot\text{OH}$ ($k' > 10^7 \text{ M}^{-1}\cdot\text{s}^{-1}$), but much more slowly with HSO_5^- radical ($k' < 10^3 \text{ M}^{-1}\cdot\text{s}^{-1}$). The second-order rate constant for *tert*-butanol reaction with $\cdot\text{OH}$ ($k' = 6 \times 10^8 \text{ M}^{-1}\cdot\text{s}^{-1}$) exceeds that of $\text{SO}_4^{\cdot-}$ ($k' = 4 \times 10^4 \text{ M}^{-1}\cdot\text{s}^{-1}$) by more than two orders of magnitude. Ethanol also scavenges phosphate and chloride radicals. The concentration of chloride in the reaction mixtures is low (18 μM), and radical chlorine species are not expected to contribute to the transformation. The second order rate of phosphate radical formation is 100 times slower than the reaction of $\cdot\text{OH}$ and $\text{SO}_4^{\cdot-}$ with amino acids so phosphate radicals are not expected to contribute. Hence, a decrease in the rate of amino acid transformation in the presence of ethanol can be attributed to

either $\text{SO}_4^{\cdot-}$ or $\cdot\text{OH}$. For reactions that are quenched by ethanol, reactions conducted in the presence of *tert*-butanol allow discrimination between $\text{SO}_4^{\cdot-}$ and $\cdot\text{OH}$ ($\cdot\text{OH}$ -mediated reactions would be quenched, while those with would not be $\text{SO}_4^{\cdot-}$).

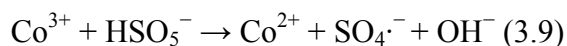
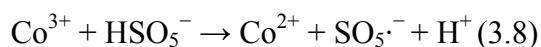
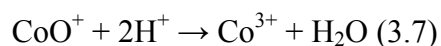
The rate of Trp transformation increased with the addition of the cobalt catalyst relative to reaction with unactivated HSO_5^- (Figure 3.3). Reactions with alcohol quenchers (ethanol, *tert*-butanol) led to the conclusion that sulfate and hydroxyl radicals are the primary oxidant for Trp in the $\text{HSO}_5^- + \text{Co(II)}$ system. The rate of reaction in the presence of ethanol decreased by 92% indicating that $\text{SO}_4^{\cdot-}$ or $\cdot\text{OH}$ was, in contrast the rate decreased by 55% in the presence of *tert*-butanol indicating some contribution by $\cdot\text{OH}$. Reactions of Ala and His were completely quenched (100%) in the presence of ethanol suggesting that either $\text{SO}_4^{\cdot-}$ or $\cdot\text{OH}$ were the major oxidants in this reaction. Further experiments with *tert*-butanol are required to determine the relative contribution of these two radicals.

Previously published rate second-order rate constants for $\text{SO}_4^{\cdot-}$ and $\cdot\text{OH}$ for some amino acids and the data from the quenching experiments allowed us to estimate steady-state concentrations of these radical species. To do this we used the second-order rate constants reported in the literature for the reaction Trp with $\text{SO}_4^{\cdot-}$ and $\cdot\text{OH}$ (Table S6) and the observed rate constants from this study. We estimate the steady state concentrations for $\text{SO}_4^{\cdot-}$ and $\cdot\text{OH}$ to be 1.1×10^{-11} M and 7.9×10^{-12} M, respectively. Assuming that both $\text{SO}_4^{\cdot-}$ and $\cdot\text{OH}$ participate in the Ala and His reactions, we calculated the k_{obs} with the calculated steady state concentration of $\text{SO}_4^{\cdot-}$ and $\cdot\text{OH}$ and their reported second-order rate constants (Table S6). The experimental and theoretical values of k_{obs} for Ala were similar (within a factor of 0.25): $k_{\text{obs}} = 3.6 (\pm 0.4) \times 10^{-3} \text{ s}^{-1}$ and $0.9 \times 10^{-3} \text{ s}^{-1}$, respectively. Assuming that Ser also reacts with $\text{SO}_4^{\cdot-}$ and $\cdot\text{OH}$ the k_{obs} were similar (within a factor of 1.8): $k_{\text{obs}} = 6.9 (\pm 0.1) \times 10^{-3} \text{ s}^{-1}$ and $3.7 \times 10^{-3} \text{ s}^{-1}$, respectively.

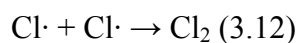
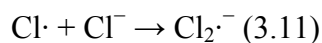
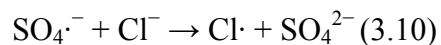
This suggests that the calculated steady state concentrations of $\text{SO}_4^{\cdot-}$ and $\cdot\text{OH}$ are reasonable. In the case of His the experimental and theoretical values differed by a factor of 23: $k_{\text{obs}} = 2.3 (\pm 0.4) \times 10^{-3} \text{ s}^{-1}$ and $5.2 \times 10^{-2} \text{ s}^{-1} \times 10^{-2} \text{ s}^{-1}$, respectively. The second-order rate constant for the reaction of His with hydroxyl radical was reported at pH 7.5. The transformation of His by HSO_5^- and singlet oxygen varies by pH due the protonation of the imidazole sidechain (Ruiz et al).⁴¹ The fraction of His present as the base are 0.91 and 0.97 at pH 7 and 7.5, respectively. This change, although small, might explain the difference between the calculated and experimental k_{obs} values for His. To test this hypothesis the transformation of His at pH 7 could be studied.

In contrast to Trp, Ala and His, the rates of Leu, Lys and Val transformation by cobalt-activated HSO_5^- did not decrease when ethanol was added to the reaction mixture (Figure 3.4a). Two possible reasons for the lack of quenching are the formation of caged radicals (i.e., those that are not freely diffusible) or that neither hydroxyl nor sulfate radicals are major participants in the reaction. Based on the transformation of 2,4-dichlorophenol in the presence of and absence of ethanol and *tert*-butanol Anipsitakis et al. concluded that the Co(II)-activated HSO_5^- system results in the generation of almost exclusively freely diffusible $\text{SO}_4^{\cdot-}$ (eq 3.3),¹⁴ arguing against the presence of caged radicals. The concentration of $\text{SO}_4^{\cdot-}$ was not quantified in that study.¹⁴ Radical scavengers are generally presumed to be unable to quench caged radicals, and lack of quenching by scavengers in systems with known radical species is typically taken as indication of their formation.^{14,42} Caged radical is a broad term for a radical that undergoes a reaction faster than it can diffuse and includes solvent-associated radicals, resonance-stabilized radical pairs, and radicals that react quickly at the site of formation (i.e., bound free radicals).^{43–45} A caged radical could form bound to an amino acid residue in the metal binding site of a protein. This has been assumed for Lys residues in protein metal binding sites in the case of the Fenton reagent (see

review by Stadtman).^{42,46} The formation of Lys-caged radical, due to complexation to Fe(II) by the sidechain amino group, was assumed because $\cdot\text{OH}$ scavengers failed to quench the reaction. Values for cobalt complexation constants by some amino acids are presented in Table S5. The complexation constants ($\log K$) for Lys are 4.5⁴⁶ and 1.785⁴⁷ with Fe (II) and Co(II), respectively. Histidine has a larger complexation constant ($\log K = 9.3$)⁴⁶ than does Leu and Lys, but its transformation was completely inhibited by ethanol (Figure 4a). The complexation constants of these amino acids may not be sufficient to explain the effect of alcohol quenching in our study. Because no quenching was observed in the presence of $\text{SO}_4^{\cdot-}$ or $\cdot\text{OH}$ scavengers, other oxidants might be driving Leu, Lys and Val transformation. Peroxymonosulfate radical ($\text{SO}_5^{\cdot-}$) can be formed during regeneration of the cobalt catalyst (eq 3.5), chlorine radical species can be formed when chloride is present in solution (eq 3.10-3.12) and hypochlorous acid (HOCl) can be formed when HSO_5^- reacts with chlorine (eq 3.13). Sulfate and peroxymonosulfate radicals can be formed during the regeneration of the catalyst (eqs 3.7-3.9):³²



In the presence of chloride, propagation reactions can lead to the formation of chloride ($\text{Cl}\cdot$) and chlorine ($\text{Cl}_2^{\cdot-}$) radicals:



Chlorine can also react with peroxymonosulfate to yield hypochlorous acid:^{49,50}



Cobalt chloride is commonly used in the cobalt activation of HSO_5^- ; the presence of chloride can lead to formation of chlorine radicals which have been shown to contribute to the transformation of 2,4-dichlorophenol and diesel contaminated soil.^{19,27} Sulfate radicals can oxidize chloride ions to Cl^\bullet (eq 3.10), which react rapidly with Cl^- to form $\text{Cl}_2^{\bullet-}$ ($k' = 6.5 \times 10^9$ to $2.1 \times 10^9 \text{ s}^{-1} \text{ M}^{-1}$, eq 11). The standard reduction potentials are 2.4 and 2.0 V for $(\text{Cl}^\bullet/\text{Cl}^-)$ and $(\text{Cl}_2^{\bullet-}/2\text{Cl}^-)$, respectively.⁵¹ The reduction potential is 1.611 V ($\text{HOCl} + \text{H}^+ + \text{e}^- \rightleftharpoons \frac{1}{2} \text{Cl}_2 + \text{H}_2\text{O}$).⁵² Chloride radical can also react with itself ($k' = 8.8 \times 10^7 \text{ s}^{-1} \text{ M}^{-1}$, eq 3.12) forming Cl_2 , which in turn reacts with water to form hypochlorous acid (eq 3.13). These radical species are not expected to be important in the reactions due to the low chloride concentration (18 μM).

To determine the possible contribution of chloride radical to the transformation of different classes of amino acids, we compared initial rates of amino acid reaction with cobalt-activated HSO_5^- in which the Co(II) counterion was sulfate or chloride (Figure 3.4b) for the aliphatic (Ala, Leu, Val, Ile), some charged (His, Lys) and aromatic (His, Trp) amino acids. These included the fastest reacting amino acids (Trp, Lys, and Leu), amino acids that were for which the rates of reaction did not decrease in the presence of ethanol (Lys, Leu, and Val), and amino acids that were transformed by either $\text{SO}_4^{\bullet-}$ or $\cdot\text{OH}$ (Trp, His, Ala). With the exception of His and Val, the rate of transformation decreased in when SO_4^{2-} was substituted for chloride as Co(II) counterion. In no case was the reaction completely inhibited when SO_4^{2-} was substituted for Cl^- as the counterion in the cobalt salt. These results suggest that chlorine species contribute to the transformation of these amino acids. Ethanol is also a scavenger for Cl^\bullet (Table 3.1) therefore if the transformation of Lys and Leu was due to Cl^\bullet the reaction rate would decrease in

the presence of ethanol, but quenching was observed for Leu and Lys in the presence of ethanol. Another explanation of the decrease observed in the transformation of Ala, Leu, Lys, Ile, and Trp in the absence of Cl^- is the formation of HOCl (eq 3.13), which can react with amino acids.^{53–55}

Another possible oxidant is HSO_5^- radical that is formed in the regeneration of the cobalt catalyst (eq 3.6). Peroxymonosulfate radical has calculated formal reduction potential of 0.95 V at pH 7 ($\text{SO}_5^{\cdot-}/\text{SO}_5^{2-}$).⁵⁶ Peroxymonosulfate radical reacts with phenols and aromatic amines with second order rate constants ranging from $8 \times 10^4 \text{ M}^{-1}\cdot\text{s}^{-1}$ to $1.4 \times 10^8 \text{ M}^{-1}\cdot\text{s}^{-1}$.^{57–59} We hypothesize that the major oxidant in solution is HSO_5^- radical for Lys, Leu and Val, to test this hypothesis further experiments could be conducted with a radical scavenger for HSO_5^- radical, or by producing HSO_5^- radical from the reaction of sulfite with oxygen.^{57–59} Such experiments would allow us to determine if the oxidation occurs by free or caged radicals.

In the case of Fenton reaction, and in the copper decomposition of H_2O_2 , the oxidant species were found to depend on pH.⁶⁰ At neutral and alkaline pH high valent iron and copper are participating oxidants, possibly Fe(IV) and Cu(III) . The standard reduction potential is estimated to be $\sim 2 \text{ V}$ for Fe(IV) ⁶¹ and is 2.4 V for Cu(III) .⁵² Transformation by Co(III) , with a standard reduction potential of 1.92 V ,⁵² must also be considered. To test the hypothesis that Co(III) is an oxidant in the reactions experiments could be conducted with Co(III) salts or complexes.

Products of oxidation. We investigated the products of oxidation by cobalt-activated HSO_5^- by LC-MS/MS for Met and the fastest reacting amino acids: Trp, Lys, and Leu. We examined MS2 chromatograms for peaks appearing in the product mixture that were absent in controls. We assigned possible structures to these products. When available authentic standards

were purchased, and products identities were confirmed based on matches to chromatographic retention times and fragmentation pattern. A list of possible products is summarized in Table 3.2.

The reaction of Trp with $\text{SO}_4^{\cdot-}$ and $\cdot\text{OH}$ produced by Co^{2+} -activation of HSO_5^- resulted in the formation of products with m/z shifts relative to the parent compound of +4, and +16. These corresponded to a gain of oxygen for the +16 m/z product and a rearrangement with a net increase for the +4 m/z product. Kynurenine was confirmed by LC-MS/MS as a product of reaction for Trp oxidation by Co^{2+} -activated HSO_5^- with the use of an authentic standard (i.e. the product had the same retention time and fragmentation pattern as the standard, Table 3S.6), and was not detected when ethanol was added to the reaction, indicating that Kyn is a product formed by the reaction of Trp with either hydroxyl or sulfate radicals. Kynurenine has been reported as a product of Trp oxidation by sulfate radical⁶² and by $\cdot\text{OH}$ produced in the metal-catalyzed oxidation of proteins,^{63,64} but not in water radiolysis (generates $\cdot\text{OH}$, solvated electrons (e_{aq}^-), and hydronium ions (H_3O^+)) of tryptophan amide (Trp-NH_2).³⁸ The formation kynurenine results from the hydrolysis and loss of the carbonyl group of *N*-formylkynurenine (+32 m/z), which is formed by the addition of two oxygen atoms followed by cleavage of the indole.⁶³

The +16 m/z product could correspond to hydroxy-tryptophan. We compared its retention time and fragmentation pattern to a commercially available standard of 5-hydroxy tryptophan (5-OH-Trp), but the retention time of the standard differed from that of the transformation product (retention time 5.6 and 7 min for 5-OH-Trp and Trp + 16 m/z respectively) (Table 3S.7). The dissimilarity in retention time relative to 5-OH-Trp may indicate that the product is not hydroxylated on the aromatic ring. Another possible product would be oxindolylalanine, which is also formed in the reaction of Trp with H_2O_2 .⁶⁵ The hydroxylation mechanism of aromatic compound by Co^{2+} -activated HSO_5^- formation of sulfate radicals has been studied.¹⁹ The

proposed mechanism occurs by an initial step of a sulfate radical attack, which leads to the formation of carbon-centered radicals via electron transfer from the organic compound to the sulfate radical. Hydrolysis of the carbon-centered radical leads to the formation of hydroxylated radical products, and then further reaction with O_2 produces hydroxylated products. The hydroxylated molecule can undergo further transformation via hydrogen abstraction. Attack by $\cdot OH$ can also form a carbon centered radical via hydrogen abstraction, explaining why similar products are observed in oxidation by $\cdot OH$ and $SO_4^{\cdot -}$.^{28,29,66} The oxidation of phenol by hydroxyl and sulfate radicals yielded similar phenol products and resulted mainly in the addition of oxygen followed by ring cleavage.⁶⁷ Anipsitakis et al., also found addition of oxygen in the cobalt-mediated oxidation of phenol, with positive m/z mass shifts of 14 and 16.

In the case of Leu two products were observed, with m/z shifts of +14 and +16, which may correspond to a leucine carbonyl and hydroxy-leucine respectively. The mass shift of +16 m/z could correspond to the addition of oxygen whereas +14 m/z could be the formation of a carbonyl.⁶⁸ Mass shifts of +14 and +16 m/z have previously been observed in the oxidation of amino acid residues in a protein structure by $SO_4^{\cdot -}$ and $\cdot OH$, with a higher abundance of the +16 m/z product.⁶² The reaction of aliphatic amino acids by $\cdot OH$ is not selective and the hydroxylation or formation of carbonyl can occur at various position.⁶⁹ Hydroxyl radical attacks by hydrogen abstraction to give a carbon-centered radical, which reacts with molecular oxygen to form a peroxy radical. The peroxy radical can undergo a series of radical reactions, giving rise to a hydroperoxide (+32 m/z), hydroxide (+16 m/z), or carbonyl (+14 m/z); a the +32 m/z product was not observed in our reactions. Sulfate radical can react with Leu by hydrogen abstraction,⁷⁰ and carbon centered radicals have been previously observed in the reaction of $SO_4^{\cdot -}$ with Leu residues.⁷⁰ The transformation of Leu was not quenched by ethanol suggesting

that neither $\text{SO}_4^{\cdot-}$ nor $\cdot\text{OH}$ were driving the transformation. Another radical that can be formed is peroxymonosulfate radical (eq 3.9). Peroxymonosulfate radical reacts by one electron transfer with derivatized phenols and aromatic amines, but the products of reaction have not been studied.⁵⁷⁻⁵⁹ Based on the observed mass shifts of +16 and + 14 m/z , which are observed in the products of $\text{SO}_4^{\cdot-}$ and $\cdot\text{OH}$ with amino acids, we propose that the reaction of $\text{SO}_5^{\cdot-}$ with Leu is similar to that of $\text{SO}_4^{\cdot-}$ and $\cdot\text{OH}$ and starts with the formation of an organic radical, which reacts with molecular oxygen to form a peroxy radical that could lead to the formation of the hydroxylated and carbonyl products. This hypothesis could be tested by conducting reactions in the absence of molecular oxygen or by using $^{18}\text{O}_2$ to verify that molecular oxygen is adding to the amino acids.

The transformation of Lys resulted in a mass shift of +16 m/z , indicative of a hydroxylation product such as hydroxyl-lysine. In the presence of oxygen, the attack of $\cdot\text{OH}$ by hydrogen abstraction results in several hydroxy-Lys products.⁶⁹ Hydroxy-lysine has also been reported in the oxidation by $\text{SO}_4^{\cdot-}$, which abstracts a hydrogen from Lys and can also lead to the formation of nitrogen-centered radicals.^{70,71} As is the case with Leu, the lack of quenching of the reaction observed in the presence of ethanol suggests that neither $\text{SO}_4^{\cdot-}$ nor $\cdot\text{OH}$ are transforming Lys. If $\text{SO}_5^{\cdot-}$ is a reactant in the system the formation of carbon- and nitrogen- centered radicals should be further studied, possibly with electron spin resonance (ESR).

The products of transformation of methionine were Met-sulfoxide and Met-sulfone, these products were confirmed with authentic standards by LC-MS/MS (the products of reaction had the same retention time and fragmentation pattern as the standards). These products of reaction were also observed in the reaction with unactivated peroxymonosulfate (Ruiz et al. 2015). The reaction of methionine with both $\text{SO}_4^{\cdot-}$ and $\cdot\text{OH}$ can lead to the formation of Met-sulfoxide and

Met-sulfone.^{38,62} Xu et al, studied the transformation of Met residues by $\cdot\text{OH}$, initiated by the addition of $\cdot\text{OH}$ forming a sulfur radical that reacts with oxygen, an oxygen radical is formed and dehydration occurs resulting in methionine sulfoxide⁶⁸

No chlorinated products were observed. This might be due to the low concentrations of amino acids and chloride used in the reactions. Reactive chlorine species that can form in Co^{2+} -activated peroxymonosulfate systems containing chloride include $\text{Cl}\cdot$, $\text{Cl}_2\cdot^-$ and HOCl (eq 3.10-3.13). At the low Cl^- concentration used (18 μM) only $\text{Cl}\cdot$ and HOCl (eq 3.13) are expected to be present in higher chloride concentrations.

Environmental Implications. Consistent with expectations, the reaction of amino acids by cobalt-activated peroxymonosulfate resulted in higher rates of oxidation than peroxymonosulfate alone (Ruiz et al. 2015). The transformation of free amino acid is expected to differ from the oxidation of amino acid residues in a protein. In a protein structure both the amino acid side chain and the peptide backbone are liable to oxidation by hydroxyl radical.⁷² The rate tryptophan oxidation by H_2O_2 decreases in the order of free Trp > short peptides containing Trp > protein (lysozyme).⁶⁵ The reaction kinetics of amino acid residues in a protein differ from those of free amino acids in part due to their location in the tertiary structure. Lundeen et al., found that the rates of singlet oxygen transformation of free amino acid and residues in peptides was faster than in proteins, and that solvent accessible amino acids had higher rates of reaction than amino acid residues present in the inside of the protein.⁷³ Sulfate radical generated by cobalt-activated peroxymonosulfate has been shown to degrade microcystin-LR, a peptidic contaminant.²⁶ Based on the degradation of microcystin-LR, and our study, cobalt-activated peroxymonosulfate has the potential to degrade proteinaceous and peptidic contaminants, such as prion protein, ricin, and cyanotoxins. Activation of peroxymonosulfate to produce sulfate

radicals can also be achieved with iron (II, III), which might be a better alternative than cobalt due to toxicity concerns and the presence of iron oxides and minerals in the environment.^{14,74} Iron oxides (goethite, ferrihydrite, pyrolusite) and iron-bearing clays have been used in the slow activation of persulfate (S_2O_8).^{12,14} The activation of HSO_5^- by iron-bearing minerals has not been examined, but warrants investigation. Although no chlorinated products were observed in this study further research must be conducted as chlorinated products are expected at higher chloride concentrations. The concentration of chloride in soils ranges from 20 to 900 $mg \cdot kg^{-1}$ with a mean of $\sim 100 \text{ } mg \cdot kg^{-1}$, and from <0.5 to $>6000 \text{ } mg \cdot L^{-1}$ soil solutions, higher than the concentration used in our study ($0.6372 \text{ } mg \cdot L^{-1}$).⁷⁵ A better understanding of the products of reaction for proteins will help us determine if cobalt-activated peroxymonosulfate is a viable oxidant for remediation technologies.

ACKNOWLEDGEMENTS

This work was funded in part by the United States Geological Survey (G10AC00676). MR was funded by a Graduate Engineering Research Scholars fellowship. We thank Christy Remucal and Megan McConville for use of the LC-MS/MS instrument and helpful discussions.

REFERENCES

- (1) Park, H. D.; Watanabe, M. F.; Harda, K.; Nagai, H.; Suzuki, M.; Watanabe, M.; Hayashi, H. Hepatotoxin (microcystin) and Neurotoxin (anatoxin-A) Contained in Natural Blooms and Strains of Cyanobacteria from Japanese Freshwaters. *Nat. Toxins* **1993**, *1*, 353–360.
- (2) Kotak, B. G.; Zurawell, R. W. Cyanobacterial Toxins in Canadian Freshwaters: A Review. *Lake Reserv. Manag.* **2007**, *23*, 109–122.
- (3) Darling, R. G.; Woods, J. B. *USAMRIID's Medical Management of Biological Casualties*; 5th ed.; 2004.
- (4) Johnson, C. J.; Phillips, K. E.; Schramm, P. T.; McKenzie, D.; Aiken, J. M.; Pedersen, J. a. Prions Adhere to Soil Minerals and Remain Infectious. *PLoS Pathog.* **2006**, *2*, e32.
- (5) Seidel, B.; Thomzig, A.; Buschmann, A.; Groschup, M. H.; Peters, R.; Beekes, M.; Terytze, K. Scrapie Agent (Strain 263K) Can Transmit Disease via the Oral Route after Persistence in Soil over Years. *PLoS One* **2007**, *2*.
- (6) Miller, M. W.; Williams, E. S.; Hobbs, N. T.; Wolfe, L. L. Environmental Sources of Prion Transmission in Mule Deer. *Emerg. Infect. Dis.* **2004**, *10*, 1003–1006.
- (7) Georgsson, G.; Sigurdarson, S.; Brown, P. Infectious Agent of Sheep Scrapie May Persist in the Environment for at Least 16 Years. *J. Gen. Virol.* **2006**, *87*, 3737–3740.
- (8) Rutala, W. A.; Weber, D. J. Guideline for Disinfection and Sterilization of Prion-Contaminated Medical Instruments. *Infect. Control Hosp. Epidemiol.* **2010**, *31*, 107–117.
- (9) *Handbook on Advance Photochemical Oxidation Processes*; Cincinnati, 1998.
- (10) Lewis, S.; Lynch, a; Bachas, L.; Hampson, S.; Ormsbee, L.; Bhattacharyya, D. Chelate-Modified Fenton Reaction for the Degradation of Trichloroethylene in Aqueous and Two-Phase Systems. *Environ. Eng. Sci.* **2009**, *26*, 849–859.

- (11) Huling, S. G.; Pivetz, B. E. *In-Situ Chemical Oxidation*; 2006.
- (12) Liu, H.; Bruton, T. a.; Doyle, F. M.; Sedlak, D. L. In Situ Chemical Oxidation of Contaminated Groundwater by Persulfate: Decomposition by Fe(III)^- and Mn(IV)^- Containing Oxides and Aquifer Materials. *Environ. Sci. Technol.* **2014**, 140818115708002.
- (13) Neta, P.; Huie, R. E.; Ross, A. B. Rate Constants for Reactions of Inorganic Radicals in Aqueous Solutions. *J. Phys. Chem. Ref. Data* **1988**, 17, 1027–1284.
- (14) Anipsitakis, G. P.; Dionysiou, D. D. Radical Generation by the Interaction of Transition Metals with Common Oxidants. *Environ. Sci. Technol.* **2004**, 38, 3705–3712.
- (15) Neta, P.; Madhavan, V.; Zemel, H.; Fessenden, R. W. Rate Constants and Mechanism of Reaction of $\text{SO}_4^{\bullet-}$ with Aromatic Compounds. *J. Am. Chem. Soc.* **1977**, 99, 163–164.
- (16) Pham, A. L.-T.; Doyle, F. M.; Sedlak, D. L. Kinetics and Efficiency of H_2O_2 Activation by Iron-Containing Minerals and Aquifer Materials. *Water Res.* **2012**, 46, 6454–6462.
- (17) Pham, A. L.; Doyle, F. M.; Sedlak, D. L. Kinetics and Efficiency of H_2O_2 Activation by Iron-Containing Minerals and Aquifer Materials. *Water Res.* **2012**, 46, 6454–6462.
- (18) Kwan, W. P.; Voelker, B. M. Rates of Hydroxyl Radical Generation and Organic Compound Oxidation in Mineral-Catalyzed Fenton-like Systems. *Environ. Sci. Technol.* **2003**, 37, 1150–1158.
- (19) Anipsitakis, G. P.; Dionysiou, D. D.; Gonzalez, M. A. Cobalt-Mediated Activation of Peroxymonosulfate and Sulfate Radical Attack on Phenolic Compounds. Implications of Chloride Ions. *Environ. Sci. Technol.* **2006**, 40, 1000–1007.
- (20) Anipsitakis, G. P.; Tufano, T. P.; Dionysiou, D. D. Chemical and Microbial Decontamination of Pool Water Using Activated Potassium Peroxymonosulfate. *Water Res.* **2008**, 42, 2899–2910.
- (21) Shukla, P.; Fatimah, I.; Wang, S.; Ang, H. M.; Tadé, M. O. Photocatalytic Generation of Sulphate and Hydroxyl Radicals Using Zinc Oxide under Low-Power UV to Oxidise

Phenolic Contaminants in Wastewater. *Catal. Today* **2010**, *157*, 410–414.

- (22) Yang, S.; Wang, P.; Yang, X.; Shan, L.; Zhang, W.; Shao, X.; Niu, R. Degradation Efficiencies of Azo Dye Acid Orange 7 by the Interaction of Heat, UV and Anions with Common Oxidants: Persulfate, Peroxymonosulfate and Hydrogen Peroxide. *J. Hazard. Mater.* **2010**, *179*, 552–558.
- (23) Guan, Y.-H.; Ma, J.; Li, X.-C.; Fang, J.-Y.; Chen, L.-W. Influence of pH on the Formation of Sulfate and Hydroxyl Radicals in the UV/peroxymonosulfate System. *Environ. Sci. Technol.* **2011**, *45*, 9308–9314.
- (24) Hebert, V. R.; Miller, G. C. Depth Dependence of Direct and Indirect Photolysis on Soil Surfaces. *J. Agric. Food Chem.* **1990**, *38*, 913–918.
- (25) Chan, K. H.; Chu, W. Degradation of Atrazine by Cobalt-Mediated Activation of Peroxymonosulfate: Different Cobalt Counteranions in Homogenous Process and Cobalt Oxide Catalysts in Photolytic Heterogeneous Process. *Water Res.* **2009**, *43*, 2513–2521.
- (26) Antoniou, M. G.; de la Cruz, A. a.; Dionysiou, D. D. Degradation of Microcystin-LR Using Sulfate Radicals Generated through Photolysis, Thermolysis and e[−] Transfer Mechanisms. *Appl. Catal. B Environ.* **2010**, *96*, 290–298.
- (27) Do, S.-H.; Jo, J.-H.; Jo, Y.-H.; Lee, H.-K.; Kong, S.-H. Application of a Peroxymonosulfate/cobalt (PMS/Co(II)) System to Treat Diesel-Contaminated Soil. *Chemosphere* **2009**, *77*, 1127–1131.
- (28) Bosio, G.; Criado, S.; Massad, W.; Rodríguez Nieto, F. J.; Gonzalez, M. C.; García, N. A.; Mártire, D. O. Kinetics of the Interaction of Sulfate and Hydrogen Phosphate Radicals with Small Peptides of Glycine, Alanine, Tyrosine and Tryptophan. *Photochem. Photobiol. Sci.* **2005**, *4*, 840–846.
- (29) Criado, S.; Marioli, J. M.; Allegretti, P. E.; Furlong, J.; Rodríguez Nieto, F. J.; Mártire, D. O.; García, N. a. Oxidation of Di- and Tripeptides of Tyrosine and Valine Mediated by Singlet Molecular Oxygen, Phosphate Radicals and Sulfate Radicals. *J. Photochem. Photobiol. B.* **2001**, *65*, 74–84.
- (30) Redpath, J. L.; Willson, R. L. Chain Reactions and Radiosensitization: Model Enzyme

- Studies. *Int. J. Radiat. Biol. Relat. Stud. Phys., Chem. Med.* **1975**, 27, 389–398.
- (31) Richard C. Thompson. Catalytic Decomposition of Peroxymonosulfate in Aqueous Perchloric Acid by the Dual Catalysts Ag^+ and $\text{S}_2\text{O}_4^{2-}$ and by Co^{2+} . *Inorg. Chem.* **1981**, 20, 1005–1010.
 - (32) Kim, J.; Edwards, J. O. A Study of Cobalt Catalysis and Copper Modification in the Coupled Decompositions of Hydrogen Peroxide and Peroxomonosulfate Ion. *Inorganica Chim. Acta* **1995**, 235, 9–13.
 - (33) Steele, W. V; Appelman, E. H. The Standard Enthalpy of Formation of Peroxymonosulfate (HSO_5^-) and the Standard Electrode Potential of the Peroxymonosulfate-Bisulfate Couple. *J. Chem. Thermodyn.* **1982**, 14, 337–344.
 - (34) Ball, D. L.; Edwards, J. O. The Kinetics and Mechanism of the Decomposition of Caro's Acid. I. *J. Am. Chem. Soc.* **1956**, 78, 1125–1129.
 - (35) Maruthamuthu, P.; Neta, P. Radiolytic Chain Decomposition of Peroxomonophosphoric and Peroxomonosulfuric Acids. *J. Phys. Chem.* **1977**, 81, 937–940.
 - (36) Xu, G.; Chance, M. R. Radiolytic Modification of Sulfur-Containing Amino Acid Residues in Model Peptides: Fundamental Studies for Protein Footprinting. *Anal. Chem.* **2005**, 77, 2437–2449.
 - (37) Cohen, S. A. Applications of Amino Acid Derivatization with 6- Carbamate Analysis of Feed Grains , Intravenous Glycoproteins Solutions and. **1994**, 661, 25–34.
 - (38) Xu, G.; Chance, M. R. Radiolytic Modification and Reactivity of Amino Acid Residues Serving as Structural Probes for Protein Footprinting. *Anal. Chem.* **2005**, 77, 4549–4555.
 - (39) Qi, F.; Chu, W.; Xu, B. Catalytic Degradation of Caffeine in Aqueous Solutions by Cobalt-MCM41 Activation of Peroxymonosulfate. *Appl. Catal. B Environ.* **2013**, 134-135, 324–332.
 - (40) Anipsitakis, G. P.; Dionysiou, D. D. Degradation of Organic Contaminants in Water with Sulfate Radicals Generated by the Conjunction of Peroxymonosulfate with Cobalt.

Environ. Sci. Technol. **2003**, 37, 4790–4797.

- (41) Chu, C.; Lundeen, R. a.; Remucal, C. K.; Sander, M.; McNeill, K. Enhanced Indirect Photochemical Transformation of Histidine and Histamine through Association with Chromophoric Dissolved Organic Matter. *Environ. Sci. Technol.* **2015**, 49, 5511–5519.
- (42) Stadtman, E. R.; Levine, R. L. Free Radical-Mediated Oxidation of Free Amino Acids and Amino Acid Residues in Proteins. *Amino Acids* **2003**, 25, 207–218.
- (43) Ito, K. A Theory Generalized to Cage Effects in Radical Formation for Determining Initiator Efficiency. *Polym. J.* **1985**, 17, 421–426.
- (44) Pryor, W. A.; Squadrito, G. L. The Chemistry of Peroxynitrite: A Product from the Reaction of Nitric Oxide with Superoxide. *Am. J. Physiol.* **1995**, 268, L699–L722.
- (45) Wondrak, G. T.; Varadarajan, S.; Butterfield, D. A.; Jacobson, M. K. Formation of a Protein-Bound Pyrazinium Free Radical Cation during Glycation of Histone H1. *Free Radic. Biol. Med.* **2000**, 29, 557–567.
- (46) Amici, A.; Levine, R. L.; Tsai, L.; Stadtman, E. R. Conversion of Amino Acid Residues in Proteins and Amino Acid Homopolymers to Carbonyl Derivatives by Metal-Catalyzed Oxidation Reactions. *J. Biol. Chem.* **1989**, 264, 3341–3346.
- (47) Furia, T. E. Sequestrants in Foods. In *CRC Handbook of Food Additives*; Intechmark Corporation: Palo Alto, 1972; pp. 275–277.
- (48) Boruah, D. Interaction of Cobalt (II) and Nickel (II) Ions with Amino Acids in Aqueous Solution : A Spectrophotometric Study. **2012**, 2, 3–6.
- (49) Francis, R. C.; Troughton, N. A.; Zhang, X.-Z.; Hill, R. T. Carboxylate Delignification Enhancement by Halides. *Tappi J.* 77, 135–141.
- (50) Fortnum, D. H.; Battaglia, C. J.; Cohen, S. R.; Edwards, J. The Kinetics of the Oxidation of Halide Ions by Monosubstituted Peroxides. *J. Am. Chem. Soc.* **1960**, 82, 778–782.

- (51) Alegre, M.; Gerone, M.; Rosso, J. A.; Bertolotti, S. G.; Braun, A. M.; Mártire, D. O.; Gonzalez, M. C. Kinetic Study of the Reactions of Chlorine Atoms and $\text{Cl}_2^{\bullet-}$ Radical Anions in Aqueous Solutions . 1 . Reaction with Benzene. *J. Phys. Chem. A* **2000**, *104*, 3117–3125.
- (52) Vanýsek, P. Electrochemical Series. In *Handbook of Chemistry & Physics*; CRC; pp. 5.80–85.89.
- (53) Pattison, D. I.; Davies, M. J. Absolute Rate Constants for the Reaction of Hypochlorous Acid with Protein Side Chains and Peptide Bonds. *Chem. Res. Toxicol.* **2001**, *14*, 1453–1464.
- (54) Hawkins, C. L.; Davies, M. J. Reaction of HOCl with Amino Acids and Peptides: EPR Evidence for Rapid Rearrangement and Fragmentation Reactions of Nitrogen-Centred Radicals. *J. Chem. Soc. Perkin Trans. 2* **1998**, 1937–1946.
- (55) Sivey, J. D.; Howell, S. C.; Bean, D. J.; Mccurry, D. L.; Mitch, W. A.; Wilson, C. J. Role of Lysine during Protein Modification by HOCl and HOBr: Halogen-Transfer Agent or Sacrificial Antioxidant? *Biochemistry* **2013**, *52*, 1260–1271.
- (56) Das, T. N.; Huie, R. E.; Neta, P. Reduction Potentials of $\text{SO}_3^{\bullet-}$, $\text{SO}_5^{\bullet-}$, and $\text{S}_4\text{O}_6^{\bullet 3-}$ Radicals in Aqueous Solution. *J. Phys. Chem. A* **1999**, *103*, 3581–3588.
- (57) Huie, R. E.; Neta, P. One-Electron Redox Reactions in Aqueous Solutions of Sulfite with Hydroquinone and Other Hydroxyphenols. *J. Phys. Chem.* **1985**, *89*, 3918–3921.
- (58) Neta, P.; Huie, R. E. One-Electron Redox Reactions Involving Sulfite Ions and Aromatic Amines. *J. Phys. Chem.* **1985**, *89*, 1783–1787.
- (59) Huie, R. E.; Neta, P. Chemical Behavior of $(\text{SO}_3^{\bullet-})$ and $(\text{SO}_5^{\bullet-})$ Radicals in Aqueous Solutions. *J. Phys. Chem.* **1984**, *88*, 5665–5669.
- (60) Lee, H.; Lee, H.-J.; Sedlak, D. L.; Lee, C. pH-Dependent Reactivity of Oxidants Formed by Iron and Copper-Catalyzed Decomposition of Hydrogen Peroxide. *Chemosphere* **2013**, *92*, 652–658.

- (61) Moore, G.; Pettigrew, G. W. *Cytochromes c*; Springer-Verlag Berlin Heidelberg, 1990.
- (62) Gau, B. C.; Chen, H.; Zhang, Y.; Gross, M. L. Sulfate Radical Anion as a New Reagent for Fast Photochemical Oxidation of Proteins. *Anal. Chem.* **2010**, *82*, 7821–7827.
- (63) Finley, E. L.; Dillon, J.; Crouch, R. K.; Schey, K. L. Identification of Tryptophan Oxidation Products in Bovine Alpha-Crystallin. *Protein Sci.* **1998**, *7*, 2391–2397.
- (64) Guedes, S.; Vitorino, R.; Domingues, R.; Amado, F.; Domingues, P. Oxidation of Bovine Serum Albumin: Identification of Oxidation Products and Structural Modification. *Rapid Commun. Mass Spectrom.* **2009**, *23*, 2307–2315.
- (65) Simat, T.; Steinhart, H. Oxidation of Free Tryptophan and Tryptophan Residues in Peptides and Proteins. *J. Agric. Food Chem.* **1998**, *46*, 490–498.
- (66) Ito, T.; Morimoto, S.; Fujita, S.; Nishimoto, S. Radical Intermediates Generated in the Reactions of L-Arginine with Hydroxyl Radical and Sulfate Radical Anion: A Pulse Radiolysis Study. *Radiat. Phys. Chem.* **2009**, *78*, 256–260.
- (67) Olmez-Hanci, T.; Arslan-Alaton, I. Comparison of Sulfate and Hydroxyl Radical Based Advanced Oxidation of Phenol. *Chem. Eng. J.* **2013**, *224*, 10–16.
- (68) Xu, G.; Chance, M. R. Hydroxyl Radical-Mediated Modification of Proteins as Probes for Structural Proteomics. *Chem. Rev.* **2007**, *107*, 3514–3543.
- (69) Morin, B.; Bubb, W. a; Davies, M. J.; Dean, R. T.; Fu, S. 3-Hydroxylysine, a Potential Marker for Studying Radical-Induced Protein Oxidation. *Chem. Res. Toxicol.* **1998**, *11*, 1265–1273.
- (70) Rustgi, S. N.; Riesz, P. An E.S.R. and Spin-Trapping Study of the Reactions of the SO_4^- Radical with Protein and Nucleic Acid Constituents. *Int. J. Radiat. Biol.* **1978**, *34*, 301–316.
- (71) Ito, T.; Morimoto, S.; Fujita, S.; Kobayashi, K.; Tagawa, S.; Nishimoto, S. Carbon- and Nitrogen-Centered Radicals Produced from L-Lysine by Radiation-Induced Oxidation: A Pulse Radiolysis Study. *Chem. Phys. Lett.* **2008**, *462*, 116–120.

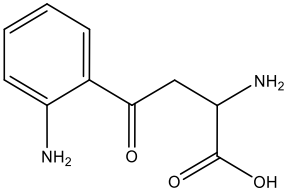
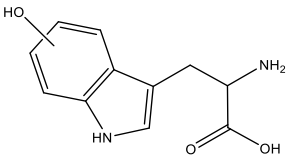
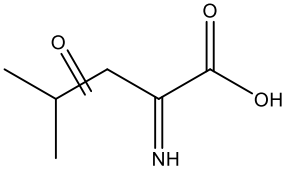
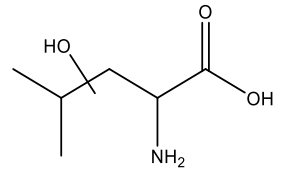
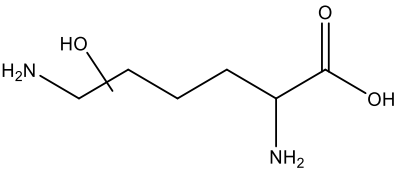
- (72) Garrison, W. M.; Jayko, M. E.; Bennett, W. Radiation-Induced Oxidation of Protein in Aqueous Solution. *Radiat. Res.* **1962**, *16*, 483–502.
- (73) Lundeen, R. a.; McNeill, K. Reactivity Differences of Combined and Free Amino Acids: Quantifying the Relationship between Three-Dimensional Protein Structure and Singlet Oxygen Reaction Rates. *Environ. Sci. Technol.* **2013**, *47*, 14215–14223.
- (74) Zou, J.; Ma, J.; Chen, L.; Li, X.; Guan, Y.; Xie, P.; Pan, C. Rapid Acceleration of Ferrous Iron/peroxymonosulfate Oxidation of Organic Pollutants by Promoting Fe(III)/Fe(II) Cycle with Hydroxylamine. *Environ. Sci. Technol.* **2013**, *47*, 11685–11691.
- (75) Mordtvedt., J. J. Bioavailability of Micronutrients. In *Handbook of Soil Science*; Sumner, M. E., Ed.; CRC Press, 2000.
- (76) Buxton, G. V.; Greenstock, C. L.; Helman, W. P.; Ross, A. B. Critical Review of Rate Constants for Reactions of Hydrated Electrons, Hydrogen Atoms and Hydroxyl Radicals (OH/O⁻) in Aqueous Solution. *J. Phys. Chem. Ref. Data* **1988**, *17*, 513–515 – 34.
- (77) Hayon, E.; Treinin, A.; Wilf, J. Electronic Spectra, Photochemistry, and Autoxidation Mechanism of the Sulfite-Bisulfite-Pyrosulfite Systems. SO₂⁻, SO₃⁻, SO₄⁻, and SO₅⁻ Radicals. **1972**, *94*, 47–57.
- (78) Khmelinskii, I. V.; Plyusnin, V. F.; Grivin, V. P. Mechanism of the Formation of the Cl₂⁻ Ion Radical in the Photolysis of the FeCl₄⁻ Complex in Ethanol Saturated with HCl. *Russ. J. Phys. Chem.* **1989**, *63*, 1494–1497.
- (79) Hasegawa, K.; Neta, P. Rate Constants and Mechanisms of Reaction of Cl₂⁻ Radicals. *J. Phys. Chem.* **1978**, *82*, 854–857.

Table 3.1. Reaction rate constants of ethanol and *tert*-butyl alcohol with sulfate, hydroxyl, and peroxymonosulfate, phosphate, and chloride radicals.^a

Quencher	Radical	k' ($\text{M}^{-1}\cdot\text{s}^{-1}$)	References
$\text{CH}_3\text{CH}_2\text{OH}$	$\text{SO}_4^{\cdot-}$	$1.6 \times 10^7 - 7.7 \times 10^7$	13
	$\cdot\text{OH}$	1.9×10^9	76
	$\text{SO}_5^{\cdot-}$	$<10^3$	77
	$\text{HPO}_4^{\cdot-}$	2.0×10^7	13
	$\text{H}_2\text{PO}_4^{\cdot}$	7.7×10^7	13
	$\text{Cl}\cdot$	1×10^9	78
	$\text{Cl}_2^{\cdot-}$	4.5×10^4	13
$(\text{CH}_3)_3\text{COH}$	$\text{SO}_4^{\cdot-}$	4.0×10^5	77
	$\cdot\text{OH}$	6×10^8	76
	$\text{Cl}_2^{\cdot-}$	1.9×10^6	79

^a No data are available for reaction of $\text{SO}_5^{\cdot-}$ with *tert*-butyl alcohol.

Table 3.2. Products of amino acid oxidation by $\text{HSO}_5^- + \text{Co}^{2+}$

Amino Acid	$\text{M}+\text{H}^+$ (m/z)	Possible products	
		Name	Structure
Trp	209	kynurenine	
	221	hydroxy-tryptophan	
Leu	146	carbonyl-leucine*	
	148	hydroxy-leucine*	
Lys	163	hydroxyl-lysine*	

*The reaction of Lys and Leu with hydroxyl radical and sulfate radical results in a mixture of products at different positions.

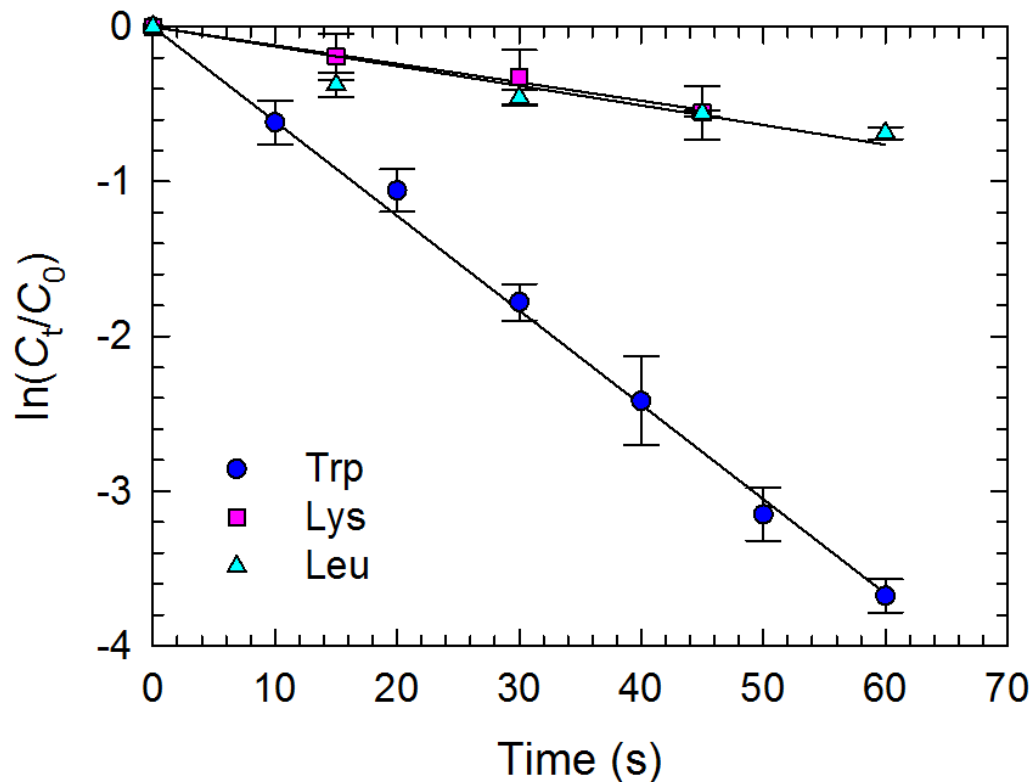


Figure 3.1. Amino acid oxidation by cobalt-activated peroxydisulfate. Experimental conditions: $[\text{amino acid}]_0 = 0.45 \text{ mM}$, $[\text{HSO}_5^-]_0 = 4.5 \text{ mM}$, $[\text{CoCl}_2]_0 = 9 \text{ }\mu\text{M}$, pH 7 (0.1 M phosphate). Error bars represent one standard deviation ($n = 3$).

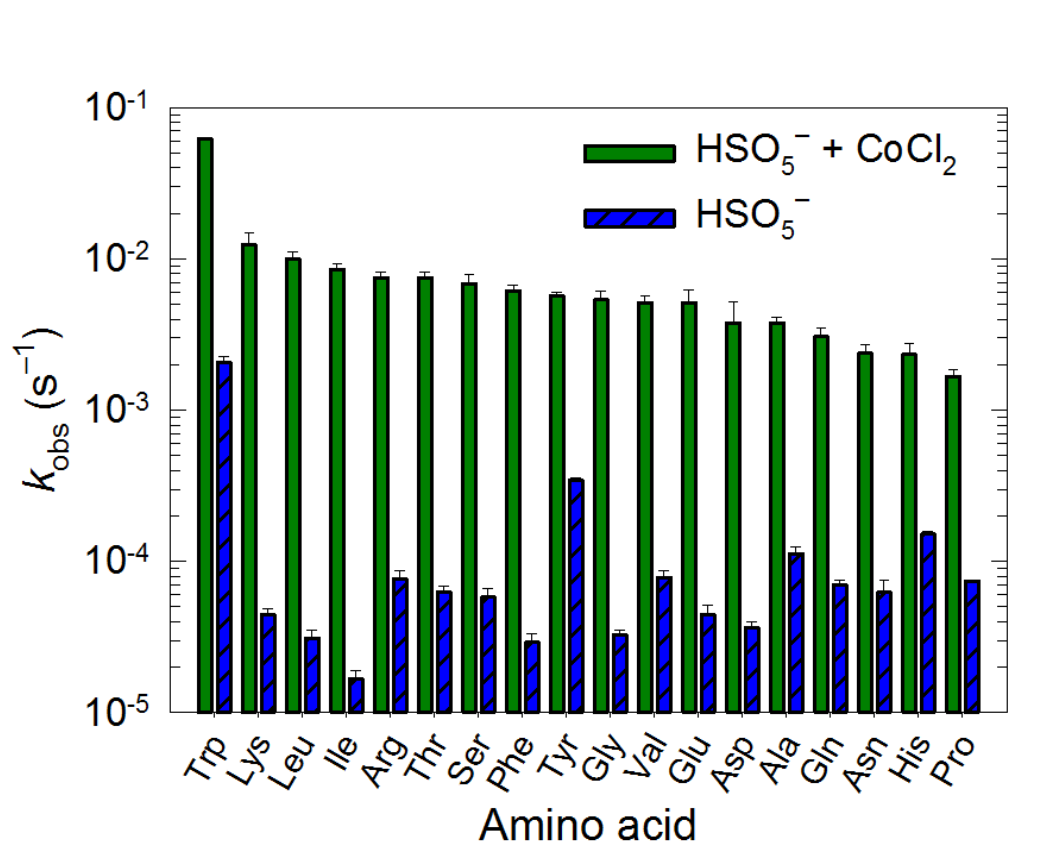


Figure 3.2. Pseudo first-order rate constants for amino acid by transformation by peroxymonosulfate and cobalt-activated peroxymonosulfate. Experimental conditions: [amino acid]₀ = 0.45 mM, [HSO₅⁻]₀ = 4.5 mM, [CoCl₂]₀ = 9 μM, pH 7 (0.1 M phosphate). Unactivated HSO₅⁻ data adapted from (Ruiz et al., 2015). Error bars represent one standard deviation ($n = 3$).

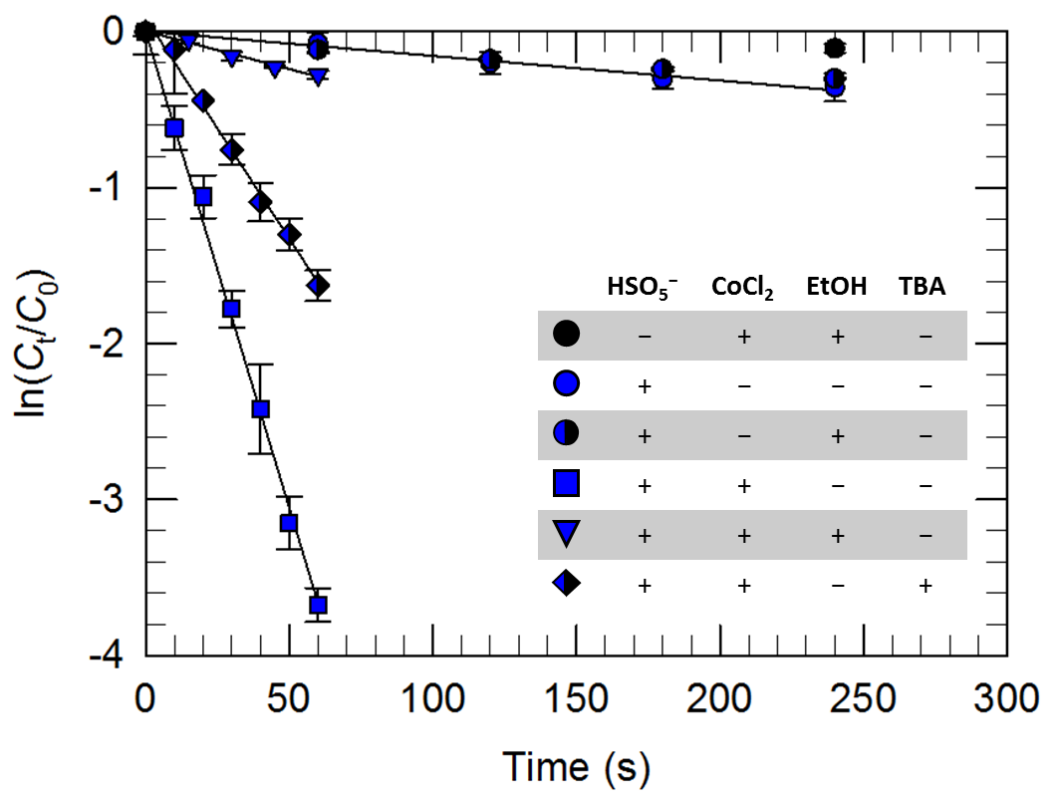


Figure 3.3. Tryptophan oxidation by cobalt-activated peroxymonosulfate. Experimental conditions: $[\text{Trp}]_0 = 0.45 \text{ mM}$, $[\text{HSO}_5^-]_0 = 4.5 \text{ mM}$, $[\text{CoCl}_2]_0 = 9 \text{ }\mu\text{M}$, pH 7 (0.1 M phosphate). The control was Trp in the absence of HSO_5^- and presence of CoCl_2 . Error bars represent one standard deviation ($n = 3$).

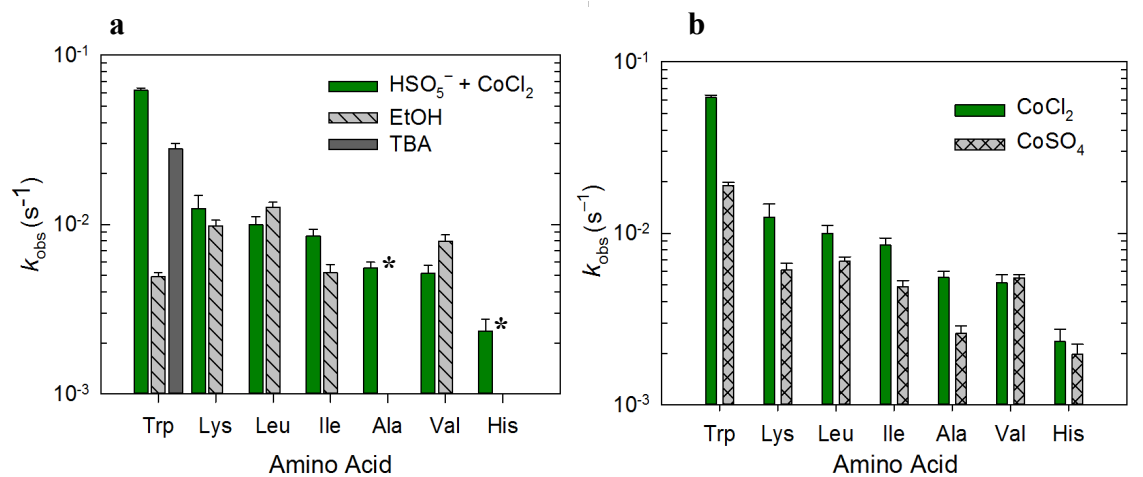


Figure 3.4. The effect of (a) radical quenchers and (b) cobalt counterion on the oxidation of amino acid by cobalt-activated peroxydisulfate. Experimental conditions: [amino acid]₀ = 0.45 mM, [HSO₅[−]]₀ = 4.5 mM, [Co²⁺]₀ = 9 μM, pH 7 (0.1 M phosphate), alcohol:HSO₅[−] 1000:1. Error bars represent one standard deviation (*n* = 3). (a) *The presence of EtOH and TBA completely quenched the reaction of Ala and His (>98%, >90% amino acid remaining respectively). (b) The rate constant decreased in the absence of chloride except for Val and His.

Chapter 3S. Supporting information for: Transformation of Amino Acids by Cobalt-activated Peroxymonosulfate

This chapter is part of a manuscript is going to be submitted with the following co-author:

Joel A. Pedersen

Environmental Chemistry and Technology Program, University of Wisconsin, Madison, WI
53706, USA

Text S1. HPLC parameters

Text 3S.2 LC-MS/MS parameters

Text 3S.3. Stability of amino acids in reaction conditions

Text 3S.4. Filtration

Table 3S.1. Pseudo first order observed rate constant of amino acid oxidation by $\text{HSO}_5^- + \text{Co}^{2+}$

Table 3S.2. Agilent 1050 HPLC mobile phases and gradients

Table 3S.3. Agilent 1260 HPLC separation conditions

Table 3S.4. MRM parameters for amino acids and product standards

Table 3S.5. Stability constant of amino acid complexes with cobalt (II)

Table 3S.6. Reaction rates of some radical species

Table 3S.7. Retention times of standards and observed products of oxidation

Table 3S.8. Observed rate constants of amino acid transformation by $\text{HSO}_5^- + \text{Co}^{2+}$ in the presence of radical scavengers and HSO_5^- activated with CoSO_4

3S.1. Supporting Materials and Methods

Stability of amino acids in reaction conditions. The stability of all studied amino acids in the absence of peroxymonosulfate under our experimental conditions was assessed (see main text). Additional controls were performed for the alcohol quenching studies, with the appropriate alcohol added to the control reaction in the absence of peroxymonosulfate. The concentration of each amino acid at the end of the control experiments was $\geq 96\%$ (data not shown) of the initial concentration for all the amino acid studied.

Filtration. Samples were filtered prior to analysis because cobalt can precipitate in the presence of phosphate, $\text{Co}_3(\text{PO}_4)_2$ ($K_{\text{sp}} = 2.05 \times 10^{-35}$). Initial experiments with tryptophan were conducted to determine if the amino acid was lost to the filter. No loss of tryptophan was observed (data not shown). For the rest of the amino acids control experiments were conducted that included filtration.

3S.2. LC-MS/MS Parameters. Source Parameters. Gas temperature 300 °C, gas flow 7 L·min⁻¹, nebulizer 310 kPa, sheath gas temperature 350 °C, sheath gas flow 10 L·min⁻¹. Capillarity 3500 V, nozzle voltage 500 V.

LC-MS/MS mobile phase gradient. The column temperature was controlled at 40 °C, the sample volume was 10-50 µL, and the flow rate was 0.25 mL·min⁻¹. The mobile phase consisted of (A) 10 mM ammonium acetate pH 7.5 with 10% acetonitrile and (B) acetonitrile. The elution gradient was 0-5 min 100% A, 20 min 60% A, 20-30 min 100% A.

Table 3S.1. Observed rate constants of amino acid transformation by $\text{HSO}_5^- + \text{Co}^{2+}$

Amino Acid	$k_{\text{obs}} (\text{s}^{-1})$	R^2
Trp	$6.2 (\pm 0.2) \times 10^{-2}$	1.00
Lys	$1.2 (\pm 0.2) \times 10^{-2}$	0.74
Leu	$1.0 (\pm 0.1) \times 10^{-2}$	0.87
Ile	$8.5 (\pm 0.7) \times 10^{-3}$	0.88
Arg	$7.5 (\pm 0.7) \times 10^{-3}$	0.91
Thr	$7.5 (\pm 0.7) \times 10^{-3}$	0.91
Ser	$6.9 (\pm 0.1) \times 10^{-3}$	0.81
Phe	$6.2 (\pm 0.6) \times 10^{-3}$	0.92
Tyr	$5.7 (\pm 0.4) \times 10^{-3}$	0.96
Gly	$5.4 (\pm 0.8) \times 10^{-3}$	0.83
Val	$5.2 (\pm 0.6) \times 10^{-3}$	0.91
Glu	$5.0 (\pm 1) \times 10^{-3}$	0.76
Asp	$4.0 (\pm 1) \times 10^{-3}$	0.99
Ala	$3.6 (\pm 0.4) \times 10^{-3}$	0.94
Gln	$3.1 (\pm 0.4) \times 10^{-3}$	0.81
Asn	$2.4 (\pm 0.3) \times 10^{-3}$	0.80
His	$2.3 (\pm 0.4) \times 10^{-3}$	0.75
Pro	$1.7 (\pm 0.2) \times 10^{-3}$	0.85

Table 3S.2. Agilent 1050 HPLC mobile phases and gradients

Amino acid	Mobile phase	Gradient
Glu, Asp	A = Formic acid 0.1 % B = 60:40 ACN:H ₂ O	0 min 80% A, 20 min 50 % A, 21 min 50 % A, 21.01 min 80 % A, 28 min 80% A.
Tyr	A = NaAc 15 mM pH 5 B = ACN	0-0.5 min 90% A, 0.6-2 min 80 % A, 2.01-8 min 65 % A, 8.05-12 min 90 % A.
Trp	A = NaAc 15 mM pH 5 B = ACN	0-2 min 90% A, 2.01-5 min 75 % A, 5.01-6 min 65 % A, 7.01-8.0 min 90 % A.
Remaining	A = NaAc 15 mM pH 5 B = 60:40 ACN:H ₂ O	0 min 80% A, 20 min 50 % A, 21 min 50 % A, 21.01 min 80 % A, 28 min 80% A.

Abbreviations: ACN, acetonitrile; NaAc, sodium acetate.

Table 3S.3. Agilent 1260 HPLC separation conditions

Amino acid	Mobile phase
Trp	90% A 2 min.
Ala, His, Leu, Lys, Val	0-1.5 min 100% A. 3-4 min 70% A. 5-10 min 100% A

Table 3S.4. MRM parameters for amino acids and product standards

Compound Name	Precursor Ion (<i>m/z</i>)	Product Ion (<i>m/z</i>)	Dwell time (ms)	Fragmentor (V)	Collision Energy (eV)
Trp-OH	221.1	204.1	75	85	8
		162.1	75	85	20
Kyn	209.1	146.1	75	90	20
		94.1	75	90	12
		65.1	75	90	64
Trp	205.2	188.1	75	80	8
		146.1	75	80	16
Methionine-sulfone	182	56	75	90	24
Methionine-sulfoxide	166	74	75	85	12
		56.1	75	85	24
Met	150	104	75	95	8
		56	75	95	16
Lys	147.2	130.1	200	80	8
		84.1	200	80	20
Leu	132.2	86.2	200	80	8
		44.2	200	80	28

All samples were analyzed in positive mode with a cell accelerator voltage of 4 V.

Table 3S.5. Stability constant of amino acid complexes with cobalt (II)

Amino Acid	log <i>K</i>
Alanine	4.82 ^b
Aspartic acid	5.9 ^b
Cysteine	9.3 ^b
Glutamic acid	5.06 ^b
Histidine	7.3 ^b
Leucine	4.49 ^b
Lysine	1.785 ^a
Proline	2.35 ^a
Threonine	1.981 ^a

^a Data obtained from Boruah et al.¹ Experimental conditions pH 5.04, 5.29, 5.88 for proline, threonine and lysine respectively. ^b Data obtained from the *CRC Handbook of Food Additives*.²

Table 3S.6. Reaction rates of some radical species^a

Reaction	k' (M ⁻¹ s ⁻¹)	pH
Chlorine oxide radical		
$\text{ClO}_2\cdot + \text{Cl}_2\cdot^- \rightarrow$	1.0×10^9	5
$\text{ClO}_2\cdot + \cdot\text{OH} \rightarrow \text{ClO}_3^- + \text{H}^+$	4.0×10^9	~7
$\text{ClO}_2\cdot + \text{ClO}_2\cdot \rightarrow$	$(2.5-7.5) \times 10^9$	
$\text{ClO}_2\cdot + \text{Ala} \rightarrow$	$< 10^2$	8
$\text{ClO}_2\cdot + \text{CysSH} \rightarrow$	$\sim 1 \times 10^2 - \sim 1 \times 10^3$	2.5-3.5
$\text{ClO}_2\cdot + \text{TrpH} \rightarrow$	7.6×10^5	~12
$\text{ClO}_2\cdot + \text{TyrOH} \rightarrow$	8.2×10^7	~12
Dichloride radical		
$\text{Cl}_2\cdot^- + \text{Cl}_2\cdot^- \rightarrow \text{Cl}^- + \text{Cl}_3^-$	$(2-8.5) \times 10^9$	7
$\text{Cl}_2\cdot^- + \text{Co}^{2+} \rightarrow \text{Cl}^- + \text{CoCl}^{2+}$	$(2.3-1.4) \times 10^6$	~1
$\text{Cl}_2\cdot^- + \text{CH}_3\text{CH}_2\text{OH} \rightarrow$	4.5×10^4	1
$\text{Cl}_2\cdot^- + \text{Ala} \rightarrow$	1.3×10^5	1
$\text{Cl}_2\cdot^- + \text{CysSH} \rightarrow$	8.5×10^8	1.8
$\text{Cl}_2\cdot^- + \text{Glu} \rightarrow$	2.3×10^5	1
$\text{Cl}_2\cdot^- + \text{Gly} \rightarrow$	$< 10^4$	1
$\text{Cl}_2\cdot^- + \text{His} \rightarrow$	1.4×10^7	1.8
$\text{Cl}_2\cdot^- + \text{Ser} \rightarrow$	1.2×10^5	1
$\text{Cl}_2\cdot^- + \text{TrpH} \rightarrow$	2.5×10^9	1.8
$\text{Cl}_2\cdot^- + \text{TyrOH} \rightarrow$	2.7×10^8	1.8
Chloride radical		
$\text{Cl}\cdot + \text{Cl}\cdot \rightarrow \text{Cl}_2$	8.8×10^7	
$\text{Cl}\cdot + \text{Cl}^- \rightarrow \text{Cl}_2\cdot^-$	$6.5 \times 10^9 - 2.1 \times 10^9$	
$\text{Cl}\cdot + \text{OH}^- \rightarrow \text{ClOH}^-$	1.8×10^{10}	
$\text{Cl}\cdot + \text{ClO}_2^- \rightarrow \text{ClO}_2\cdot + \text{Cl}^-$	8.2×10^9	
Sulfate radical		

$\text{SO}_4^{\cdot-} + \text{SO}_4^{\cdot-} \rightarrow \text{S}_2\text{O}_8^{2-}$	$3.8 \times 10^8 - 1.8 \times 10^9$	<0-5.8
$\text{SO}_4^{\cdot-} + \text{Cl}^- \rightarrow \text{SO}_4^{2-} + \text{Cl}^{\cdot}$	$(2.0-3.1) \times 10^8$	1.4-6.8
$\text{SO}_4^{\cdot-} + \text{Co}^{2+} \rightarrow \text{SO}_4^{2-} + \text{Co}^{3+}$	2.0×10^6	<0
$\text{SO}_4^{\cdot-} + \text{OH}^- \rightarrow \text{SO}_4^{2-} + \cdot\text{OH}$	$(4.6-8.3) \times 10^7$	>11
$\text{SO}_4^{\cdot-} + \text{H}_2\text{O} \rightarrow \text{SO}_4^{2-} + \text{HO}_2^{\cdot} + \text{H}^+$	$<6 \times 10^1$	7
$\text{SO}_4^{\cdot-} + \text{S}_2\text{O}_8^{2-} \rightarrow \text{SO}_4^{2-} + \text{S}_2\text{O}_8^{\cdot-}$	1.2×10^6	
$\text{SO}_4^{\cdot-} + \text{HSO}_4^- \rightarrow$	$<1 \times 10^5$	
$\text{SO}_4^{\cdot-} + \text{CH}_3\text{CH}_2\text{OH} \rightarrow \text{SO}_4^{2-} + \text{CH}_3\text{CHOH} + \text{H}^+$	$(1.6-7.7) \times 10^7$	4.8-8
$\text{SO}_4^{\cdot-} + \text{Ala} \rightarrow$	1.0×10^7	7
$\text{SO}_4^{\cdot-} + \text{Gly} \rightarrow$	1.0×10^7	7
$\text{SO}_4^{\cdot-} + \text{His} \rightarrow$	$\sim 2.5 \times 10^6$	7
$\text{SO}_4^{\cdot-} + \text{Met} \rightarrow$	1.1×10^9	>3
$\text{SO}_4^{\cdot-} + \text{Ser} \rightarrow$	2.3×10^7	7
$\text{SO}_4^{\cdot-} + \text{TrpH} \rightarrow$	$\sim 2 \times 10^9$	7
$\text{SO}_4^{\cdot-} + \text{TyrOH} \rightarrow$	3.2×10^9	7

Peroxymonosulfate radical



Phosphate radical formation^b



Hydroxyl radical^c



^a Table adapted from Neta et. al.³; ^b values obtained from Maruthamuthu and Neta (1978).⁴ ^c values obtained from Xu and Chance (2005).⁵

Table 3S.7. Retention times of standards and observed products of oxidation

<i>m/z</i>	Standard	Standard Retention time (min)	Sample Retention time (min)
221	5-hydroxy tryptophan	5.6	7
209	Kynurenine	6.8	6.8
205	Trp	8.7	8.7
132	Leu	5.6	5.6
146	2-(hydroxyimino)-4-methylpentanoic acid	NA	4.6
148	Leu-hydroxide	NA	4.6
147	Lys	5.3	5.3
162	Lys-hydroxide	NA	5.6

 NA no standard obtained

Table 3S.8. Observed rate constants of amino acid transformation by $\text{HSO}_5^- + \text{Co}^{2+}$ in the presence of radical scavengers and HSO_5^- activated with CoSO_4

Amino Acid	Ethanol k_{obs} (s^{-1})	<i>tert</i> -Butanol k_{obs} (s^{-1})	CoSO_4 k_{obs} (s^{-1})
Ala	NA*	NA	$2.6 (\pm 0.3) \times 10^{-3}$
His	NA*	NA	$2.0 (\pm 0.3) \times 10^{-3}$
Ile	$5.2 (\pm 0.6) \times 10^{-3}$	NA	$4.9 (\pm 0.4) \times 10^{-3}$
Leu	$1.3 (\pm 0.1) \times 10^{-2}$	NA	$6.9 (\pm 0.4) \times 10^{-3}$
Lys	$1.8 (\pm 0.8) \times 10^{-3}$	NA	$6.1 (\pm 0.6) \times 10^{-3}$
Val	$8.0 (\pm 0.7) \times 10^{-3}$	NA	$5.5 (\pm 0.5) \times 10^{-3}$
Trp	$4.9 (\pm 0.3) \times 10^{-3}$	$2.8 (\pm 0.2) \times 10^{-2}$	$1.9 (\pm 0.1) \times 10^{-2}$

NA values not obtained. *The reaction of His and Ala was completely quenched in the presence of ethanol

References

- (1) Boruah, D. Interaction of Cobalt (II) and Nickel (II) Ions with Amino Acids in Aqueous Solution : A Spectrophotometric Study. **2012**, 2, 3–6.
- (2) Furia, T. E. Sequestrants in Foods. In *CRC Handbook of Food Additives*; Intechmark Corporation: Palo Alto, 1972; pp. 275–277.
- (3) Neta, P.; Huie, R. E.; Ross, A. B. Rate Constants for Reactions of Inorganic Radicals in Aqueous Solutions. *J. Phys. Chem. Ref. Data* **1988**, 17, 1027–1284.
- (4) Maruthamuthu, P.; Neta, P. Phosphate Radicals. Spectra, Acid-Base Equilibriums, and Reactions with Inorganic Compounds. *J. Phys. Chem.* **1978**, 82, 710–713.
- (5) Xu, G.; Chance, M. R. Radiolytic Modification and Reactivity of Amino Acid Residues Serving as Structural Probes for Protein Footprinting. *Anal. Chem.* **2005**, 77, 4549–4555.

Chapter 4. Sorption of Clarithromycin and Tetracycline to Natural Organic Matter in the Presence and Absence of Calcium

This chapter is part of a manuscript under will be submitted with the following co-authors:

Iso Christl^a, Jordan R. Schmidt^b and Joel A. Pedersen^{b,c}

^a Institute of Biogeochemistry and Pollutant Dynamics, ETH Zurich, 8092 Zürich, Switzerland

^b Department of Chemistry, University of Wisconsin, Madison, WI 53706, USA

^c Environmental Chemistry and Technology Program, University of Wisconsin, Madison, WI 53706, USA

ABSTRACT

A variety of organic contaminants exist as cations in pH values typical of the environment. The sorption of ionizable compounds to natural organic matter is affected by solution conditions (i.e. pH, ionic strength, competing cations) and the presence of competing cations.¹⁻³ Calcium is an abundant inorganic cation in the environment that binds to natural organic matter.⁴ We studied the pH-, ionic strength-, and concentration-dependent binding of the antibiotics clarithromycin and tetracycline (large, multifunctional organic cations and zwitterions) to soil humic acid in the absence and presence of calcium. The sorption of tetracycline was found to depend strongly on pH, with maximum sorption at pH 4, where the cation and zwitterion predominate. Sorption decreased with increasing pH as the predominant species shift from the zwitterion to the negative species (i.e., monoanion and dianion). Calcium inhibited clarithromycin binding to humic acid and promoted tetracycline binding at different pH values. The data were fitted with the NICA-Donnan model, which has been previously used to describe sorption of inorganic cations binding to natural organic matter as a function of solution chemistry and is able to capture the effect of competing cations. The solubility of clarithromycin was an important parameter in the model, but the reported literature values vary significantly, therefore the solubility of clarithromycin at pH 12 was determined and found to be $0.083 \pm 0.006 \text{ mg}\cdot\text{L}^{-1}$ ($\log K_{\text{sp}} = -7.0$). This value is within the range of reported values $\log K_{\text{sp}} = -6.4$ to -7.8 .^{5,6} The NICA-Donnan model was able to describe the concentration-, ionic strength- and pH-dependence of clarithromycin and tetracycline sorption to soil humic acid, and captured the effects of calcium on sorption.

INTRODUCTION

The widespread use of antibiotics in human medicine, veterinary medicine, and as growth promoters for animals have resulted in their release to the environment. Since not all of the antibiotics administered are metabolized the percentage of unchanged antibiotics excreted ranges from 10-90%.⁷ Antibiotics have been detected in natural waters and in sediments.^{8,9} Release into the environment can occur through wastewater discharges, biosolids and manure applications, and/or agricultural run-off.^{10,11} The efficacy of antibiotic removal by wastewater treatment plants varies and ranges between 20-90%.¹²⁻¹⁵ Antibiotics in the environment can alter the structure of the microbial community, inhibit or promote ecological functions, and affect the magnification of antibiotic resistance (see review by Ding et al).¹⁶

Natural organic matter (NOM) is a ubiquitous component of the environment. It is described as a heterogeneous polydisperse mixture composed primarily of the degradation products of vegetation and microorganisms.¹⁷ Humic substances are a subset of natural organic matter that represent about 60% of the dissolved organic matter in aqueous systems.¹⁸ Humic substances are involved in the transport and sorption of organic molecules. Organic contaminants may engage in hydrogen bonding and electrostatic interactions with humic substances, as well as van der Waals interactions.¹⁹⁻²¹ Some contaminants may also covalently bind with humic substances.²² Natural organic matter can also affect the bioavailability of contaminants in the environment, which can decrease in the presence of NOM.^{23,24} The charge and supramolecular structure of NOM are also affected by changes in pH and ionic strength.²⁵ Natural organic matter possesses a variety of functional groups that are ionizable, including carboxyl (COOH), phenolic (Ph-OH), amine, sulfhydryl, and phosphate groups.²⁶

In the past the study of organic contaminants was focused on hydrophobic organic contaminants but the focus has shifted to obtain a greater understanding about the fate of polar contaminants. Models that have been used to predict sorption of organic cations include FITEQL (models sorption as a function of pH),^{1,2,27} and polyparameter linear free energy relationships (estimates partition coefficients)²⁸⁻³² Aristilde and Sposito developed a simple affinity spectrum model that describes the sorption of organic cations as a function of pH.³³ The non-ideal competitive adsorption (NICA)-Donnan model, described by Kinniburgh et al.,³⁴ has been effective in describing inorganic cation binding to humic substances, over large ranges of pH and cation concentrations. The model was built on the assumption that cations interact with humic substances by two main mechanisms, specific and nonspecific binding. The specific interactions occur between the cation and negatively charged functional groups on the humic substances, which is described by the NICA model. The nonspecific interactions are due to accumulation of cations in the humic substance, which is depicted as a gel phase with a uniform distribution of negative charge in the Donnan model, due to residual negative charge. The negative charges arise from primarily carboxylic and phenolic functional groups in the humic acid.

The objectives of this study were to determine sorption behavior of clarithromycin and tetracycline, relatively large organic cations and zwitterions, to natural organic matter and to evaluate the ability of the NICA-Donnan model to describe the sorption of organic cations. To achieve these objectives we first investigated the pH-, ionic strength-, and concentration-dependent sorption of CLA and TC to Elliott soil humic acid by equilibrium dialysis using ³H-labeled antibiotics with quantification by liquid scintillation counting. We hypothesized that sorption would decrease in presence of divalent cations due to competition. To test this hypothesis, we conducted equilibrium dialysis experiments in the presence of calcium to

determine the effects of this common alkaline earth metal cation on binding. We also hypothesized that sorption of TC would decrease with increasing pH due to a decrease in the cationic species. This hypothesis was tested by determining the amount of bound TC at different pH values.

The antibiotic molecules studied were clarithromycin (CLA) and tetracycline (TC). CLA is a macrolide used to treat both humans and animals, it has been detected in wastewater treatment plants, sediments, and in natural water.^{35–38} It has a $pK_a = 8.9^5$ and exhibits a positive charge across most of the pH range relevant for the natural environment. Tetracycline is a broad-spectrum antibiotic mainly used in veterinary settings, for treatment of diseases and as an animal growth promoter in the USA. It is also used to treat human diseases. Tetracycline has been detected in sediments and natural waters.^{39,40} Tetracycline has three ionizable functional groups (pK_a values of 3.30, 7.68, and 9.69),⁴¹ and can therefore be present as a cation, zwitterion, and anion at environmentally relevant pH values. In this study we hope to broaden the understanding of sorption mechanisms that contribute to the distribution of polar organic contaminants. Specifically we studied the sorption of ionizable antibiotics to natural organic matter as a function of pH, contaminant concentration, and the effect of calcium (representing a competing divalent cation). My contribution to the overall study described in Christl et al. (submitted) consisted of obtaining the pH-dependent sorption data for TC at two ionic strengths, and the concentration-dependent data at different pH values and calcium concentration-dependent data under acidic and alkaline conditions for TC and CLA. These data in conjunction to the data sets of Sibley and Pedersen² and Gu et al.,¹ were used to test the applicability of the NICA-Donnan model for organic ions. This work was motivated by the desire to evaluate use of the NICA-Donnan model with organic cations. Inorganic cations are well-described by the model, and

application of the model to organic cations could improve understanding of the behavior of cationic organic contaminants in the environment. Additionally, due to a significant variability in published data on CLA solubility in aqueous media,^{5,6} We determined CLA solubility at pH 12 by equilibrating an excess of solid CLA for 48 h in a 0.01 M phosphate solution.

MATERIALS AND METHODS

Chemicals. All solutions were prepared fresh for each experiment, and filter-sterilized (0.22 μ m Corning polystyrene membrane filter). Sodium phosphate monobasic dihydrate (>99%), sodium phosphate tribasic dodecahydrate (98+%), succinic acid (99%), were purchased from Acrös Organics, NJ. Boric acid (99.9%), sodium hydroxide (99.9%), calcium chloride (98.4%), and sodium chloride (USP) were purchased from Fisher. Sodium succinate hexahydrate (99%) was purchased from Alfa Aesar. Sodium tetraborate decahydrate (ACS) was purchased from Mallinckrod Chemical Works. Phosphoric acid (ACS) was purchased from Baker and Adamson. Clarithromycin (CLA) was purchased from TCI America, and tetracycline (TC) from Aldrich. Radiolabeled antibiotics (CLA, TC) were purchased from Moravek Biochemicals. Biosafe II liquid scintillation cocktail was purchased from Research Products International Corp., Mount Prospect, IL.

Glassware. All dialysis glass vials were silanized to reduce nonspecific binding.

Humic Acid. Elliott soil humic acid (ESHA, 1S102H), obtained from the International Humic Substances Society, was adjusted to pH 9 with NaOH, stirred for 24 h in the dark, filtered (0.22 μ m Corning polystyrene membrane filter), and stored in the dark at 4 °C. Elliott soil is present in Midwestern USA (Illinois, Indiana, Ohio, and Wisconsin), and used for crop cultivation (e.g. corn, soybeans, small grain, and meadow).⁴²

Clarithromycin Solubility. The published data on CLA solubility in aqueous media varies considerably. Reported values for $\log K_{SP}$ range from -6.4 to -7.8 .^{5,6} We therefore determined the solubility of neutral CLA (CLA⁰) by the saturation shake-flask method followed by centrifugation.⁴³ Solubility experiments were conducted in triplicate. Clarithromycin solutions (0.01 M phosphate buffer, pH 12) containing a solid excess were equilibrated for 48 h. Samples were centrifuged at 397,000g for 1 h (Beckman Coulter Optima™ L-90K Ultracentrifuge), and the supernatant was collected. The CLA concentration in the supernatant was determined by liquid chromatography-tandem mass spectrometry using a Synergi MAX-RP 250 × 4.6 mm, 4 μm column (Phenomenex, Torrance, CA) and separated at 700 μL·min⁻¹ by a binary gradient (A = 0.01 M ammonium formate in 0.1% formic acid, B = methanol:acetonitrile (50:50)) employing an Agilent 1100 HPLC system (Santa Clara, CA). The gradient expressed in percent mobile phase B was as follows: 0 min = 5%, 3.5 min = 5%, 10 min = 80%, 13 min = 80%, 13.1 min = 100%, 21 min = 100%, 21.1 min = 5%, 30 min = 5%). Detection was achieved with an AB SCIEX API 4000 MS/MS system (Framingham, MA) operating with positive mode Turbo Ion Spray ionization and multiple reaction monitoring (MRM) detection. Pertinent MS/MS conditions follow: CLA quantitative MRM (m/z) = 748.5/158.2; CLA qualitative MRM (m/z) = 748.5/590.4; ERY ISTD MRM (m/z) = 736.5/160.3; curtain gas (CUR) = 25 psig; nebulizer gas (GS1) = 20 psig; drying gas (GS2) = 40 psig; source temperature (TEM) = 500 °C; collision gas (CAD) = 8 psig; and Turbo Ion Spray voltage (IS) = 5000 V.

Standards Preparation. A 1.0 mg·mL⁻¹ methanolic solution of clarithromycin (SigmaAldrich, St Louis, MO) neat standard was prepared and was diluted to 1000 ng·mL⁻¹ in methanol for a working solution. The 1000 ng·mL⁻¹ solution of CLA in methanol was further diluted in methanol:water (50:50) in microcentrifuge tubes to the following concentrations for a

calibration curve: 5, 10, 25, 50, 100, 250, and 500 ng·mL⁻¹. A 100 mg·mL⁻¹ acetonitrile solution of mass labeled erythromycin (ERY ISTD) (erythromycin (90-95% erythromycin A), *N,N*-dimethyl-¹³C₂, ~90%, Cambridge Isotope Laboratories Inc., Andover, MA) was diluted 1:10 in methanol for a 10 mg·mL⁻¹ ERY ISTD working solution.

Sample Preparation. Samples containing CLA were diluted 1:100 in methanol:water (50:50). Microcentrifuge tubes were labeled for each calibration standard, method blank, and sample. A 10 µL aliquot of mg·mL⁻¹ ERY ISTD solution was added to each microcentrifuge tube, and the solvent was evaporated to dryness under a gentle stream of nitrogen at 40 °C. A 100 µL aliquot of each calibration standard, method blank, and sample was added to the appropriate microcentrifuge tube and vortexed for 15 s. These solutions were then transferred into tapered polypropylene autosampler vials with crimp caps.

Equilibrium Dialysis Experiments. The partitioning of the antibiotics to dissolved humic acid was investigated by equilibrium dialysis as described previously. Briefly, dialysis tubing (Spectra/Por 7 regenerated cellulose, 2 kDa nominal molecular weight cutoff; Spectrum Laboratories) was rinsed with ultrapure H₂O (18 MΩ·cm; Barnstead Nanopure Water System) to remove NaN₃ storage solution and stored overnight in ultrapure H₂O at 4 °C. Tubing was then filled with 4.5 mL of 50 mg_{OC}·L⁻¹ ESHA solution (pH 9), sealed with polypropylene Spectra/Por closures, and predialyzed for 24 h against 3.4 mM buffer of desired pH (borate pH 8-9, phosphate pH 4-10, succinate pH 3-4.5). Ionic strength was adjusted to 10 mM with NaCl unless otherwise noted. The humic acid was predialyzed to equilibrate with the desired background solutions prior to addition into antibiotic-containing solutions and to decrease amount of ESHA molecules that pass across the dialysis tubing through the course of the experiment. The amount of ESHA inside the dialysis tubing at the end of the experiment was calculated based on the

linear relationship between pH loss of ESHA, for the same dialysis tubing employed in this study, found by Sibley and Pedersen.²

Sorption experiments were initiated by placing pre-dialyzed ESHA into 30 mL of a buffered solution containing the desired concentrations of ³H-labeled and unlabeled antibiotic. Vials were sealed and placed in a reciprocal shaker in the dark for 72 h. At the end of the experiment pH was measured. Aliquots were collected from the internal (freely dissolved and ESHA-bound antibiotic) and external (freely dissolved antibiotic) compartments of the dialysis tubing respectively. Subsequently, aliquots were spiked with 15 mL of Biosafe II, and ³H-activity was measured by liquid scintillation counting (LSC; Packard Tri Carb 2500TR).

The amount of bound ³H-labeled antibiotic was calculated from the difference between internal (free + bound antibiotic) and external (free antibiotic) ³H-activities. The organic carbon-normalized distribution coefficient (K_{OC} , L·kg⁻¹_{OC}) was calculated directly from ³H-activities of the antibiotics and reflects the ratio of bound and freely dissolved concentrations of antibiotics:

$$K_{OC} = \frac{(DPM_{\text{internal}} - DPM_{\text{external}})}{(DPM_{\text{external}})[DOC]} \quad (4.1)$$

where DPM_{internal} and DPM_{external} represent the ³H-activities in the aliquots collected from the internal and external compartments of the dialysis tubing, and $[DOC]$ represents the ESHA concentration (kg_{OC}·L⁻¹). All sorption experiments were conducted in triplicate.

Antibiotics sorption was examined as a function of concentration, and sorption isotherms were constructed for different solution conditions and fit to the Freundlich equation (eq 4.2).⁴⁴ The Freundlich affinity parameter (K_F) expresses the sorption capacity, and the Freundlich exponent (n_F) is related to the distribution of sorption site energies.

$$\log Q_{\text{DOC}} = n_F \cdot \log C_w + \log K_F \quad (4.2)$$

where Q_{DOC} represents the amount of antibiotic sorbed to ESHA ($\text{mol} \cdot \text{kg}_{\text{OC}}^{-1}$) and C_w represents the amount of freely dissolved antibiotic ($\text{mol} \cdot \text{L}^{-1}$). Q_{DOC} and C_w were calculated from ^3H -activity at equilibrium and the total concentration of unlabeled antibiotic used in the experiment.

Additional experiments examined cation competition by including calcium (as CaCl_2) to sorption experiments. The effect of calcium was studied as a function of pH and total calcium concentration. Calcium experiments were conducted with succinate and borate buffers.

NICA-Donnan Modeling (Iso Christl). A detailed description of the NICA-Donnan model has been presented elsewhere.³⁴ Briefly, humic acids are considered a gel-like phase that exhibit a uniformly distributed negative potential resulting from deprotonation of various functional groups in humic acids. The negative charge of the humic phase is compensated by counter cation accumulation within the Donnan volume, V_D ($\text{L} \cdot \text{kg}^{-1}$), according to the empirical relationship

$$\log V_D = b(1 - \log I) - 1 \quad (4.3)$$

where I is ionic strength and b is an empirical parameter describing the change in the Donnan volume with I to describe ionic strength-dependent conformational changes in humic substances. In the NICA-Donnan model, the amount of cation i specifically bound to humic acid, Q_i , is given by (eq 4.4):

$$Q_i = \frac{n_{1,i}}{n_{1,H}} \cdot Q_{\text{max}1,H} \cdot \frac{(\tilde{K}_{1,i} C_i)^{n_{1,i}}}{\sum_1 (\tilde{K}_{1,i} C_i)^{n_{1,i}}} \cdot \frac{\left[\sum_1 (\tilde{K}_{1,i} C_i)^{n_{1,i}} \right]^{p_1}}{1 + \left[\sum_1 (\tilde{K}_{1,i} C_i)^{n_{1,i}} \right]^{p_1}} + \frac{n_{2,i}}{n_{2,H}} \cdot Q_{\text{max}2,H} \cdot \frac{(\tilde{K}_{2,i} C_i)^{n_{2,i}}}{\sum_1 (\tilde{K}_{2,i} C_i)^{n_{2,i}}} \cdot \frac{\left[\sum_1 (\tilde{K}_{2,i} C_i)^{n_{2,i}} \right]^{p_2}}{1 + \left[\sum_1 (\tilde{K}_{2,i} C_i)^{n_{2,i}} \right]^{p_2}}$$

where C_i denotes the concentration in the Donnan phase, the subscripts 1 and 2 correspond to

low and high proton-affinity sites (primarily carboxylic and phenolic sites, respectively), n_H are heterogeneity parameters for proton binding, n_i describe cation-specific heterogeneity parameters, $Q_{\max H}$ represent the maximum proton site densities of the humic substance for each distribution ($\text{mol}\cdot\text{kg}^{-1}$), \tilde{K}_i is median affinity distribution constant, and the p represent the widths of the distribution and describes the intrinsic heterogeneity of the humic substance. The total amount of cation i associated with humic acid is calculated as the sum of specifically bound cations Q_i and the amount of cation i accumulated in the Donnan phase due to non-specific electrostatic interactions.

Based on the pH-dependence of CLA binding to ESHA reported previously,² only positively charged CLA- H^+ was assumed to interact with ESHA. For TC binding, the triply protonated TC- H_3^+ cation and the doubly protonated TC- H_2^\pm zwitterion were considered to interact with ESHA. For fitting NICA-Donnan model parameters specific to antibiotic binding (viz. the affinity constants \tilde{K}_i and ion-specific heterogeneity parameters n_i) log-transformed data on CLA and TC binding were used. Model parameters were optimized using the programs ECOSAT⁴⁵ and FIT.⁴⁶ The Akaike Information Criterion corrected for small sample size (AIC_C) was used to select among competing assumptions on interactions considered in modeling.⁴⁷ Based on the best fits, the effect of Ca^{2+} present in solution was predicted. Generic NICA-Donnan model parameters for ESHA and ion-specific parameters for H^+ and Ca^{2+} binding to ESHA were taken from Christl.⁴⁸ In addition to NICA-Donnan model equilibria (*vide supra*), all calculations considered the complete aqueous speciation of all components present in solution (viz. background electrolytes, CLA, and TC including Ca-TC complex formation).⁴⁹

Molecular Modeling (J.R. Schmidt). Density functional theory calculations on clarithromycin, tetracycline, and sulfathiazole monomers were conducted using Gaussian 09⁵⁰ in

conjunction with the B3LYP density functional. Monomer geometries were optimized in the gas phase using the 6-31G(d) basis; the molecular electrostatic potential (MEP) was calculated from the density at the B3LYP/cc-pVDZ level in the presence of a polarizable continuum solvation model (PCM). All reported MEP values are maxima along the $\rho = 0.03 \text{ e}/\text{\AA}^3$ electron density isosurface, corresponding approximately to the molecular van der Waals radius.

Specific binding interactions were examined by modeling interaction of cationic/zwitterionic monomers with a benzoic acid anion. Dimer binding energies were calculated with respect to isolated ions (including PCM solvation) at the B3LYP/cc-pVTZ/PCM level, including augment functions on O atoms. Reported energies were counterpoise corrected using the corresponding gas phase dimer at the same geometry.

RESULTS AND DISCUSSION

Clarithromycin solubility. Published values of solubility for CLA vary considerably (reported $\log K_{\text{SP}}$ range from -6.4 to -7.8).^{5,6} The solubility of neutral clarithromycin (CLA^0) was found to be an important parameter in the modeling of CLA data at higher pH values where the CLA^0 is a significant species. We therefore determined the solubility of CLA^0 experimentally at pH 12 and found to be $0.083 \pm 0.006 \text{ mg}\cdot\text{L}^{-1}$ ($\log K_{\text{sp}} = -7.0$).

Clarithromycin. To determine the concentration-dependence of CLA sorption to ESHA at alkaline conditions isotherms were conducted at pH 8.7 and 9 (Figure 4.1). The concentration dependent sorption of CLA at near neutral pH (6.5) had been studied by Sibley and Pedersen² but not at alkaline pH where CLA^0 becomes a significant species (Figure 4.3a). Freundlich parameters for the isotherms are summarized in Table 1. The fits described well the data ($R^2 \geq 0.99$) and n_F values near unity were obtained. The isotherm at pH 8, although it has a lower K_F

value, is comparable to the isotherm (pH = 6.5) of Sibley and Pedersen² the K_F are 1910 ± 400 and 1300 ± 300 and the n_F are 0.85 ± 0.01 and 0.84 ± 0.01 for Sibley and Pedersen and this study respectively. The fraction of clarithromycin present as CLA^+ was 1.00 and 0.61 at pH 6.5 and 8.7 respectively. The isotherm at pH 9 a K_F of 270 ± 170 and n_F of 0.82 ± 0.03 were obtained, at pH 9 the fraction of CLA^+ is 0.44. The decrease of K_F observed at both pH used in this study compared to Sibley and Pedersen² could be due to the decrease of cationic CLA present, at pH 9 the decrease in sorption is more evident. From the isotherms we obtained n_F which corresponds to the ion-specific heterogeneity parameters n_i used in the NICA-Donnan model. Clarithromycin exists mainly as a cation over environmentally relevant pH values as can be observed in its speciation (Figure 4.3a). Sibley and Pedersen² found that clarithromycin sorption depends strongly with pH, with a maximum at pH 6.4, sorption decreases as the amount of cationic CLA decreases. Binding of CLA to humic acid under alkaline conditions was found to be controlled by the amount of cationic clarithromycin (CLA-H^+) and the solubility of CLA^0 .

Tetracycline. The concentration-dependent sorption of TC was studied at pH values where different species predominate. Freundlich parameters for the isotherms conducted for TC (3, 4.3, 6.3, and 9.2; Figure 4.2) are summarized in Table 4.1. The fits described well the data ($R^2 \geq 0.99$) and n_F values near unity were obtained. The isotherms at pH 4.3, $I = 0.01$ M conducted by Gu et al¹ and this study differ considerably, the values are K_F 4290 ± 940 and 16000 ± 6400 , and n_F at 0.99 ± 0.02 and 0.93 ± 0.02 , respectively. The main difference in the two studies was the [TC] used. The second isotherm has some non-linearity which could result in higher partitioning at lower C_w . Tetracycline is present as a cation, zwitterion, a monoanion and a dianion over the pH values studied (Figure 4.3b) and sorption occurs even when the cation is not the major species. Tetracycline contains three ionizable functionalities and is present as a cation

(TC-H₃⁺) at pH < pK_{a1}, a zwitterion (TC-H₂^{+/-}) at pK_{a1} < pH < pK_{a2}, a net monoanion (TC-H₁^{+/-}) exhibiting one positive and two negative charges at pK_{a2} < pH < pK_{a3}, and a dianion (TC²⁻) at pH > pK_{a3} (Figure 4.3b). The species expected to drive sorption are TC-H₃⁺, TC-H₂^{+/-}, and TC-H₁^{+/-} since it does not possess a positively charged moieties that can bind to NOM, the dianion is not expected to contribute since it does not have any positively charged moiety.

We studied the sorption of TC to ESHA as a function of pH at two ionic strengths (*I* = 0.01 M, 0.1 M). Results are presented in Figure 4.4. Tetracycline has pK_a values of 3.30, 7.68, and 9.69 and exists as a cation, zwitterion, monoanion, and dianion over the pH range studied (3-10).⁴¹ Gu et al¹ studied the sorption of TC to ESHA as a function of pH (*I* = 0.01 M, 0.1 M), as a function of concentration at pH 4.3, and in the presence of calcium (0.2 mM at different pH values). In this study sorption increased with increasing pH in the acidic range with a maximum sorption observed at pH 4, indicating competition for binding sites with H⁺. As pH increases from 4 to 8 sorption decreases steadily with a marked decrease at pH > 8 where the speciation is dominated by anionic species. This suggests that sorption is driven mainly by the cationic and zwitterionic species binding to the deprotonated moieties in the ESHA. Even so sorption, also occurred when the monoanionic and dianionic species predominate, suggesting they are able to associate with NOM as well the dianion is not expected to sorb (*vide supra*). The monoanion (TC-H₁^{+/-}) retains a positively charged moiety, the dimethylamino group (Figure 4.3b), which could bind to the negatively charged NOM. At higher ionic strength (*I* = 0.1 M) the sorption of TC decreased in comparison to the lower ionic strength data (*I* = 0.01 M) for all of the pH point studied except at pH > 8 (Figure 4.4). The effect of ionic strength on sorption might be due to charge screening, at higher ionic strength the higher concentration of Na⁺ screening the negative charge thus reducing the electrostatic attraction between the positively charged TC and the

zwitterion, resulting in lower sorption. However at $\text{pH} > 8$, there is a reduction in the electrostatic repulsion that could allow accumulation of the negatively charged species, the monoanion and the dianion, resulting in an increase of sorption at higher ionic strength in comparison to the lower ionic strength.

Effect of calcium on the sorption of tetracycline and clarithromycin to ESHA. In natural systems, the presence of inorganic cations (especially Ca^{2+} and Mg^{2+}) is expected to affect organic cation binding to humic substances. Calcium is present as a dissolved ion in surface and groundwater at concentrations ranging from 0.15-1.1 mM.⁵¹ We studied the effect of calcium at low concentrations ranging from 0.001-10 μM . Our experimental data show that total calcium concentrations exceeding 0.1 μM affect the binding of trace amounts of clarithromycin to ESHA at pH 5.6 and 9.1 (Figure 4.4a). Antibiotic sorption as a function of total Ca^{2+} concentration was studied (Figure 4.4), and the K_{OC} values are represented in Figure 4.6. As the concentration of calcium increased the amount of CLA sorbed decreased (Figure 4.4a). In the absence of calcium the K_{OC} at pH 5.6 was $19000 \pm 290 \text{ L} \cdot \text{kg}^{-1}_{\text{OC}}$ whereas in the presence of the highest Ca^{2+} employed (10 μM), the K_{OC} of CLA decreased to $560 \pm 220 \text{ L} \cdot \text{kg}^{-1}_{\text{OC}}$. Clarithromycin sorption was completely inhibited in the presence of 10 μM Ca^{2+} at pH 9 (no detectable sorbed CLA). Clarithromycin has a pK_a of 8.9, at pH 5.6 CLA^+ is the dominant species in solution and competes with Ca^{2+} , but at pH 9 the speciation shifts and CLA^0 is the major species in solution (44% of the molecule is present as CLA^+ at pH 9), decreasing the concentration of CLA^+ able to bind to ESHA. Calcium competes readily for binding sites with CLA at pH 5.6 and 9 (Figure 4.5a).

Sorption of TC to ESHA increased with total Ca^{2+} concentration at both pH values examined (pH 5.6 and 9): at pH 5.7 the K_{OC} was $13000 \pm 810 \text{ L} \cdot \text{kg}^{-1}_{\text{OC}}$ and $19000 \pm 720 \text{ L} \cdot \text{kg}^{-1}_{\text{OC}}$

in the absence of Ca^{2+} and at $10\ \mu\text{M}\ \text{Ca}^{2+}$, respectively. At pH 9 the promotion TC sorption to ESHA is more pronounced the K_{OC} increases from $6100 \pm 920\ \text{L}\cdot\text{kg}^{-1}_{\text{OC}}$ in the absence of calcium to $26000 \pm 1500\ \text{L}\cdot\text{kg}^{-1}_{\text{OC}}$ in the presence of $10\ \mu\text{M}\ \text{Ca}^{2+}$ (Figure 4.5b). Our results agree with those of Gu et al.,¹ who demonstrated that TC sorption to ESHA increased with calcium concentration ($[\text{Ca}^{2+}]$ employed in that study was $0.2\ \text{mM}$), the two studies show that at higher calcium concentration the sorption of TC to ESHA increases. Tetracycline can form complexes with Ca^{2+} ,^{52–54} and the increase in sorption could be explained by the formation of TC-Ca complexes binding to ESHA. Of the TC calcium complexes (Figure 4.7) TC-Ca^0 , TC-Ca^{2+} , and $\text{TC}_2\text{-H}_2\text{-Ca}^-$ are the most abundant at pH 9 among these species TC-Ca^{2+} bears a positive charge. At increased pH electrostatics favor the interactions between TC-Ca^{2+} , which could explain the increased sorption observed at pH 9 in comparison to pH 5.7 at pH 5.7 no TC-calcium complexes are present in solution (fractional abundance < 0.001) whereas at pH 9 the species TC-Ca^0 , TC-Ca^{2+} , and $\text{TC}_2\text{-H}_2\text{-Ca}^-$ the fraction present are 0.9, 0.02, and 0.01 respectively (Figure 4.7).

Results from the model. (Refer to Christl et al.). The data, from the experimental results gathered in this study, the CLA data set from Sibley and Pedersen,² and the sorption data for TC in the presence of calcium from Gu et al.,¹ was fitted with the NICA-Donnan model that has been applied to describe the sorption of inorganic cations to NOM in different solution conditions (i.e. pH, ionic strength) and in the presence of competing cations.^{34,55} The NICA-Donnan model was able to capture the sorption behavior of CLA and TC at different solution conditions (i.e., pH, ionic strength, presence of Ca^{2+}), and determine the extent of binding due to specific and non-specific sorption. In the case specific binding, the NICA-Donnan model was able to attribute sorption to sites of low or high proton affinity (i.e., due primarily to carboxylic

and phenolic sites respectively). The importance of the interaction of the different ionic species with the binding sites was selected based on The Akaike Information Criterion corrected for small sample size (AIC_C)⁴⁷ was used to select the combination of antibiotic species and binding sites that resulted in the highest quality model. The results lead to the conclusion that both CLA and TC bind through specific binding with minimal non-specific accumulation in the Donnan phase. For CLA, the selected model attributed CLA^+ binding mainly to low proton affinity (e.g., carboxylate) sites. The contribution of CLA^0 to the overall sorption of clarithromycin was found to be negligible. Tetracycline, with a more complex speciation, binds to both sites with low and high proton affinity: the positively charged species ($TC-H_3^+$) binds to both high and low proton affinity sites, while the zwitterionic ($TC-H_2^\pm$) binds mainly to high proton affinity sites. The anionic species were found to have negligible contribution on sorption based on the modeling of the data.

Calcium binds preferably to low proton affinity sites, albeit with a lower affinity than CLA^+ : $\log \tilde{K}_1 = -1.7$,⁴ and 0.2 ± 0.1 for calcium and clarithromycin respectively. Both CLA^+ and Ca^{2+} compete for these sites, and the model agrees with the experimental data at pH 9, with increasing Ca^{2+} concentration the amount of sorbed CLA^+ decreases. In the case of pH 5.6 the model underestimates the effect of calcium because it attributes Ca^{2+} non-specific accumulation to the Donnan phase, leaving more low proton affinity sites available (*in silico*), leading to the competition between the two cations not being well captured.

For tetracycline, several calcium complexes form depending on solution pH (Figure 4.7). Among the Ca-TC complexes, $TC-Ca_2^{2+}$ is net positively charged and may associate with negatively charged humic acids due to non-specific, electrostatic binding. The results from the model, fitted to the data set of Gu et al.,¹ suggest that the promoting effect of calcium on sorption

is due to electrostatic interaction of positively charged tetracycline-Ca complexes with humic acid rather than due to the formation of ternary complexes.

Environmental implications. The present study demonstrates that solution conditions (e.g., pH, ionic strength, calcium concentration) strongly influence the interactions of cationic and zwitterionic antibiotics with humic substances. Sorption to NOM decreases the bioavailability of organic compounds,^{23,24} and the bioavailability of ionizable compounds is therefore expected to depend on the factors affecting sorption (e.g. pH, ionic strength, and the presence of competing cations), with the lowest bioavailability expected at pH 4 for TC. Calcium was found to inhibit sorption of CLA but promote TC sorption, due to electrostatic interaction of positively charged tetracycline-Ca complexes with humic acid at high TC concentration (i.e., 0.1 mM); TC has been detected at 9-32 $\mu\text{g}\cdot\text{kg}^{-1}$ in sediments.^{13,35,39} The extent of sorption promotion by calcium for other organic compounds is expected to depend on the relative magnitude of complexation constants and the concentrations of relevant ligands. The impact of Ca^{2+} on association with humic acid was shown to depend on the ability of the compound to form complexes with calcium and solution conditions. Apart from effects of Ca^{2+} at trace antibiotic levels, the NICA-Donnan model described experimental data on clarithromycin and tetracycline binding to a soil humic acid well over a very wide range of conditions with respect to pH, antibiotic concentration, and ionic strength. In terrestrial and aquatic systems, inorganic cations other than Ca^{2+} such as Mg^{2+} , Ba^{2+} , Sr^{2+} , Mn^{2+} , and Fe^{2+} are typically present at concentrations exceeding those of antibiotics. The affinities of these divalent cations for humic acids are similar to that Ca^{2+} or even higher.⁵⁵ Based on the results of this study, we expect that in natural systems, the interactions of natural organic matter with antibiotics bearing positively charged moieties are influenced by the presence of these ubiquitous cations. Therefore we need to better

understand the impact of naturally occurring cations on the sorption of cationic contaminants. The NICA-Donnan model is able to capture the effect of calcium on TC sorption. This model therefore appears to hold promise for determining the effects of naturally occurring cations on the sorption of cationic contaminants.

ACKNOWLEDGEMENTS

Iso Christl modeled the data with the NICA-Donnan model. J.R. Schmidt conducted the molecular electrostatic potentials calculations shown in Figure 4.3. Curtis J. Hedman quantified clarithromycin for the solubility experiment samples. I thank Sam Sibley for helpful assistance during this project.

REFERENCES

- (1) Gu, C.; Karthikeyan, K. G.; Sibley, S. D.; Pedersen, J. A. Complexation of the Antibiotic Tetracycline with Humic Acid. *Chemosphere* **2007**, *66*, 1494–1501.
- (2) Sibley, S. D.; Pedersen, J. A. Interaction of the Macrolide Antimicrobial Clarithromycin with Dissolved Humic Acid. *Environ. Sci. Technol.* **2008**, *42*, 422–428.
- (3) Richter, M. K.; Sander, M.; Krauss, M.; Christl, I.; Dahinden, M. G.; Schneider, M. K.; Schwarzenbach, R. P. Cation Binding of Antimicrobial Sulfathiazole to Leonardite Humic Acid. *Environ. Sci. Technol.* **2009**, *43*, 6632–6638.
- (4) Christl, I. Ionic Strength- and pH-Dependence of Calcium Binding by Terrestrial Humic Acids. *Environ. Chem.* **2012**, *9*, 89.
- (5) Nakagawa, Y.; Itai, S.; Yoshida, T.; Nagai, T. Physicochemical Properties and Stability in the Acidic Solution of a New Macrolide Antibiotic, Clarithromycin, in Comparison with Erythromycin. *Chem. Pharm. Bull. (Tokyo)*. **1992**, *40*, 725–728.
- (6) Kümmerer, K. Eintrag von Antibiotika in Die Aquatische Umwelt. Prüfung Der Biologischen Abbaubarkeit Ausgewählter Antibiotika, Ihr Vorkommen Im Abwasser Und Ihr Möglicher Einfluss Auf Die Reinigungsleistung Kommunaler Kläranlagen. Identifizierung von Risikofeldern; Um. *Umweltbundesamt F&E-Vorhaben* **2003**, 298, 722.
- (7) Kümmerer, K. Promoting Resistance by the Emission of Antibiotics from Hospitals and Households into Effluent. *Clin. Microbiol. Infect.* **2003**, *9*, 1203–1214.
- (8) Kümmerer, K. Antibiotics in the Aquatic Environment - A Review - Part I. *Chemosphere* **2009**, *75*, 417–434.
- (9) Wei, Y.; Zhang, Y.; Xu, J.; Guo, C.; Li, L.; Fan, W. Simultaneous Quantification of Several Classes of Antibiotics in Water, Sediments, and Fish Muscles by Liquid Chromatography-Tandem Mass Spectrometry. *Front. Environ. Sci. Eng.* **2014**, *8*, 357–371.
- (10) Kinney, C. A. Survey of Organic Wastewater Contaminants in Biosolids Destined for Land Application. *Environ. Sci. Tech* **2006**, *40*, 7207–7215.
- (11) Kinney, C. A.; Furlong, E. T.; Werner, S. L.; Cahill, J. D. Presence and Distribution of

- Wastewater-Derived Pharmaceuticals in Soil Irrigated with Reclaimed Water. *Environ. Toxicol. Chem.* **2006**, *25*, 317–326.
- (12) McArdell, C. S.; Molnar, E.; Suter, M. J. F.; Giger, W. Occurrence and Fate of Macrolide Antibiotics in Wastewater Treatment Plants and in the Glatt Valley Watershed, Switzerland. *Environ. Sci. Technol.* **2003**, *37*, 5479–5486.
 - (13) Miao, X. S.; Bishay, F.; Chen, M.; Metcalfe, C. D. Occurrence of Antimicrobials in the Final Effluents of Wastewater Treatment Plants in Canada. *Environ. Sci. Technol.* **2004**, *38*, 3533–3541.
 - (14) Batt, A. L.; Snow, D. D.; Aga, D. S. Occurrence of Sulfonamide Antimicrobials in Private Water Wells in Washington County, Idaho, USA. *Chemosphere* **2006**, *64*, 1963–1971.
 - (15) Karthikeyan, K. G.; Meyer, M. T. Occurrence of Antibiotics in Wastewater Treatment Facilities in Wisconsin, USA. *Sci. Total Environ.* **2006**, *361*, 196–207.
 - (16) Ding, C.; He, J. Effect of Antibiotics in the Environment on Microbial Populations. *Appl. Microbiol. Biotechnol.* **2010**, *87*, 925–941.
 - (17) Sutton, R.; Sposito, G. Molecular Structure in Soil Humic Substances: The New View. *Environ. Sci. Technol.* **2005**, *39*, 9009–9015.
 - (18) Stevenson, F. J. *Humus Chemistry: Genesis, Composition, Reactions*; John Wiley & Sons, 1994.
 - (19) Schwarzenbach, R. P.; Gschwend, P. M.; Imboden, D. M. *Environmental Organic Chemistry*; 2nd. ed.; Wiley-Interscience: New York, 2003.
 - (20) Keiluweit, M.; Kleber, M. Molecular-Level Interactions in Soils and Sediments: The Role of Aromatic π -Systems. *Environ. Sci. Technol.* **2009**, *43*, 3421–3429.
 - (21) Nguyen, T. H.; Goss, K.-U.; Ball, W. P. Polyparameter Linear Free Energy Relationships for Estimating the Equilibrium Partition of Organic Compounds between Water and the Natural Organic Matter in Soils and Sediments. *Environ. Sci. Technol.* **2005**, *39*, 913–924.
 - (22) Gulkowska, A.; Sander, M.; Hollender, J.; Krauss, M. Covalent Binding of Sulfamethazine to Natural and Synthetic Humic Acids: Assessing Laccase Catalysis and Covalent Bond Stability. *Environ. Sci. Technol.* **2013**, *47*, 6916–6924.

- (23) Akkanen, J.; Kukkonen, J. Measuring the Bioavailability of Two Hydrophobic Organic Compounds in the Presence of Dissolved Organic Matter. *Env. Toxicol Chem* **2003**, *22*, 518–524.
- (24) Kungolos, A.; Samaras, P.; Tsiridis, V.; Petala, M.; Sakellaropoulos, G. Bioavailability and Toxicity of Heavy Metals in the Presence of Natural Organic Matter. *J Env. Sci Heal. A Tox Hazard Subst Env. Eng.* **2006**, *41*, 1509–1517.
- (25) Ghosh, K.; Schnitzer, M. Macromolecular Structures of Humic Substances. *Soil Sci.* **1980**, *129*, 266–276.
- (26) Takács, M.; Alberts, J. J.; Egeberg, K. Characterization of Natural Organic Matter From Eight Norwegian Surface Waters: Proton and Copper Binding. *Environ. Int.* **1999**, *25*, 315–323.
- (27) Buschmann, J.; Sigg, L. Antimony(III) Binding to Humic Substances: Influence of pH and Type of Humic Acid. *Environ. Sci. Technol.* **2004**, *38*, 4535–4541.
- (28) Droge, S.; Goss, K.-U. Effect of Sodium and Calcium Cations on the Ion-Exchange Affinity of Organic Cations for Soil Organic Matter. *Environ. Sci. Technol.* **2012**, *46*, 5894–5901.
- (29) Droge, S. T. J.; Goss, K. U. Development and Evaluation of a New Sorption Model for Organic Cations in Soil: Contributions from Organic Matter and Clay Minerals. *Environ. Sci. Technol.* **2013**, *47*, 14233–14241.
- (30) Schenzel, J.; Goss, K.-U.; Schwarzenbach, R. P.; Bucheli, T. D.; Droge, S. T. J. Experimentally Determined Soil Organic Matter-Water Sorption Coefficients for Different Classes of Natural Toxins and Comparison with Estimated Numbers. *Environ. Sci. Technol.* **2012**, *46*, 6118–6126.
- (31) Stenzel, A.; Goss, K.-U.; Endo, S. Prediction of Partition Coefficients for Complex Environmental Contaminants: Validation of COSMOtherm, ABSOLV, and SPARC. *Environ. Toxicol. Chem.* **2014**, *33*, 1537–1543.
- (32) Bronner, G.; Goss, K.-U. Predicting Sorption of Pesticides and Other Multifunctional Organic Chemicals to Soil Organic Carbon. *Environ. Sci. Technol.* **2011**, *45*, 1313–1319.
- (33) Aristilde, L.; Sposito, G. Complexes of the Antimicrobial Ciprofloxacin with Soil, Peat, and Aquatic Humic Substances. *Environ. Toxicol. Chem.* **2013**, *32*, 1467–1478.

- (34) Kinniburgh, D. G.; Milne, C. J.; Benedetti, M. F.; Pinheiro, J. P.; Filius, J.; Koopal, L. K.; Van Riemsdijk, W. H. Metal Ion Binding by Humic Acid: Application of the NICA-Donnan Model. *Environ. Sci. Technol.* **1996**, *30*, 1687–1698.
- (35) Hirsch, R.; Ternes, T.; Haberer, K.; Kratz, K. L. Occurrence of Antibiotics in the Aquatic Environment. *Sci. Total Environ.* **1999**, *225*, 109–118.
- (36) Christian, T.; Schneider, R. J.; Färber, H. a.; Skutlarek, D.; Meyer, M. T.; Goldbach, H. E. Determination of Antibiotic Residues in Manure, Soil, and Surface Waters. *Acta Hydrochim. Hydrobiol.* **2003**, *31*, 36–44.
- (37) Calamari, D.; Zuccato, E.; Castiglioni, S.; Bagnati, R.; Fanelli, R. Strategic Survey of Therapeutic Drugs in the Rivers Po and Lambro in Northern Italy. *Environ. Sci. Technol.* **2003**, *37*, 1241–1248.
- (38) Alexy, R.; Sommer, A.; Lange, F. T.; Kümmerer, K. Local Use of Antibiotics and Their Input and Fate in a Small Sewage Treatment Plant - Significance of Balancing and Analysis on a Local Scale vs. Nationwide Scale. *Acta Hydrochim. Hydrobiol.* **2006**, *34*, 587–592.
- (39) Kim, S. C.; Carlson, K. Quantification of Human and Veterinary Antibiotics in Water and Sediment Using SPE/LC/MS/MS. *Anal. Bioanal. Chem.* **2007**, *387*, 1301–1315.
- (40) Kolpin, D. W.; Furlong, E. T.; Meyer, M. T.; Thurman, E. M.; Zaugg, S. D.; Barber, L. B.; Buxton, H. T. Pharmaceuticals, Hormones, and Other Organic Wastewater Contaminants in U.S. Streams, 1999–2000: A National Reconnaissance. *Environ. Sci. Technol.* **2002**, *36*, 1202–1211.
- (41) Mitscher, L. A. *The Chemistry of the Tetracycline Antibiotics*.; New York, 1978.
- (42) Elliott Series https://soilseries.sc.egov.usda.gov/OSD_Docs/E/ELLIOTT.html.
- (43) Baka, E.; Comer, J. E. A.; Takács-Novák, K. Study of Equilibrium Solubility Measurement by Saturation Shake-Flask Method Using Hydrochlorothiazide as Model Compound. *J. Pharm. Biomed. Anal.* **2008**, *46*, 335–341.
- (44) Freundlich, H. M. F. Über Die Adsorption in Lösungen. *Z Phys Chem.* **1906**, *57*, 385–470.
- (45) Keizer, M. G.; van Riemsdijk, W. H. ECOSAT, 2006.

- (46) Kinniburgh, D. G.; Tang, C. K. FIT, 2004.
- (47) Burnham, K. P. Multimodel Inference: Understanding AIC and BIC in Model Selection. *Sociol. Methods Res.* **2004**, *33*, 261–304.
- (48) Christl, I. Ionic Strength- and pH-Dependence of Calcium Binding by Terrestrial Humic Acids. *Environ. Chem.* **2012**, *9*, 89.
- (49) Martell, A. E.; Smith, R. M.; Motekaitis, R. J. *NIST Critically Selected Stability Constants of Metal Complexes*; Version 8.; National Institute of Standards and Technology: Gaithersburg, MD, 2004.
- (50) Frisch, M. J.; Trucks, G. W.; Schlegel, H. B.; Scuseria, G. E.; Robb, M. A.; Cheeseman, J. R.; Scalmani, G.; Barone, V.; Mennucci, B.; Petersson, G. A.; et al. Gaussian 09 Revision A.2, 2009.
- (51) Williamson, J. E.; Carter, J. M. *Water-Quality Characteristics in the Black Hills Area, South Dakota: U.S. Geological Survey Water-Resources Investigations Report 01-4194*.
- (52) Wessels, J. M.; Ford, W. E.; Szymczak, W.; Schneider, S. The Complexation of Tetracycline and Anhydrotetracycline with Mg^{2+} and Ca^{2+} : A Spectroscopic Study. *J. Phys. Chem. B* **1998**, *102*, 9323–9331.
- (53) Schmitt, M. O.; Schneider, S. Spectroscopic Investigation of Complexation between Various Tetracyclines and Mg^{2+} or Ca^{2+} . *PhysChemComm* **2000**, *3*, 42.
- (54) Gu, C.; Karthikeyan, K. G. Interaction of Tetracycline with Aluminum and Iron Hydrous Oxides. *Environ. Sci. Technol.* **2005**, *39*, 2660–2667.
- (55) Milne, C. J.; Kinniburgh, D. G.; Tipping, E. Generic NICA-Donnan Model Parameters for Proton Binding by Humic Substances. *Environ. Sci. Technol.* **2001**, *35*, 2049–2059.

Table 4.1. Freundlich parameters for tetracycline and clarithromycin sorption to dissolved Elliott soil humic acid.

Antibiotic	pH	K_F	n_F
TC	3.0	17400 ± 5400	0.92 ± 0.02
TC	4.3	16000 ± 6400	0.93 ± 0.02
TC	6.3	3300 ± 550	0.88 ± 0.01
TC	9.2	2100 ± 900	0.93 ± 0.02
CLA	8.7	1300 ± 300	0.84 ± 0.01
CLA	9.0	270 ± 170	0.82 ± 0.03

Errors represent propagated error of the $\log Q$ vs. $\log C$ linear fit ($R^2 \geq 0.99$).

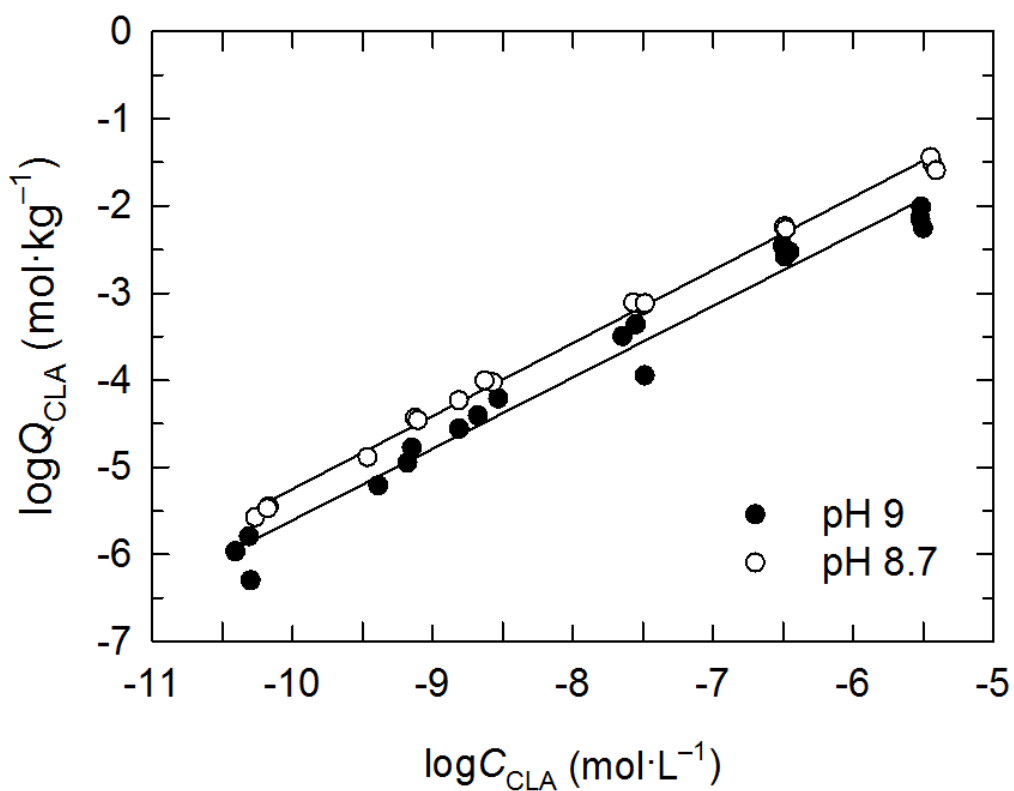


Figure 4.1. Sorption of clarithromycin (CLA) to Elliott soil humic acid as a function of non-sorbed CLA at pH 8.7 and 9 (phosphate buffer). $[\text{DOC}] = 42 \text{ mg} \cdot \text{L}^{-1}$.

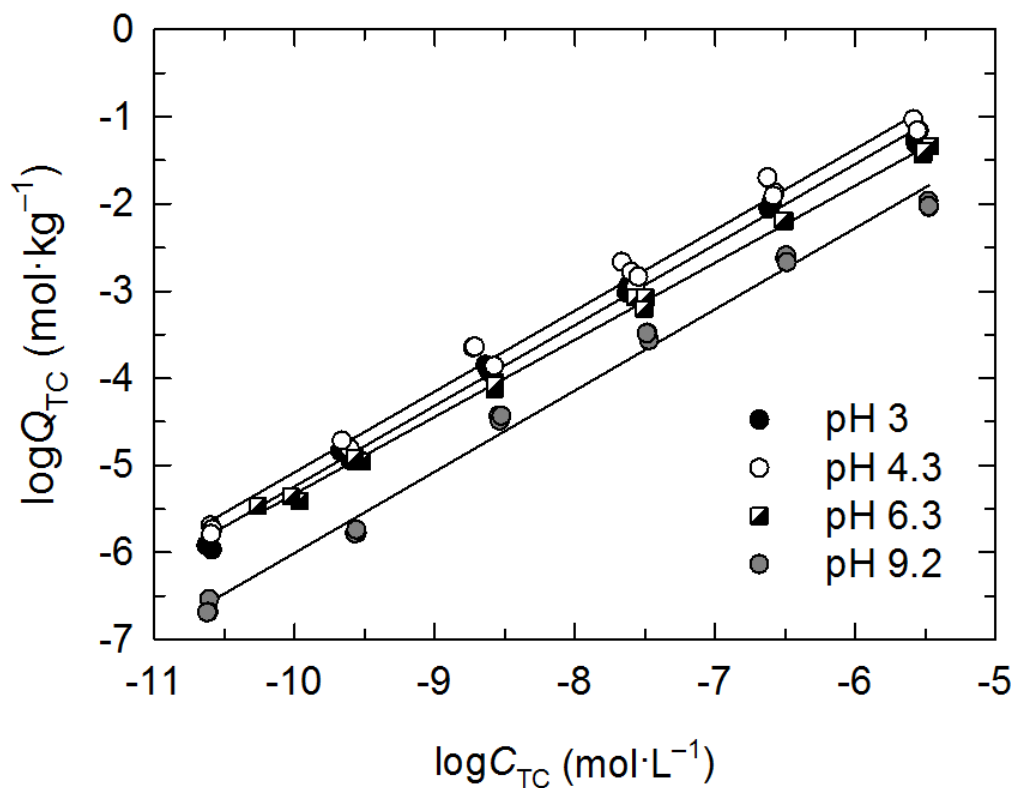


Figure 4.2. Sorption of tetracycline (TC) to Elliott soil humic acid as a function of non-sorbed TC at pH 3, 4.3, 6.3 and 9.2 (phosphate buffer). $[\text{DOC}] = 37\text{-}42 \text{ mg} \cdot \text{L}^{-1}$.

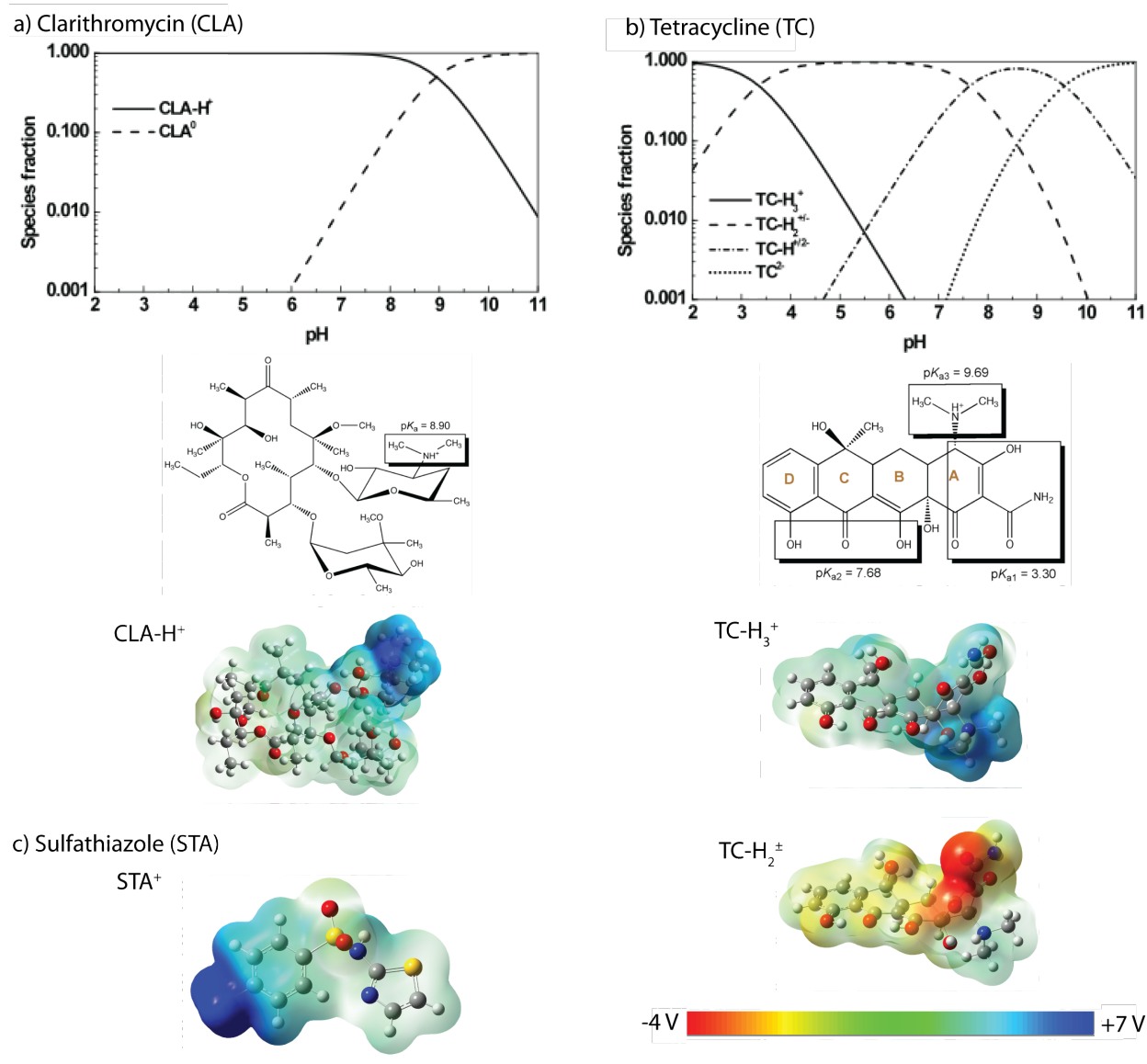


Figure 4.3. Speciation as a function of pH, skeletal formulae and molecular electrostatic potentials (MEPs) of (a) clarithromycin and (b) tetracycline, and (c) MEP for sulfathiazole cation. Speciation was calculated for an ionic strength of 0.01 M and a total clarithromycin or tetracycline concentration of 1 μ M. Macroscopic dissociation constants (pK_a) for clarithromycin and tetracycline were taken from Nakagawa et al.⁵ and Mitscher,⁴¹ respectively. Molecular electrostatic potentials were calculated along the $\rho = 0.03 \text{ e}/\text{\AA}^3$ electron density isosurface and are superimposed over ball-and-stick structures. Atoms in the ball-and-stick structures are color-

coded as follows: white, H; grey, C; blue, N; red, O; and yellow, S. Abbreviations: CLA^0 , neutral clarithromycin; CLA-H^+ , clarithromycin cation; STA, sulfathiazole cation; TC-H_3^+ , tetracycline cation; $\text{TC-H}_2^{+/-}$, tetracycline zwitterion; $\text{TC-H}^{+/2-}$, tetracycline monoanion; TC^{2-} , tetracycline dianion. From Christl et al.

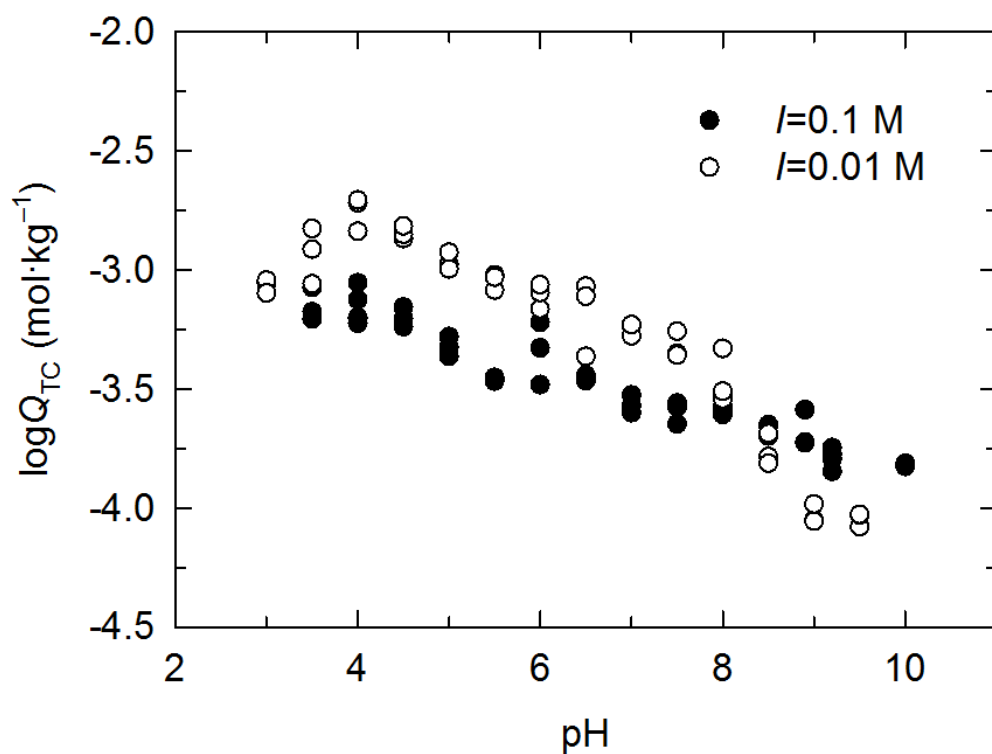


Figure 4.4. Sorption of tetracycline (TC) to Elliott soil humic acid as a function of pH ($I = 0.01$ M and 0.1 M). $[TC] = 1 \mu M$, $[DOC] = 37\text{--}43 \text{ mg}\cdot\text{L}^{-1}$. Buffers used were phosphate for pH 3-4 and 6-10 and succinate pH 4-5.5.

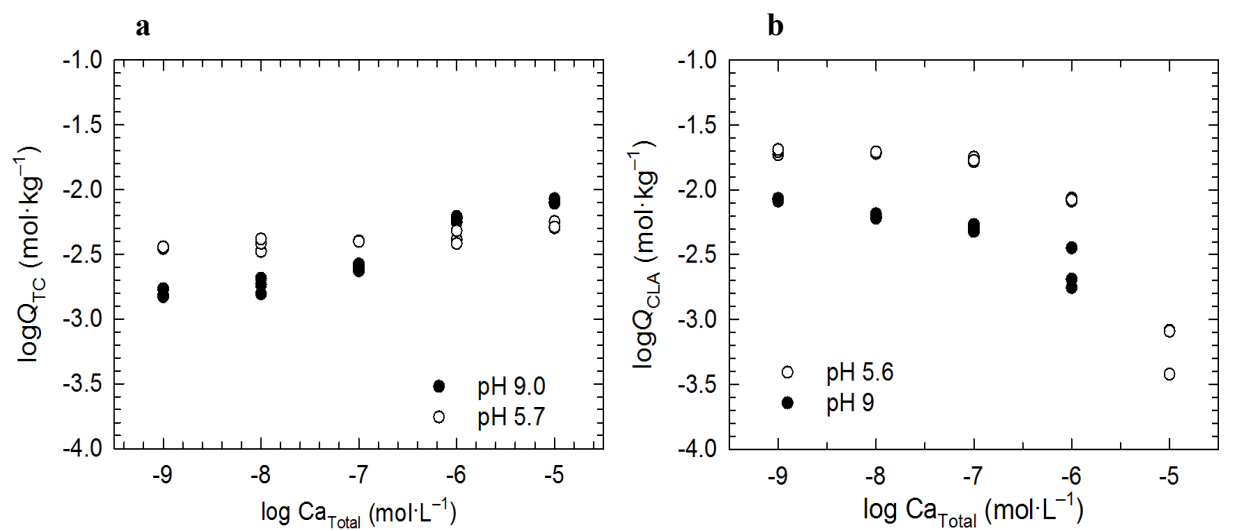


Figure 4.5. Sorption of antibiotics tetracycline (TC) and clarithromycin (CLA) to Elliott soil humic acid (ESHA) as a function of total calcium concentration. **a)** $[TC] = 1 \mu\text{M}$, **b)** $[CLA] = 1 \mu\text{M}$ $[\text{DOC}] = 39$ and $42 \text{ mg} \cdot \text{L}^{-1}$ for pH 5.6 (succinate buffer) and 9 (phosphate buffer) respectively.

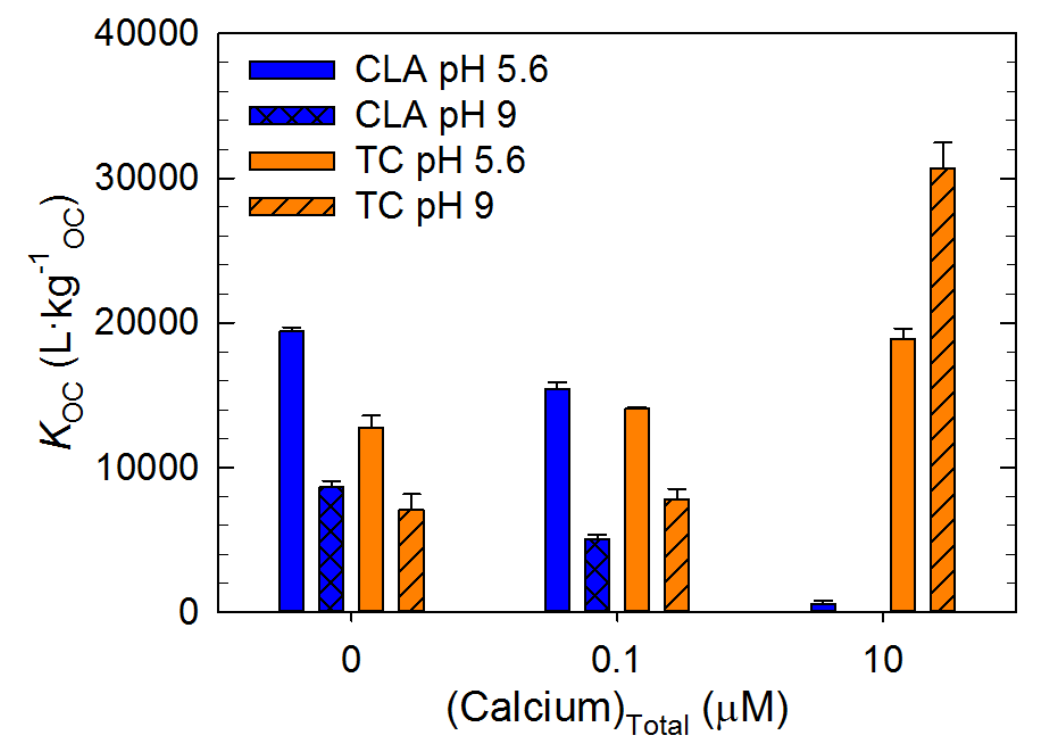


Figure 4.6. Organic carbon-normalized distribution coefficient (K_{OC} , $L \cdot kg^{-1}_{OC}$) as a function of pH 5.6 (succinate buffer) and 9 (borate buffer) and $[Ca^{+2}]_{total}$ (0, 0.1, 10 μM). Ionic strength was 10 mM, $[DOC] = 39$ and $42 \text{ mg} \cdot L^{-1}$ for pH 5.6 and 9 respectively, and antibiotic concentration was 1 μM . The K_{OC} of clarithromycin (CLA) decreased with increasing $[Ca^{+2}]_{total}$ and pH. Competition between CLA and calcium was more pronounced at pH 9. The K_{OC} of tetracycline (TC) increased with increasing $[Ca^{+2}]_{total}$, this effect was more apparent at pH 9.

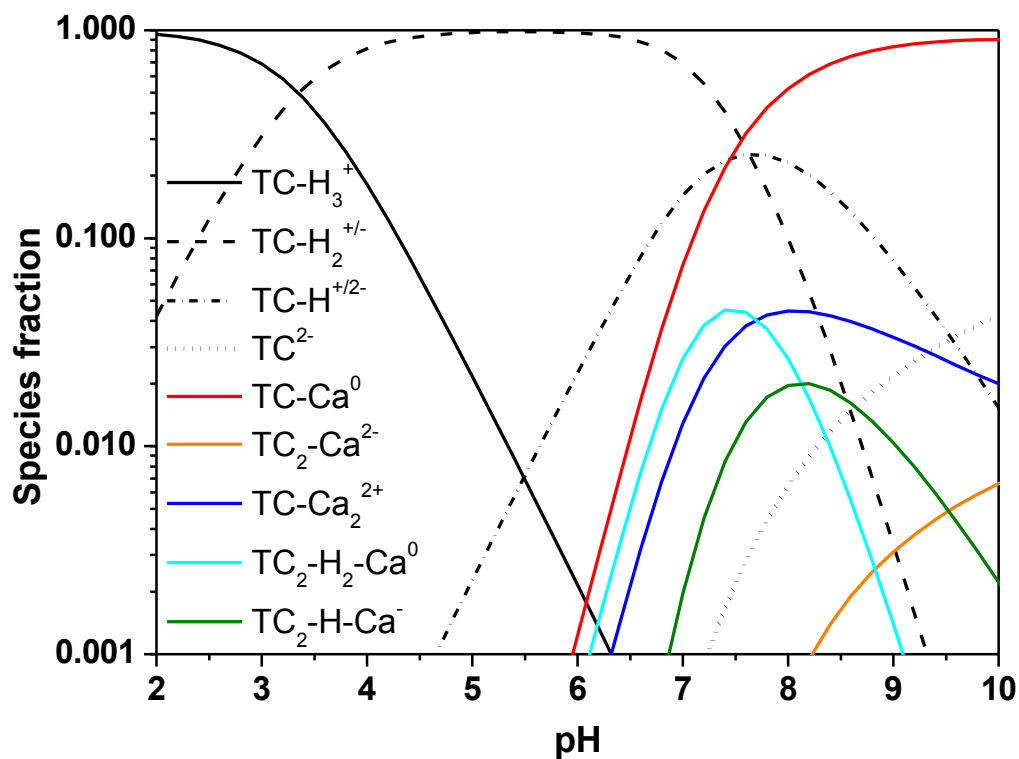


Figure 4.7. Speciation of dissolved tetracycline (TC) as a function of pH in the presence of 2×10^{-4} M Ca^{2+} at $I = 0.01$ M and a total tetracycline concentration of 10^{-4} M. Complexation constants for TC- Ca^{2+} species were taken from Martell et al.⁴⁹ From Christl et al.

Chapter 5. Summary, Conclusions, and Future Directions

SUMMARY AND CONCLUSIONS

In regards to the oxidation of amino acids by peroxymonosulfate, we found that peroxymonosulfate by itself is capable of oxidizing all off the amino acids studied with rates decreasing in the order of methionine > tryptophan > tyrosine > histidine > alanine for the fastest reacting amino acids. The results agree with the ranking of oxidation of amino acids by other oxidants (i.e., hydroxyl radical, sulfate radical, singlet oxygen, ozone), with the aromatic and sulfur-containing amino acids being oxidized at higher rates. Natural organic matter did not impact on the overall rate of oxidation of tryptophan.

In the case of the oxidation of amino acids by cobalt-activated peroxymonosulfate, we found the pseudo first-order rate constant to increase by at least one order of magnitude for all the amino acids studied compared to the unactivated reaction. The ranking was found to differ with the fastest reacting amino acids decreasing in the order of tryptophan > lysine > leucine. The activation of peroxymonosulfate with cobalt is known to form primarily sulfate radicals.³ To test the hypothesis that sulfate radicals are the major oxidation of amino acids by cobalt activated peroxymonosulfate we used known radical scavengers (i.e., ethanol, *tert*-butanol) to determine the effect of the different radical species. The results from tryptophan agree with our hypothesis that sulfate radical is the primary oxidant, but we found that different mechanisms take place for the amino acid studied. In the case of lysine and leucine no decrease in the rate of oxidation in the presence of ethanol, which scavenges sulfate and hydroxyl radical. This finding could imply two things, either peroxymonosulfate radical or bound radical species of sulfate or hydroxyl radicals are driving the oxidation. Further tests are needed to determine the impact of said radical species.

We were able to identify some products of oxidation of amino acids by LC-MS/MS. In the case of methionine the products of oxidation include methionine sulfoxide and sulfone. In the case of tryptophan, kynurenine was observed as a product of oxidation in the cobalt-activated reaction indicating that this product forms by the reaction of tryptophan with sulfate and hydroxyl radicals. Mass shifts of (+16 g·mol⁻¹) corresponding to hydroxylation were observed for tryptophan, histidine, leucine and lysine. In the case of tyrosine a mass shift of (+48 g·mol⁻¹) was observed that could correspond to three hydroxylations.

Pertaining to the sorption of tetracycline and clarithromycin to Elliott soil humic acid, we found the sorption to be dependent on pH. For tetracycline the highest sorption was found in the acidic range, close to the first pK_a. Calcium had a pronounced effect for both antibiotics, in the case of clarithromycin, a decrease in sorption was observed with increasing calcium concentration, however the sorption of tetracycline increased. Clarithromycin competes with calcium for binding sites, which becomes increasingly important at higher calcium concentrations. Tetracycline can form complexes with calcium, and ternary complexes with both calcium and humic matter, which was found to be the main cause for the increase in sorption by the NICA-Donnan model. The data, along with data sets from Sibley and Pedersen¹ and from Gu et al.,² were modeled by our collaborator Iso Christl using the NICA-Donnan model. By applying the Akaike Information Criterion corrected for small sample size the importance of binding sites and ionic species was determined.

FUTURE DIRECTIONS

While the study of free amino acids will give us an idea of which residues will most likely be oxidized in a protein and to which degree, further experiments with proteins must be conducted, including the oxidation of intact proteins, extent of inactivation after exposure to

peroxymonosulfate, and more complex matrices (e.g., soil, surface water, and waste water). By studying proteins with known structures and the site-specific oxidation we can determine the solvent accessibility of peroxymonosulfate, information that will be important if we want to apply the system to inactivate different proteins.

More experiments need to be conducted to identify the products of oxidation. Chlorinated products are expected to be formed when chloride is present in the cobalt activated reaction due to propagation reactions. Although no mass shifts associated with chlorinated products were observed, further experiments with increased amino acid and chloride concentrations may enable the detection of chlorinated products.

The vast differences in the sorption of clarithromycin and tetracycline with humic acids as a function of pH and calcium concentration highlights the need of developing models that describe the fate of polar organic contaminants in the environment. The application of the NICA-Donnan model for organic cations is a step in that direction. Although it had some flaws estimating the effect of calcium for both antibiotics, it was able to describe the effect of pH on sorption and to determine the extent of binding to different sites in the humic acid and the ionic species binding in each case. As of today it has only been tested on three organic cations, increasing the amount of data modeled will bring to light flaws that must be addressed as well as the chemical-physical properties required to achieve a good fit.

REFERENCES

- (1) Sibley, S. D.; Pedersen, J. a. Interaction of the Macrolide Antimicrobial Clarithromycin with Dissolved Humic Acid. *Environ. Sci. Technol.* **2008**, *42*, 422–428.
- (2) Gu, C.; Karthikeyan, K. G.; Sibley, S. D.; Pedersen, J. a. Complexation of the Antibiotic Tetracycline with Humic Acid. *Chemosphere* **2007**, *66*, 1494–1501.